AMMONIUM AND LEAD EXCHANGE IN CLINOPTILOLITE ZEOLITE COLUMN

A THESIS SUBMITTED TO
THE GRADUATE SCHOOL OF NATURAL AND APPLIED SCIENCES
OF
MIDDLE EAST TECHNICAL UNIVERSITY

BY

AHMAD DH. BAHAALLDDIN

IN PARTIAL FULFILLMENT OF THE REQUIREMENTS
FOR
THE DEGREE OF MASTER OF SCIENCE
IN
CHEMICAL ENGINEERING

DECEMBER 2010

Approval of the thesis:

AMMONIUM AND LEAD EXCHANGE IN CLINOPTILOLITE ZEOLITE COLUMN

submitted by **AHMAD DH. BAHAALDDIN** in partial fulfillment of the requirements for the degree of **Master of Science in Chemical Engineering Department, Middle East Technical University** by,

Prof. Dr. Canan Özgen _____
Dean, Graduate School of **Natural and Applied Sciences**

Prof. Dr. Gürkan Karakaş _____
Head of Department, **Chemical Engineering**

Prof. Dr. Hayrettin Yücel _____
Supervisor, **Chemical Engineering, METU**

Examining Committee Members:

Assoc. Prof. Dr. Halil Kalıpçılar _____
Chemical Engineering Dept., METU

Prof. Dr. Hayrettin Yücel _____
Chemical Engineering Dept., METU

Assoc. Prof. Dr. Naime Aslı Sezgi _____
Chemical Engineering Dept., METU

Assoc. Prof. Dr. İpek İmamoğlu _____
Environmental Engineering Dept., METU

Dr. Cevdet Öztin _____
Chemical Engineering Dept., METU

Date: December 17, 2010

I hereby declare that all information in this document has been obtained and presented in accordance with academic rules and ethical conduct. I also declare that, as required by these rules and conduct, I have fully cited and referenced all material and results that are not original to this work.

Name, Last name: Ahmad Dh. Bahaalddin

Signature:

ABSTRACT

AMMONIUM AND LEAD EXCHANGE IN CLINOPTILOLITE ZEOLITE COLUMN

Bahaalddin, Ahmad Dh.

M.Sc., Department of Chemical Engineering

Supervisor: Prof. Dr. Hayrettin Yücel

December 2010, 152 pages

Wastewaters resulted from anthropogenic influence can encompass a wide range of potential contaminants and concentrations. There are numerous procedures that can be used to clear out wastewaters depending on the type and extent of contamination, however; disposal of pollutants from wastewaters in industrial scale is a difficult and costly problem.

In this study, the use of ion exchange theory utilizing natural Turkish clinoptilolite zeolite from Gördes-Manisa as ion exchange resins in down-flow column mode is investigated. The clinoptilolite with particle size range of 0.25-0.50 mm is used in the removal of lead Pb^{2+} and ammonium NH_4^+ ions from aqueous solutions.

The aim of the study is to set up the conditions under which clinoptilolite may be used in an economical and efficient approach in the removal process. Experiments were divided into two sets: binary studies, and ternary studies, and the effects of

conditioning clinoptilolite with NaCl solution, flow rate, and initial concentration of the solutions on the removal behavior were investigated.

In binary studies, results showed that increasing the loading volumetric flow rate resulted in decreasing the breakthrough capacity and the column efficiency, while the total capacity remained constant. The maximum total capacity was determined as 1.16 meq/g of zeolite for NH_4^+, and 1.1 meq/g of zeolite for Pb^{2+} and these values were close to each other and to the sodium content of Na-form of pretreated clinoptilolite (1.16 meq/g of zeolite). In addition, by decreasing the initial contaminant concentration, an increase in breakthrough capacity and column efficiency was observed.

In ternary studies, the results showed that the removal of Pb^{2+} and NH_4^+ ions are dependent on the flow rate, in which at moderately low flow rate, a higher ion exchange capacity is yielded. That was explained as at higher flow rates, the retention time was insufficient for the ion exchange process to take place completely between clinoptilolite and lead and ammonium ions. Thus, a competition between Pb^{2+} and NH_4^+ ions for the exchange sites on clinoptilolite was observed and this competition was in favor of lead ions.

Consequently, it was observed that the clinoptilolite zeolite has affinity for both Pb^{2+} and NH_4^+ ions. However, the affinity of clinoptilolite for lead ions is higher than that for ammonium ions. Therefore, the cations selectivity for clinoptilolite according to their affinity is determined as the following sequence: $NH_4^+ > Pb^{2+} > Na^+$.

Keywords: Clinoptilolite, Ion exchange, Pretreatment, Lead, Ammonium, Removal, Column, Multicomponent.

ÖZ

KLİNOPTİLOLİT ZEOLİTİ KOLONUNDA AMONYUM VE KURŞUN DEĞİŞİMİ

Bahaalddin, Ahmad Dh.
Yüksek Lisans, Kimya Mühendisliği Bölümü
Tez Danışmanı: Prof. Dr. Hayrettin Yücel

Aralık 2010, 152 sayfa

Antropojenik etkilerden kaynaklanan atıksular, geniş bir aralıkta potansiyel kirletici ve konsantrasyonları içerebilir. Kontaminasyonun tipine ve derecesine bağlı, atıksuların arıtması için kullanılabilecek çok sayıda prosedürleri vardır. Ancak, endüstriyel ölçüde atıksulardan kirleticileri bertaraf etmek zor ve pahalı bir sorundur.

Bu çalışmada, iyon değiştirici olarak kullanılan Manisa-Gördes tipi doğal klinoplilolit zeolitinin aşağı-akışlı kolon operasyonu ile iyon değişimi incelenmiştir. Kurşun Pb^{2+} ve amonyum NH_4^+ iyonlarının sulu çözeltilerden gidermesinde parçacık boyutu 0.25-0.5 mm arasında olan klinoptilolit kullanılmıştır.

Bu çalışmanın amacı klinoptilolitin verimli ve etkili olarak ayırma proseslerinde kullanılabilmesi için koşulların belirlenmesidir. Deneyler ikili ve üçlü iyon değişim çalışması olarak iki kısma ayrılmıştır ve her iki çalışmada da; klinoptilolitin NaCl

çözeltisi ile zenginleştirilmesinin, akış hızının, ve çözeltilerin başlangıç derişiminin atık giderimine etkileri incelenmiştir.

İkili iyon değişim çalışmalarda, akış hızındaki artış salıverme kapasitesinin, ve kolon veriminin azalmasına neden olmuştur. Halbuki toplam kapasite sabit kalmıştır. Maksimum toplam kapasite 1.16 meq/g zeolit, NH_4^+ için, ve 1.1 meq/g zeolite, Pb^{2+} için belirlenmiştir, ve bu değerler hem birbirlerine hem de Na-form klinoptilolitin sodyum içeriğine yakınmıştır (1.16 meq/g zeolite). Ayrıca başlangıçtaki kirletici maddenin konsantrasyonunu azaltarak, salıverme kapasitesinin ve kolon veriminin artışı gözlenmiştir.

Üçlü iyon değişim çalışmalarda, sonuçlar gösterdi ki kurşun Pb^{2+} ve amonyum NH_4^+ iyonların gideriminin akış hızına bağlıdır ve ılımlı düşük akış hızlarında daha yüksek iyon değişim kapasitesine ulaşılmıştır. Bu durumun yüksek akış hızlarında klinoptilolit ile kurşun ve amonyum iyonlarının tamamen yer değiştirmesi için gerekli olan alıkonma süresinin yetersiz olması ile açıklanmıştır. Nitekim klinoptilolit üzerindeki değişim siteleri için Pb^{2+} ve NH_4^+ iyonları arasında bir rekabet gözlenmiştir ve bu çekişme kurşun iyonlarının lehine idi.

Sonuç olarak, klinoptilolit zeolitinin hem kurşun hem de amonyum iyonlarına karşı çekiciliğinin olması gözlenmiştir. Fakat klinoptilolitin kurşun iyonuna olan çekiciliği amonyuma göre daha fazla olduğu gözlenmiştir. Bu nedenle klinoptilolitin seçicilik sırası $NH_4^+ > Pb^{2+} > Na^+$ olarak belirlenmiştir.

Anahtar Kelimeler: Klinoptilolit, İyon Değişimi, Pretreatment, Kurşun, Amonyum, Giderim, Kolon, Çok Bileşenli.

To My Family...

ACKNOWLEDGEMENTS

First of all, I would like to express my deep sense of gratitude to my thesis supervisor Prof. Dr. Hayrettin Yücel for his permanent support, trust, precious advice and suggestions throughout this study. It was a great honor and pleasure to know him and to work with him.

I am also grateful to Mrs. Kerime Güney in instrumental laboratory for her endless valuable assistance and care, supportive comments, and for her assist in all chemical analysis throughout my study.

I am also grateful to all members and staff of the Department of Chemical Engineering in METU, for supporting me in my study and giving me chance to perform this thesis study. Many thanks go to Prof. Dr. Deniz Üner, Assoc. Prof. Dr. Halil Kalıpçılar, and Assoc. Prof. İpek İmamoğlu from Environmental Engineering Department, for giving me helpful suggestions and guidance in carrying out my thesis and for moral support.

Many thanks go to my colleagues at Chemical Engineering Department who were beside me all the time and helped me in my difficult days. I wish to thank my dearest friends Murat Erdoğan, Wisam Abdallah, Baraa Abbas Ali (God bless his soul), Hale Ay, Dominic Deo, Duygu Yılmazer, Saltuk Pirgalıoğlu, Hakan Murat İşler, Bijen Kadaifci, and Gamzenur Özsin, for their continuous helps and support.

I would like to express my great indebtedness to all my family, especially to my mother for her continuous support and encouragement. I like to convey many thanks to my father, my brother Safaaddin and my sister Mine, also to my uncle Sharaf and my aunts Mune and Salwa. I wouldn’t be able to succeed without your presence in my life.

And finally, words are inadequate in offering my thanks to the one who doesn't want to be named but she knows who she is, and so do I.

TABLE OF CONTENTS

LIST OF TABLES

TABLES

LIST OF FIGURES

FIGURES

LIST OF SYMBOLS AND ABBREVIATIONS

$A_{c.s}$: The cross-sectional area of the fixed bed

A_B : Area above the curve

A_S : Area under the curve

a_s : Surface area of clinoptilolite

A_T : The total area

BBU : Basic building unit of clinoptilolite

BV : Bed volume

C : The component ion concentration in the effluent

C_o : The component initial ion concentration in the influent

D_p : Average clinoptilolite particle diameter

E_a : Activation energy

EBZ : The equilibrium bed zone of the fixed bed

EEC : The effective exchange capacity of clinoptilolite

F : Fraction residual capacity of the mass transfer exchange zone

G_z : The total amount of cations removed by the exchange zone

$G_{z,\,max}$: Maximum quantity of ions removed by fixed bed

h_c : The column height

h_T : The mean fixed bed height

h_z : The mass transfer exchange zone height

IEC : The ideal exchange capacity of clinoptilolite

meq : Miliequivalent

M_i : Initial molarity of exchanging cations

M_f : Final molarity of exchanging cations

MTZ : The mass transfer zone of the fixed bed

M_z : Mass of the zeolite clinoptilolite

N : Total normality of the feed solution

Q_B : The breakthrough capacity of clinoptilolite

Q_T : The total exchange capacity of the bed

Q_z : Area above the breakthrough curve between breakthrough and exhaustion

REC : The real exchange capacity of clinoptilolite

S : Surface area

SBU : Secondary building unit of clinoptilolite

T : Temperature

TEC : The theoretical exchange capacity of clinoptilolite

t_f : Time of formation of mass transfer exchange zone

t_T : Time required for exhaustion of the bed

t_z : Time interval between the breakthrough and exhaustion point

UBZ : The unused bed zone of the fixed bed

U_f : Superficial fluid velocity

U_z : Rate of descent of mass transfer exchange zone

V : Volume of effluent collected

V_B : Volume of effluent collected up to the breakthrough point

V_T : Volume of effluent collected up to the exhaustion point

V_z : Volume of effluent collected between breakthrough and exhaustion point

V_w : Volume of deionized water

Greek Symbols

ε : The porosity of clinoptilolite

η_c : The column efficiency

ρ_b : The packed bed density

ρ_s : The solid density of clinoptilolite

$\emptyset$: The column diameter

$\hat{O}$: The volumetric flow rate

CHAPTER 1

INTRODUCTION

Man's influence on the environment has been receiving public and scientific research for many years. Excessive levels of pollutants are being introduced into the environment as a result of many activities conducted by human. Wastewater problem is one of the most important environmental problems because it contains a broad spectrum of contaminants affecting human health as well as the lives of plants and animals, and consequently violating the nature balance. As a result, the removal of these contaminants from aqueous wastes is a challenging task for the accurate management of waste disposal and the research is focused on using low-cost effective processes to remove such pollutants from aqueous environment.

Wastewater produced from municipal, agricultural and industrial sites creates ammonia nitrogen which subsequently mixes into lakes, rivers and drinking water reservoirs. The presence of excess nitrogen in the environment has caused serious distortions of the natural nutrient cycle between the living world and the soil, water and atmosphere. On the other hand, lead and lead components, which are present in the wastewater of many industries, are generally toxic pollutants and have hazardous effects on human life and on the aquatic environment. Therefore, raw water and wastewater with high lead and/or ammonia concentration should be treated before it reaches the consumer or the water reservoir.

Zeolites are crystalline aluminosilicates of alkali and earth-alkali elements with a framework structure enclosing cavities occupied by cations and water molecules,

both of which have considerable freedom of movement, permitting ion exchange and reversible dehydration. Zeolites form naturally on earth and its availability is broad.

Clinoptilolite, a type of natural zeolite, has a significant cation exchange property and has high selectivity for most of heavy metals. Hence it is used in the removal of some poisonous elements from wastewater including lead and ammonium.

The ion exchange method is widely used in wastewater treatment applications as a result of many advantages it held compared to other methods. However, there are several mechanisms involved in the process and many factors affecting the procedure that should be well studied in order to reach optimal conditions for practical use.

In this study, ion exchange behavior of natural zeolite clinoptilolite for lead and ammonium removal from synthetic wastewater was investigated in column mode utilizing ion exchange theory. Both binary and ternary systems were studied considering different parameters effects on the removal process: conditioning of clinoptilolite, solution flow rate in the column, and the initial feed concentration.

Finally, the results of the column studies were analyzed by utilizing the mathematical models given in literature to gain a better understanding for the mechanism of the ion exchange process using natural zeolite clinoptilolite.

CHAPTER 2

THEORETICAL BACKGROUND

2.1 Wastewater Treatment

The world is faced with increasing demands for high-quality drinking water and for treatment of municipal, agricultural, and industrial wastewaters. Heavy metals released in wastewater are among the most bothersome pollution problems due to their collective effects along the food chain. Wastewater treatment is becoming ever more critical due to diminishing water resources, increasing wastewater disposal costs, and stricter discharge regulations that have lowered permissible contaminant levels in wastewater streams.

With the rapid development of many different industries, a massive quantity of wastewater has been produced from industrial processes and was released into soil and sewage systems. Wastewater typically contains many pollutants such as cationic and anionic ions, oil and organics, which have lethal and toxic effects on ecosystems. The removal of these contaminants entails cost effective technologies and a variety of techniques have been developed in the past decades in dealing with wastewater treatment including adsorption and ion exchange processes (Wang, 2010)

Natural zeolites have potential advantages for applications in water and wastewater treatment. By using natural zeolites, a benefit is gained for wastewater treatment in their capability to undergo ion-exchange and adsorption. Furthermore, natural zeolites can be treated and modified in order to trap contaminants in wastewater.

Also, natural zeolites exist abundantly; therefore, low cost and low technology systems are required. Another benefit of using natural zeolites is their regenerative properties (Widiastuti, 2008). In addition, natural zeolites have the advantages of being a low-priced reserve (mainly when local deposits can be used) and most mined materials are available as vigorous crystal aggregates that can be processed to sizes appropriate to column use. This has resulted in a large literature describing definite and latent use of the natural species for water and wastewater treatment (Dyer, 2007).

The natural zeolite clinoptilolite is particularly useful in selectively eradicating ammonia and heavy metals such as Pb^{2+}. Generally, clinoptilolite is stable in an acidic environment and illustrates high selectivity for many heavy metals. The metal removal is greatly affected when the contact of the solid/liquid phases is short, which is a crucial restriction for treatment of wastewater (Lobo, 2003).

2.1.1 Lead Removal

Lead is the most broadly used of the heavy metals for thousands of years because it is widespread, easy to extract and easy to work with. Lead (Pb) belongs to Group 14 (IVA) of the Periodic Table of the elements having an atomic weight of 207.19 g/mole and its dominant oxidation state in most inorganic compounds is Pb^{2+} (Fergusson, 1991). Because it is the least mobile of the heavy elements in nature, metallic lead beads was found in Çatalhöyük in The Southern Anatolia of Turkey dating back to 6400 B.C. It has also been mined in Spain in the early 200 B.C. Lead was also known to the ancient Egyptians, Romans and Babylonians. Lead's symbol Pb is an abbreviation of its Latin name plumbum for soft metals (Merian et al, 2004).

Lead as a heavy metal, is not biodegradable and lean to accumulate in organisms, causing several diseases and disorders. When present in high amounts, lead has been found to be an acute toxic to human beings. As well as being poisonous, lead is also reported as a tumorigen, mutagen, and reproductive effector. Furthermore, lead is

known to damage the kidney, the liver and the reproductive system, the basic cellular processes and the brain functions (Fergusson, 1991).

Founded on the legislation currently enforced in the European Union, the maximum allowable lead concentration for discharge from industries in public waters, such as rivers, lakes and costal sea water is set at 200 μg/L (EC, 1991). According to the European Economic Community (EEC) standards, the maximum admissible concentration of lead in running water is 50 μg/L (Liu and Lipták, 1997). As a result of the toxicity of the lead, the United States Environmental Protection Agency (USEPA) since the early 2004 has lowered the concentration level in drinking water from 50 μg/L into 15 μg/L (USEPA, 2005).

Lead may enter the atmosphere naturally as a result of weathering of rocks, windblown soil, and volcanoes, and through anthropogenic acts as in the burning of leaded gas in automobiles and industrial releases. When lead is released to the atmosphere, it will generally occur as particulate matter and will be subject to gravitational settling. Therefore, lead particles are dispersed and ultimately removed from the atmosphere by wet or dry deposition (Merian et al, 2004).

In the hydrosphere, lead enters surface water from atmospheric fallout, run-off, or waste-water and little is transferred from natural minerals or leached from soil. The most stable ionic form of lead Pb^{2+} forms complexes of low solubility with major anions in the natural environment such as the hydroxide, carbonate, sulfide, and sulfate ions. The reported residence time of lead in oceans is about 290 to 850 years and in lakes is around 25 days (Fergusson, 1991).

In the lithosphere, lead is probably the least mobile of the heavy elements, and is still found in top soils that were contaminated with lead in the 4th century BC, that is because the half-life time of lead in soils lies in the range of 800 to 6000 years. In soil, lead ion Pb^{2+} will be involved in a number of chemical processes, such as

sorption into clays, coordination to both inorganic and organic ligands, and precipitation of insoluble compounds and generally follows the Langmuir and Freundlich isotherms (Merian et al, 2004).

As regards the biosphere, plants and human may bio-concentrate lead and uptake of lead in human may occur as a result of inhalation of contaminated ambient air or ingestion of polluted food or plants, and, to a limited extent, through the skin. The residence time of lead in humans were reported in the range of 270 to 370 and 2700 days according to the part or area of the body. Consequently, lead is toxic to all aquatic biota, and organisms higher up in the food chain may experience lead poisoning (Merian et al, 2004).

Even though lead is an eminent poison to human and animal health, its use in many industrial processes is still quite extensive. Many activities result in the lead presence in urban environment wastewaters, such as paint manufacturing, handicrafts, welding activities, plating, textile dyeing and printing, photography, and storage battery manufacturing and recycling (Liu and Lipták, 1997). This generates severe environmental problems, including the pollution of aquatic systems, which leads to lead involvement in hydrological-hydrochemical, and biological cycles.

Thus, treating the industrial wastewater at its source is required before the entry of the contaminants into the sewage system. To do so, many techniques are used, such as chemical precipitation, solvent extraction, ultra-filtration, electrodialysis, reverse osmosis, reduction reactions and ion exchange (Orhan and Kocaoba, 2007; Kocasoy and Şahin, 2007). Among these, ion exchange method is considered the most attractive method because its relative simplicity of its application. High removal rates of lead from aqueous solutions by clinoptilolite-containing rock samples have been observed and it is projected that natural zeolite be used to remove heavy metals from aqueous solutions. The metal binding is attributed to ion-exchange adsorption and surface precipitation processes (Lobo, 2003).

2.1.2 Ammonium Removal

The ammonium cation is a positively charged polyatomic cation of the chemical formula NH_4^+. Generally, ammonium ions are a toxic waste product of the metabolism in animals. In fish and aquatic invertebrates, it is excreted directly into the water. In mammals and amphibians, it is converted in the urea cycle to urea. In addition, many industries discharge wastes that are characterized by significant concentrations of ammonium including: iron and steel industry, fertilizer manufacturing, food processing, the manufacture of fibers, plastics, explosives, paper, and rubber, petroleum refinery, coal gasification, wood-preserving industry, and it also used as a coolant, in metal processing, and as a starting product for many nitrogen-containing compounds (Tufan, 2002; Šiljeg et al., 2010).

Although nitrogen is a nutrient vital to all forms of life as a basic building block of plant and animal protein, excess of it can be toxic. The existence of nitrogen excess in the environment has caused severe distortions of the natural nutrient cycle between the living world and the soil, water, and atmosphere (Tufan, 2002). Nitrogen in the form of ammonia or ammonium is soluble in water and can end up in ground water and drinking water. The Environmental Protection Agency (EPA) recommends a value of below 0.02 mg/L (Tchobanoglous and Schroeder, 1985), and according to the European Economic Community (EEC), the guide level is 0.05 mg/L and the utmost allowable level is 0.5 mg/L of NH_4 in drinking water (Liu and Lipták, 1997).

The ammonium ion is the most frequent cation in wastewater affecting both human and animal health (Widiastuti, 2008). As a result, the removal of ammonium ions is necessitated because of several reasons: the ammonium is toxic to fish and marine life and it contribute to tense growth of algal advancing eutrophication (Jorgensen and Weatherley, 2008; Huang et al., 2010). Also, ammonium ions cause the depletion of oxygen and it is corrosive to certain metals and materials of construction and has a negative effect on disinfection of water supplies (Mercer, 1970).

Many techniques are used in order to remove ammonium ions from drinking waters include air stripping, nitrification, distillation, reverse osmosis, breakpoint chlorination, incineration, catalytic decomposition, electrochemical treatment, algal harvesting, biological nitrification-denitrification and ion exchange (Tufan, 2002; Wang et al., 2006).

The properties of natural zeolites, and especially clinoptilolite, as ion exchangers for ammonium ions removal have a great interest in the matter even though the synthetic zeolites or organic resins have a greater total exchange capacity, since the clinoptilolite has a high selectivity for ammonium ions in solution and has a potential low cost (Koon and Kaufman, 1975). On the other hand, ion exchange processes are known to be stable with respect to product quality, and the widespread application of ion exchange processes has led to the development of equipments that operate almost automatically and requires relatively little maintenance. As a result, utilizing zeolites in ion exchange processes draw a great interest in ammonium removal from wastewater applications in literature (Hedström, 2001).

Generally, the nitrogen in aqueous solution exists in either the non-ionized ammonia form (NH_3) and/or ionized ammonium form (NH_4^+) depending on the temperature and pH of the aqueous environment. The ion exchange process can only remove the deionized form in which the pH of the aqueous solution should be kept below 7 for optimum ion exchange process (Rahmani et al., 2004).

As a result, the use of natural zeolite clinoptilolite for the removal of ammonium is considered to be a viable and efficient treatment method due to its low cost and relative simplicity of application and operation (Huang et al, 2010). However, the performance of the exchange and the magnitudes of ammonium removed are very much reliant on the origin of the material, the impurities contained, the counter ions, and the pretreatment performed on the zeolite (Abd El-Hady et al., 2001).

2.2 Natural Zeolites

2.2.1 Definition of Zeolites

The mineralogist community defines natural zeolites (or sedimentary zeolites) as crystalline aluminosilicates with a four connected tetrahedral framework structure enclosing cavities occupied by large ions and water molecules, both of which have considerable freedom of movement, permitting ion exchange and reversible dehydration to occur (Lobo, 2003). The zeolite composition can be best described as having three components: a four connected framework, extra-framework cations that balance the negative charge of the framework, and an adsorbed phase, which in this case is the water molecule in the cavities (McCusker and Baerlocher, 2007).

The term zeolite was originally coined by the Swedish mineralogist Axel Fredrik Cronstedt in 1756 who observed, upon rapidly heating a natural mineral that the stones began to vibrate about itself as the water evaporated. Using the Greek words which mean "stone that boils," he called this material zeolite (Sand and Mumpton, 1976). This property of zeolites is called “intumescence” which illustrates how zeolites can easily lose water when they are heated.

2.2.2 Crystal Structure and Chemistry of Natural Zeolites

All zeolite frameworks can be built by linking in a periodic pattern a basic building unit, the tetrahedron. In the center of the tetrahedra are atoms with relatively low electronegativities (Si^{4+}, Al^{3+}, etc.) and in the corners are oxygen anions (O^{2-}). These combinations can be depicted as $[SiO_4]^{-4}$, $[AlO_4]^{-5}$ tetrahedron. Figure 2.1. illustrates several representations of the tetrahedron. The center of the tetrahedron is occupied by a silicon or aluminum atom, with four atoms of oxygen at the vertices. It is shown in the figure that each apical oxygen is shared with the adjacent tetrahedron and thus, the framework of zeolite materials always has a metal-to-oxygen ratio of 2.

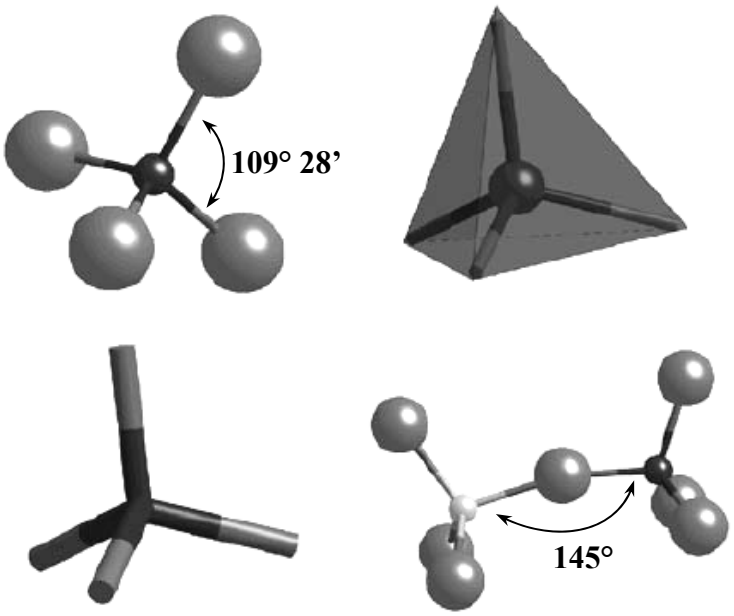

Figure 2.1. Several Representations of Basic Building Unit of Zeolite, the $[SiO_4]^{-4}$, or $[AlO_4]^{-5}$ Tetrahedron (Lobo, 2003).

Hence, a continuous framework is formed by the tetrahedra, as it is shown in Figure 2.2. resulting in a three dimensional open structure with pores, voids and channels where ions and molecules can move, allowing cation exchange and reversible dehydration to be possible (Lobo, 2003). Under normal conditions, the cavities and channels in zeolite structure are occupied by water molecules and cations. In addition, the alkali and/or alkaline earth cations are coordinated with water molecules, and located on specific sites in framework channels of the zeolite structure (McCusker and Baerlocher, 2007).

Commonly, the term TO_4 is used to describe the tetrahedral, where T stands for any tetrahedral species. The tetrahedra in zeolite materials are somewhat rigid. In general, the O-T-O angle is close to the ‘‘ideal’’ value of 109° 28’ for a geometrically perfect tetrahedron and deviations of more than a few degrees are not frequent. The T-O bond length depends on the particular metal cation. For $[SiO_4]^{-4}$ tetrahedra the bond length is d(Si-O) ≈ 1.59-1.64 Å, and for $[AlO_4]^{-5}$ the bond length is usually d(Al-O) ≈ 1.73 Å (Lobo, 2003).

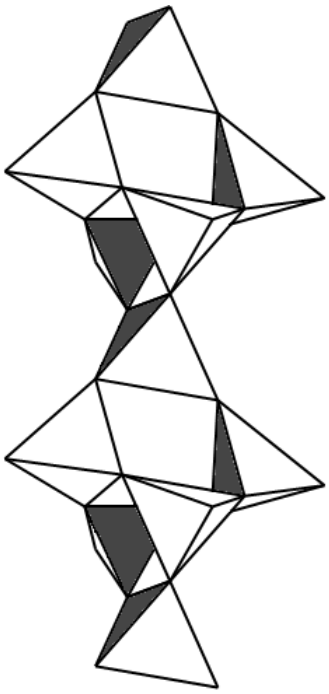

Figure 2.2. Tetrahedral Linked To Create a Three Dimensional Structure (Mumpton, 1960)

At some places in the zeolite framework Al^{3+} replaces Si^{4+} and thus the framework carries a negative charge. Loosely held cations, the extra-framework sitting within the cavities, preserve the electroneutrality of the zeolite and keep the overall framework neutral. Some of those cations are amenable to cation exchange; so, zeolites are able to reversibly adsorb polar molecules and these properties have contributed to the desiccant properties of zeolites (Payra and Dutta, 2003).

The generalized chemical formula of the zeolites is of the type $M_{x/n}[(AlO_2)_x(SiO_2)y].zH_2O$, where M is Na^+, K^+, Li^+ and/or Ca^{2+}, Mg^{2+}, Ba^{2+}, Sr^{2+}, Fe^{2+}; n is the cation charge; y/x is the silicon/aluminum ratio (Si/Al) lying within the limits of 1 to 6; and z is the number of water molecules; z/x ranges between 1 and 4; and finally (x+y) is the total number of tetrahedral in the unit cell. The composition of the tetrahedral framework is generally given in square brackets. Another way to express the zeolite composition is by the so-called oxide formula of the type: $M_{2/n}O.Al_2O_3.gSiO_2.zH_2O$ (McCusker and Baerlocher, 2007).

2.2.3 Classification of Natural Zeolites

In zeolites science, the term silicon/aluminum ratio (Si/Al) is frequently used to describe the composition of a zeolite and it is also used to classify the zeolite materials. That is because the aluminosilicates framework is the most conserved and stable component in the zeolite structure (Lobo, 2003). The silicon and aluminum contents verify the thermal and the chemical stability of the zeolite, the hydrophilic nature of the zeolite, and, in the acid form, the numbers and strengths of the acid sites (Corbin et al., 1987).

Basically, natural zeolites have relatively high Si/Al compositional ratio giving it special ion exchange selectivity for large monovalent cations (Dyer and White, 1999). Still, the properties of zeolites change as the amount of aluminum increases. In zeolite materials with higher aluminum content it is useful to think of the bonding as more ionic in character as compared to the siliceous counterparts. The thermal stability or capacity to endure high temperatures without loss of structural integrity decreases as the aluminum content increases (Armbruster, 2008).

Low-silica zeolites are unstable in acid, whereas high-silica zeolites are stable in boiling mineral acids, though unstable in basic solution. The ion-exchange capacity also increases as the number of negative charges in the framework increases. Consequently, the maximal number of acid sites (i.e., protons) increases with the amount of aluminum in the framework. Although acid site concentration decreases with the increase in Si/Al ratio, the acid "strength" and proton activity coefficients of the acid sites increase with decreasing in the fraction of aluminum in the framework. This observation can be understood on the basis of the proximity of electron-donating $[AlO_4]^-$. These groups increase the effective charge of the oxygen atom on the acid site, making it less prone to donate the proton (i.e., less acid). In addition, low-silica zeolites are hydrophilic, whereas high-silica zeolites are hydrophobic. For example, chabazite zeolites having Si/Al ratio lower than 2, are very hydrophilic.

Water molecules can coordinate to the many sodium cations present in the pores. The framework oxygen atoms are rather basic and serve as hydrogen bond acceptors to water and other molecules (Payra and Dutta, 2003).

The amount of Al within the framework can vary within the range of Si/Al = 1 to 6. The lower limit is determined by “Lowenstein's rule” in honor of the individual who first rationalized this observation. Lowenstein stated that an AlO_4 tetrahedron can not associate with another AlO_4 tetrahedron by a common oxygen atom; at Si/Al=1, in which the silicon and aluminum tetrahedral alternate to form the ordered framework. An example of the case is the chabazite material where the number of aluminum atoms per unit cell is identical to the number of silicon atoms. Lowenstein proposed that the lower limit of Si/Al=1 of a zeolite framework arises because placement of adjacent AlO_4^- tetrahedra is not favored as a result of the electrostatic repulsions between the negative charges. At other Si/Al ratios, ordered locations of Si and Al are also possible. The upper limit of the Si/Al ratio in the natural zeolites reaches up to 5 to 6, such as the case for clinoptilolite, mordenite, and ferrierite (Lobo, 2003).

A general classification of the natural zeolite materials according to the Si/Al ratios is done into three groups: low-silica or aluminum-rich zeolites; intermediate silica zeolites; and high-silica zeolites. Table 2.1 shows this classification. In the table, each framework in the zeolite structure is identified with a three-letter mnemonic code according to The Structure Commission of the International Zeolite Association (Payra and Dutta, 2003).

Table 2.1. Classification of Natural Zeolites (Payra and Dutta, 2003).

Low Silica $Si/Al \leq 2$	**Intermediate Silica** $2 < Si/Al \leq 5$	**High Silica** $5 < Si/Al$
AFG, afghanite	BOG, boggsite	FER, ferrierite
ANA, analcime	BRE, brewsterite	MEP, melanopholgite
BIK, bikitaite	CHI, chiavennite	
CHA, chabazite	DAC, dachiardite	
CAN, cancrinite	EPI, epistilbite	
EDI, edingtonite	ERI, erionite	
FRA, franzinite	FAU, faujasite	
GIS, gismondine	FER, ferrierite	
GME, gmelinite	GOO, goosecreekite	
LAU, laumonite	HEU, heulandite	
LEV, levyne	LOV, lovdarite	
LIO, liottite	MAZ, mazzite	
NAT, natrolite	MER, merlinoite	
PAR, partheite	MON, montasommaite	
PHI, phillipsite	MOR, mordenite	
ROG, roggianite	OFF, offretite	
WEN, wenkite	PAU, paulingite	
THO, thomsonite	STI, stilbite	
	YUG, yugawaralite	

2.2.4 Clinoptilolite

The natural zeolite clinoptilolite is the most regular and broadly distributed zeolite mineral found in nature. The name "clinoptilolite" was introduced by the mineralogist Waldemar T. Schaller in 1923, which is derived from the Greek words klino:oblique, ptylon:feather, and lithos:stone, to represent alkali and silica rich members of the heulandite family of zeolites (Schaller, 1923; Koyama and Takĕuchi, 1977). Its Si/Al ratio is greater than 4, and it is very stable towards dehydration, and thermally stable up to 700°C in air (Çulfaz and Yağız, 2004).

Clinoptilolite forms as white to reddish tabular monoclinic tectosilicate crystals, with a Moh's hardness of 3.5 to 4 and a specific gravity of 2.1 to 2.3 g/cm^3 (Duvarcı et al. 2007). It commonly occurs as a devitrification product of volcanic glass shards in tuff or as vesicle fillings in basalts and rhyolites. In nature, it occures as sedimentary deposits or found along with other minerals of silicate class: feldspars, quartz and other zeolites (tectosilicates subclass), clays (phylosilicates subclass), and volcanic glass (Armbruster and Gunter, 2001; Townsend and Coker, 2001).

2.2.4.1 Crystal Structure and Chemistry of Clinoptilolite

The chemical composition of the Heulandite-Clinoptilolite series is characterized according to their remarkable changes in the Si/Al ratio and depending upon composition of exchangeable cations in their structure. The Si/Al (y/x ratio) ratio changes between 4 and 5.5, and low-silica members are enriched with calcium, whereas high-silica clinoptilolite are enriched with potassium, sodium, and magnesium (Tsitsishvili et al., 1992). Generally, clinoptilolite species are mostly enriched with potassium and sodium exchangeable ions (Breck, 1971). The unit cell of clinoptilolite is usually characterized on the basis of 72 oxygen atoms and 24 water molecules (Abusafa and Yücel, 2002). The chemical composition of clinoptilolite is $(Na,K)_6[(AlO_2)_6(SiO_2)_{30}]24H_2O$.

In the structure of clinoptilolite crystals, $(Si,Al)O_4$ tetrahedra, which is the basic building unit of clinoptilolite (BBU), are linked through oxygen atoms in layers. Secondary building unit (SBU) for clinoptilolite is the 4-4-1 unit. The connection of SBU's forms the framework with monoclinic symmetry with unit cell constants: a=17.627Å, b=17.955Å, c=7.4Å and β=116.29° (Merkle and Slaughter, 1968; Coombs et al, 1998). The channel system of clinoptilolite is two dimensional consisting of ten membered (7.5 x 3.1 Å) and eight membered (4.6 x 3.6 Å) tetrahedral rings (Baerlocher et al, 2007) (Figure 2.3.). There is an additional eight membered channel cross-linked to these channels which is responsible for the two dimensional layer-like structure (Alberti, 1972; Armbruster and Gunter, 2001).

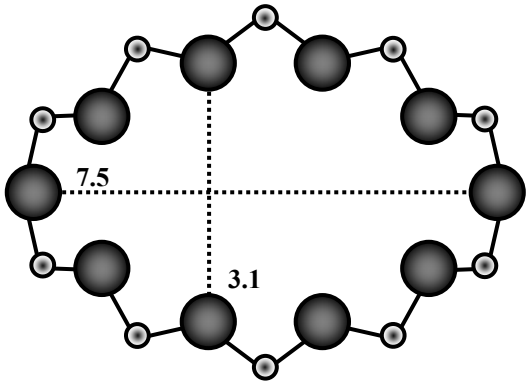

10-ring viewed along [011]

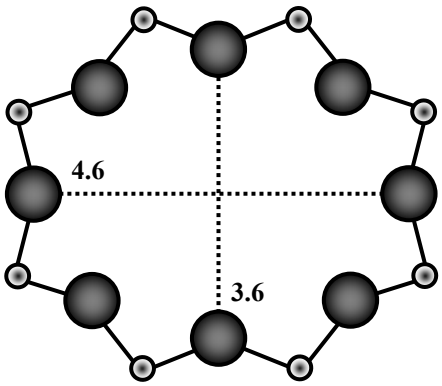

8-ring viewed along [001]

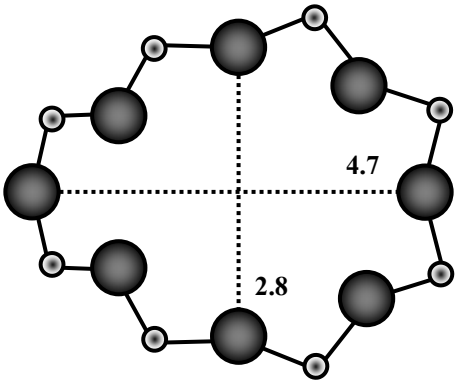

8-ring viewed along [100]

Figure 2.3. 8-ring and 10-ring Windows of Clinoptilolite (Baerlocher et al, 2007)

2.2.4.2 Tetrahedral Framework of Clinoptilolite

It is observed that all structural determinations of heulandite and clinoptilolite justify the structural scheme offered by Merkle and Slaughter (1968). In this proposed structural scheme, the $(Si,Al)O_4^-$ tetrahedra are bound in layers as it is shown in Figure 2.4. Moreover, these layers are in turn bound by the oxygen atoms in the symmetry plane and they form a three dimensional honeycomb framework structure as it is shown in Figure 2.5. In clinoptilolite, the strength of bonding in the main direction of aluminosilicate chains is greater than the strength of cross-linking of chains (Bareer, 1949).

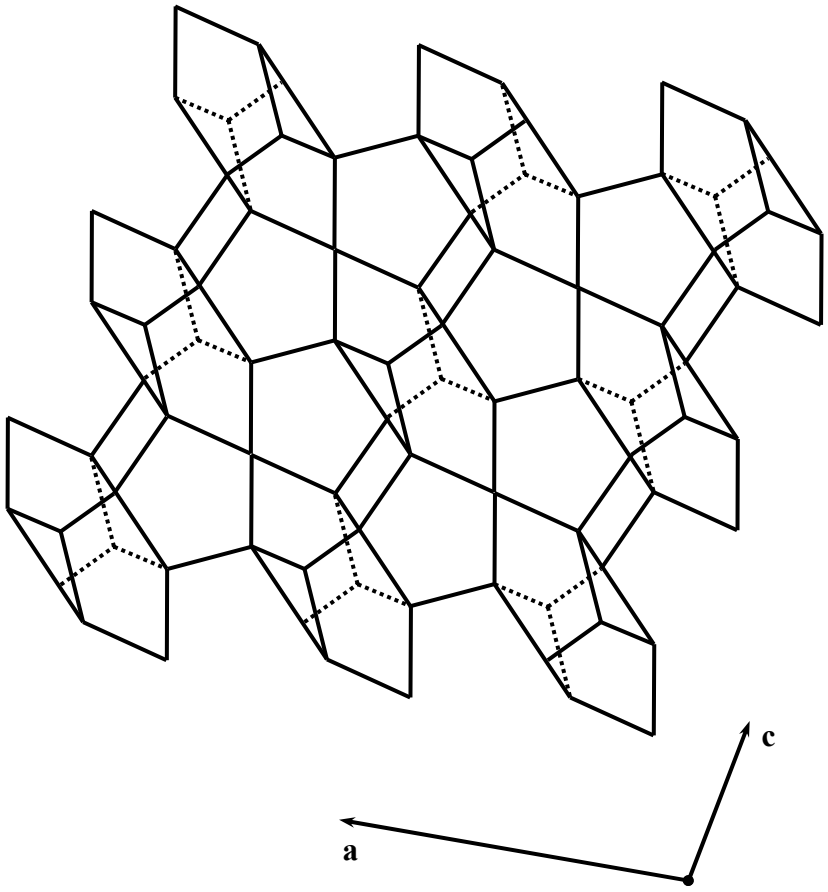

Figure 2.4. Arrangement of the 4-1-1 Units in the Framework Structure of Heulandite (Merkle and Slaughter, 1968)

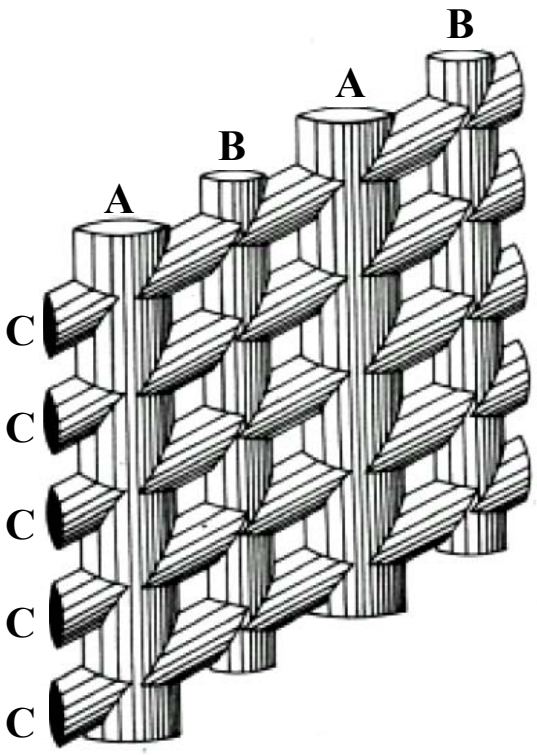

Figure 2.5. Schematic Representation of Two Dimensional Channel Systems in the ac Plane of Clinoptilolite (Koyama and Takĕuchi, 1977)

In clinoptilolite, framework units are joined in a layer like array which cause the characteristic perfect cleavage of the mineral. The channel system is 2-D, including 8 to 10 membered channels, parallel [001] and 8-tetrahedra channels along [100], termed by Koyama and Takĕuchi (1977) as A, B and C channels respectively as seen in Figure 2.5.

Regarding the porosity, clinoptilolite can be characterized by two types: the microporosity, which is caused by the specific crystal building of zeolite mineral grains; and the meso- and macroporosity, which is related to the size of zeolite, and other mineral grains in the rock as well as by structural features of the rock proper (Kowalczyk et al., 2006).

2.2.4.3 Exchangeable Cations and Water Molecules in Clinoptilolite

Clinoptilolite zeolite has high variable cation content. In nature, clinoptilolite channels are dominant with compositions as Na^+, K^+, and Ca^{2+}, and in some cases Sr^{2+}, Ba^{2+}, and Mg^{2+}, and other possible constituents are Fe^{2+} and Fe^{3+} (Merkle and Slaughter, 1968; Alberti, 1972). Still, it has stated that the most abundant single cation by a small margin is Na^+ and/or K^+ (Boles, 1972; Coombs et al, 1998).

Substitution of trivalent Al for quadrivalent Si in the silicate tetrahedral of clinoptilolite structures create fixed, negatively charge sites throughout the structure. To maintain electrical neutrality the negative charges are neutralized by the presence of an equivalent number of mobile cations and these mobile cations are loosely bonded in the crystal structure and they are free to exchange with cations in the solution surrounding it. The cation exchange occurs when ions from solution replace counter ions within the crystal structure. When presented in acidic environments, the zeolite skeleton does not vary on acidic processing but pores and channels change as a result of cations exchanging and these changes are more evident in the case of clinoptilolite (Korkuna et al., 2006).

Generally, zeolite structures have unique features that lead to unusual types of cation selectivity. However, cation selectivities in zeolites do not follow the typical rules which are evidenced by other inorganic and organic exchangers. Accordingly, The unusual selectivity of clinoptilolite that make it attractive for ion exchange applications is caused by structure related ion sieve properties. Many different mechanisms are existed which are responsible for the cation sieve properties exhibited by natural zeolites. One of them is the positive exclusion of certain cations due to the inability of these larger cations to enter the zeolite lattice in considerable amounts. The second mechanism for a cation sieve effect is the inability of the negative charge distribution on the zeolite structure to accommodate a given cation (Mumpton, 1960).

The framework of clinoptilolite points out that the hydrated mineral has four cation sites, two in the main 10-ring channels and two in the 8-ring ones. Calcium and sodium ions both occupy two sites M(1) and M(2) in channels A and B of clinoptilolite. In addition, in clinoptilolite structure there are two sites; M(3) occupied by potassium and M(4) occupied by magnesium ions (Gunter et al., 1994). Figure 2.6. illustrates cation locations in clinoptilolite structure according to the c- and a-axis projections (Koyama and Takĕuchi, 1977).

Along the c-axis, channels A and B are parallel to each other, and both are bound by 10 and membered oxygen rings. The thermodynamic parameters assigned to cation migration vary because cation movement in channels A and B meet different energy barriers. The cations in site M(1) are co-ordinate to two framework oxygen and five water molecules, while in M(2) three framework oxygen and five water molecules compose the cation environments. Therefore, cations leaving site M(2) should experience a slightly higher activation energy (E_a) in order to migrate (Dyer and White, 1999). The cation sites, as determined by Koyama and Takĕuchi (1977), are summarized in Table 2.2.

Table 2.2. Channel Characteristics and Cation Sites in Clinoptilolite (modified from Ackley and Yang, 1991).

Channel	**Tetrahedral Ring Size / Channel Axis**	**Cation Site**	**Major Cations**	**Approximate Channel Dimensions (Å x Å)**
A	10 / c	M(1)	Na^+, Ca^{2+}	7.2 x 4.4
B	8 / c	M(2)	Ca^{2+}, Na^+	4.7 x 4.1
C	8 / a	M(3)	K^+	5.5 x 4.0
A	10 / c	M(4)	Mg^{2+}	7.2 x 4.4

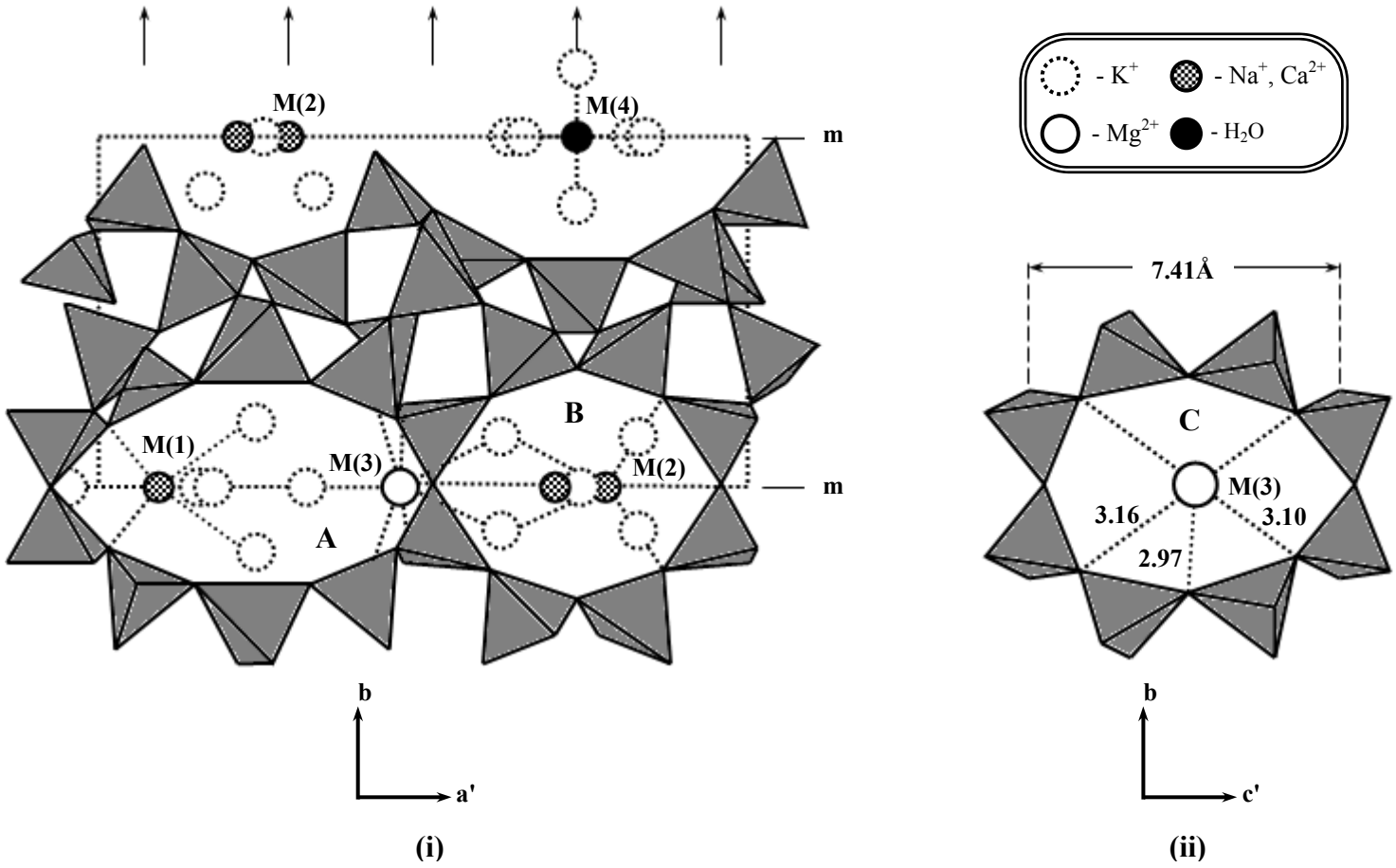

Figure 2.6. Cation Locations in Clinoptilolite Structure; i) The c-axis Projection of the Ten-Member Ring of Channels A and B, ii) The a-axis Projection of the Eight-Member Ring of Channel C. (modified from Koyama and Takĕuchi, 1977).

2.2.5 Applications of Zeolites

Applications and uses of zeolites, weather in natural or synthetic form, have attracted much attention and considerable progress has been made in utilization of zeolites in many industrial and agricultural areas in many countries, in both commercial and domestic levels. The major industrial applications which make use of zeolites are summarized according to the process involved in Table 2.3. (Passaglia and Galli, 1991; Mumpton, 1999; Townsend and Coker, 2001; Polat et al., 2004).

Table 2.3. Applications of Zeolites

Process	**Application**
Adsorption and Separation	• Regenerative (Separation based on sieving or selectivity) • Bulk Separation and gas absorption • Cryosorption • Purification
Ion Exchange	• Metal separation or removal from wastewater • Artificial kidney dialysate regeneration • Ion exchange fertilizers • Ammonium removal • Detergent Builder
Catalysis	• Hydrocarbon conversion (Alkylation, Cracking, Hydrocracking, Isomeration) • Hydrogenation and Dehydrogenation • Drying and purification of acid gases • Shape-selective reforming
Miscellaneous	• Animal nutrition and health • Construction materials • Soil conditioner • Paper filler

2.2.6 Natural Occurrence and Reservoirs of Zeolites

Natural zeolites form where volcanic rocks and ash layers react with alkaline groundwater. Zeolites also crystallized in post-depositional environments over periods ranging from thousands to millions of years in shallow marine basins. Large zeolite occurrences are found in belts of recent volcanism, frequently in rocks of Cretaceous, Paleogenic and Neogenic age (Tufan, 2002). Nowadays, cconventional open pit mining techniques are used to mine natural zeolites.

After the determination of natural zeolite reserves over the world has begun since 1950, wide natural zeolite occurrences have been seen in all of the continents (Ozaydin, 2006). According to the United States Geological Survey minerals yearbook in 2008, world production of natural zeolites is estimated in the range of 2.5 to 3 Mt (USGS, 2008).

Production estimates for individual countries are: China, 1.75 to 2.25 Mt; Jordan, 400,000 to 450,000 t, the Republic of Korea, 160,000 t; Japan, 140,000 to 160,000 t; Turkey, 100,000 t; the United States, 60,100 t; Slovakia, 60,000 t; Indonesia, 30,000 to 50,000 t; Ukraine, 20,000 to 40,000 t; Hungary, 20,000 to 30,000 t; New Zealand, 17,000 t; Cuba, 16,500 t; Bulgaria, 15,000 t; South Africa, 10,000 to 15,000 t; Australia and Spain, 5,000 to 10,000 t each; Canada, Greece, Italy, the Philippines, and Russia, 3,000 to 5,000 t each; and Mexico, 700 t (USGS, 2008).

Among world countries, Turkey has a huge occurrence of sedimentary zeolite, primarily in central and western Anatolia regions and in around the shores of the Aegean Sea due to the abundance of natural clinoptilolite in easily accessible surface deposits. However, no definite natural zeolite reserve in Turkey is determined and that is because the limits of zeolitic zones in volcanics have not yet been resolved in many of zeolite occurrences (Ozaydin, 2006). Associated to many parts of the world, the zeolitic tuffs are allied with clay minerals, borates, carbonates, and soda minerals

akin. Also, they are found in close association with lignite-bearing lacustrine rocks (Ören and Kaya, 2006).

The Western Anatolia region is rich in clinoptilolite deposits. The most important reserves of clinoptilolite in Turkey are Manisa-Gördes and Balıkesir-Bigadiç basins, with estimated reserves of 20 million tons and 500 million tons, respectively. Other basins for clinoptilolite with total reserves of 50 billion tons are in Emet-Yukarı Yoncaağaç, Kütahya-Şaphane, Gediz-Hisarcık, İzmir-Urla, Tuzköy-Kayseri and Amasya-Doğantepe (DPT, 1996).

In Turkey, only the clinoptilolite group of natural zeolite is mined and processed as a major mineral occurrence of the country. The foremost consumption purposes that are mined for are agricultural, animal feed additive, water purification, and animal litter purposes. In addition, there are other trade coded products based on clinoptilolite, such as fertilizer additive, soil amendment, and animal feed additive products, which are marketed in Turkey and exported to some companies in Europe, Israel, and the United States (Ozaydin, 2006). The price of sized clinoptilolite is 130 US Dollars/Ton FOB-Istanbul (ROTA Madencilik A.Ş).

2.3 Ion Exchange Theory

Ion exchange is the process concerning exchange (or sorption) of one or several ionic species escorted by the simultaneous dislocation (or desorption) of one or more other ionic species of the same charge. In other words, ion exchange is the exchange of ions between an insoluble solid and a surrounding aqueous solution. The charge in the solid phase is balanced by ions of the opposite charge, named counter-ions. To illustrate, when the ion exchanger, containing ions A is immersed in a liquid phase, containing ions B, then a diffusion process is established and this diffusion is a result of the considerable concentration difference between the two phases. . In zeolites, the ion exchange reaction is best regarded as involving bulk phases and not essentially a surface reaction (Townsend and Coker, 2001). Moreover, as the ions undergo a phase change, ion exchange can be considered as a sorption process, but in contrast to other sorption processes, ion exchange is necessarily stoichiometric (Helfferich, 1962).

The most significant property of the solid phase is its active charge, which is directly related to its ion exchange capacity (Ingllzakis, 2005). In zeolites, cation exchange behavior depends on different variables such as the nature of the cation species, the cation size, both anhydrous and hydrated, and cation charge; the temperature; the concentration of the cation species in solution; the anion species associated with the cation in solution; the solvent; and the structural characteristics of the particular zeolite (Breck, 1974).

The zeolite contains exchangeable ions that reside at the internal channels of its framework. These cations can be replaced more or less easily with other cations in aqueous solution, without affecting the alumina-silicate framework. The ion exchange process in zeolites involves replacing one singly-charged exchangeable atom in the zeolite by one singly-charged atom from the solution, or replacing two singly-charged exchangeable atoms in the zeolite by one doubly-charged atom from the solution. The magnitude of such cation exchange in a given zeolite is known as

its cation exchange capacity and is commonly measured in terms of moles of exchangeable cation per gram of zeolite, or in terms of equivalents of exchangeable cations per gram of zeolite (Howery and Thomas, 1965).

In ion exchange nomenclature, the specific nature of natural zeolites undergoing ion exchange processes, especially in column mode operations, creates a need for different ion exchange capacity terminologies that should be differentiated. These include: theoretical exchange capacity, ideal exchange capacity, real exchange capacity, breakthrough capacity, and total exchange capacity.

The theoretical exchange capacity (TEC) is the number of exchangeable cations per specified amount of ion exchanger. The total charge of these exchangeable cations is equal to the zeolite framework charge. The term was introduced by the International Union of Pure and Applied Chemistry (IUPAC) and Helfferich (1962) called it the maximum exchange capacity. This type of capacity is a constant used for characterizing the zeolite, and commonly can be determined by chemical analysis of the zeolite or spectrometric techniques such as X-ray diffraction or NMR techniques (Fanfan et al, 2006). Since the exchangeable cations of zeolites are Na^{+}, Ca^{2+}, Mg^{2+}, and K^{+}, the theoretical exchange capacity (TEC) is the total sum of the zeolite free cations, measured in (meq/g of zeolite):

$$TEC = \Sigma (Na^{+}, K^{+}, Ca^{2+}, Mg^{2+}) \qquad 2.1$$

However, zeolites in nature do not exist in pure form, but they rather contain several impurities, such as feldspars, quartz, clays, volcanic glass, and other zeolites (Payra and Dutta, 2003). As a result, in order to distinguish the case of zeolites with specific purity, with the case of pure zeolites, the term ideal exchange capacity (IEC) is introduced by Inglezakis (2005) that corresponds to the actual amount of the exchangeable cations in pure zeolites. The ideal exchange capacity (IEC) can be

determined using the zeolite' chemical formula, then the amount in equivalents of the exchangeable cations for each formula unit can simply be calculated.

Another term for the capacity is the real exchange capacity (REC), which refers to the amount of actual exchangeable cations of the zeolite, measured by ion exchange methods, and is a characteristic constant of the zeolite independent of the experimental conditions. The total charge of the exchangeable (or removable) cations is equal to the active negative charge of the zeolite structure. It is reported by many investigations that the real exchange capacity of clinoptilolite ranges from 1.6 to 2.0 meq/g of clinoptilolite (Kon and Kaufmann, 1975). The real exchange capacity (REC) can be calculated utilizing X-ray diffraction (XRD) technique or by performing ion exchange process (batch or column mode) in which the zeolite negative charge should be totally and fully balanced by any equivalent amount of incoming cations. In case of utilizing XRD method, the real exchange capacity for zeolite tuff can be calculated using the following equation:

$$REC = \Sigma P_i \, IEC_i \qquad 2.2$$

where (P_i) is the fraction of each mineral (i) including zeolite and impurities, in the zeolite tuff having an ideal exchange capacity of IEC_i.

The theoretical exchange capacity (TEC) is always higher than the real exchange capacity (REC) as a result of the fact that some of the zeolite cations can not be detached from the zeolite structure because of strong bonding force within the structure of the zeolite, or they are part of the zeolite impurities and thus they are not exchangeable. In summary, ideal exchange capacity (IEC) is a characteristic property of pure zeolite species, whereas theoretical exchange capacity (TEC) and real exchange capacity (REC) are characteristic properties of a zeolite sample (tuff) with a precise purity in which both of their values depend on the amount and the nature of impurities (Inglezakis, 2005).

2.3.1 Column Operations

Most ion exchange operations in practical applications (especially in continuous pollutant treatment) are carried in fixed-bed column systems, in which the ion exchange operation column units operate in continuous mode in a steady state or approximate steady state. However, the column design should provide several factors, such as it must contain and support the ion exchange resin, must distribute the service flow through the resin bed uniformly, must provide space to fluidize the resin during backwash, must include the piping, valves, and instruments needed to regulate flow of feed, regenerant, and backwash solutions. Ion exchange processes in column operations can be used for the replacement, removal, and separation of ions and non electrolytes (Barrer et al., 1967).

The simplest column operation is the replacement of counter ion in feed by another counter ion which is primarily in the ion exchanger. The counter ion from the feed is removed by the ion exchange process and it is absent in the effluent until the breakthrough occurs. The composition of the effluent and its change with time, depend on the properties of the exchanger, the composition of the feed, and the operating conditions such as flow rate, temperature, etc (Inglezakis et al., 2003).

Ion exchange processes in fixed bed column lab-scale operations are conducted using vertical columns packed with zeolite material, and the feed is introduced using a peristaltic pump, at a specific flow rate. Then, the samples are withdrawn at the exit of the bed at desired time intervals, depending on the flow rate, and analyzed for cations. It must be recognized that fixed bed column operations differ from batch operations in terms of the hydrodynamic and the mass transfer patterns. Moreover, column operations flow may suffer from non-idealities such as channeling or insufficient contact of the solution with the ion exchanger. These problems may reduce the process efficiency and lead to erroneous results in capacity

determinations. Therefore, it is recommended that the column should be long enough and operate under steady state conditions (Inglezakis, 2005).

2.3.2. Mathematics Used in Column Operation Calculations

Several definitions and methods should be considered when analyzing and designing the fixed bed operations for ion exchange processes. A common method in such is the mass transfer zone method (MTZ), which was proposed by Michaels (1952). Nevertheless, this method is applicable only for fixed bed ion exchange processes in which a sharply defined and a constant width exchange zone are formed. Generally, this behavior is characteristic of exchange in which the ion to be removed from the influent has a greater affinity for the exchanger than the ion originally in the solid.

To demonstrate, let us assume that the feed solution containing ammonium ions NH_4^+ is allowed to pass up at constant rate through a packed bed of Na-form of clinoptilolite zeolite, exchange of sodium ions of the solid for ammonium ions is taking place, so that ammonium ions are taken up by the clinoptilolite and equivalent amount of sodium ions is to be released to the external solution. As the influent moves in upward direction, the first part comes into contact with new layer of sodium saturated clinoptilolite (Michaels, 1952).

Afterwards, the uptake of ammonium ions continues, and the reaction attempts to reach a new state of equilibrium in which the amount of ammonium ions in the solution is less than in the original. According to the mass transfer zone method described by Michaels, it is supposed that the exchange process is confined in a restricted region of the bed, which is the mass transfer zone (MTZ) lying under steady state conditions, between the lower equilibrium bed zone (EBZ), and the upper unused bed zone (UBZ), as shown in Figure 2.7. Accordingly, the mass transfer zone is the area where the exchange is taking place and where exhaustion

and equilibrium have not been achieved yet, in which the fresh solution is in contact with unsaturated zeolite. The unused bed zone (UBZ) is the part of the mass transfer zone which has not yet undergone exchange (Fanfan et al, 2006).

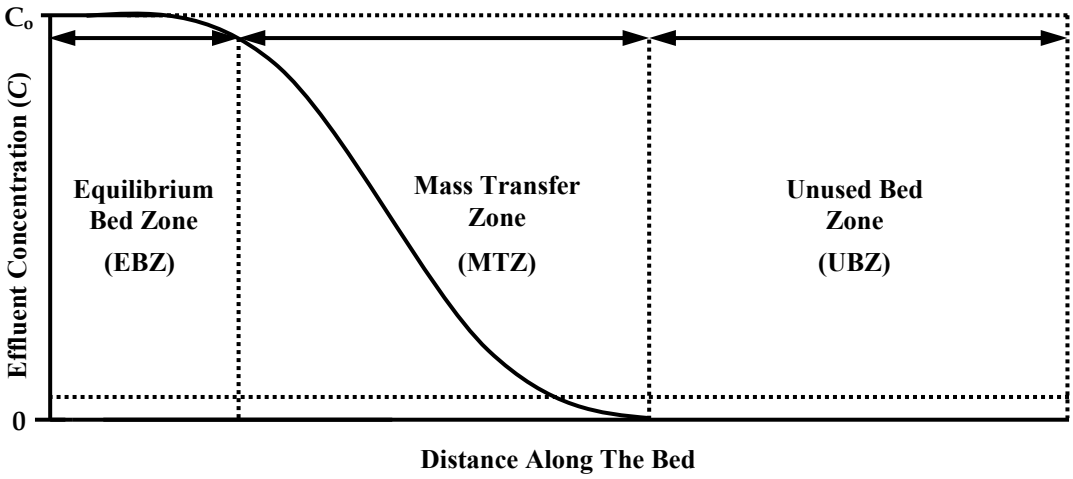

(a)

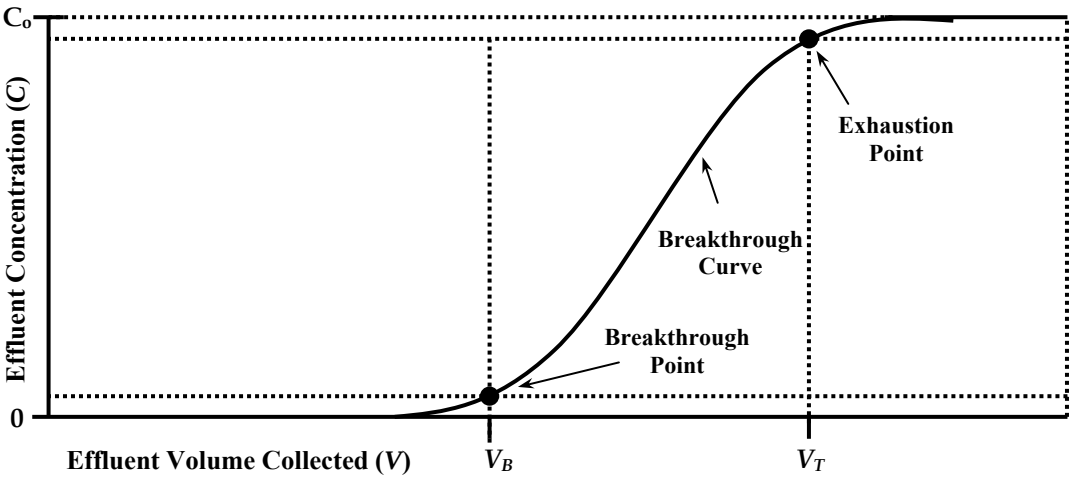

(b)

Figure 2.7. Ion Concentration Profile (Michaels, 1952)

a) in the bed

b) in the effluent

After definite amount of influent has been introduced into the column, the lower part of the clinoptilolite will be saturated with ammonium ions, whereas the upper parts are still in the sodium form. The concentration of ammonium ions in the solution is the same as the initial ion concentration in the influent (C_o) in the lower part, equal to zero in the upper part of the column. While in the intermediate zone of the column, both ammonium and sodium ions are present in the liquid as well as the solid, and the concentration changes in different points where the composition of the liquid will be a function of the distance from the bottom of the clinoptilolite bed.

The effluent from the bottom of column will be free from ammonium ions and will contain an equivalent amount of sodium ions until such an amount of solution has been run through the column that the mass transfer zone has reached the end of the bed. When a definite amount of the influent has passed through the ion exchanger bed, the so-called breakthrough point is reached, which means that ammonium ions are detected in the effluent. So, the breakthrough point can be defined as the time when the effluent concentration (C) is reaching a percentage of the influent concentration (C_o) which considered unacceptable. Accordingly, the exchange zone can be defined as the part of the ion exchange bed in which the concentration of the ion, desired to exchange with the bed, in the solution flowing through the bed falls from 95 to 5 % of its initial value (C_o) in the influent (Inglezakis, 2003).

When the concentration of the exchangeable ion in the effluent of a fixed bed ion exchange column is plotted as a function of the volume of effluent collected, characteristic S-shaped curves can be obtained (Figure 2.8.). Mathematically, competitive ion binding experiments will often need a nonlinear regression model. This model has to level off at both extremes to represent almost no binding at one end and saturated binding at the other end. This behavior is usually represented by an S-shaped curve in which it specifies a nonlinear regression functional relationship, where populations existing in favorable circumstances. The sharp S-shape of the

curves is due to optimal choice of the ratio of particle/column diameters, and the ratio of bed depth/column diameter (Medvidović et al., 2008).

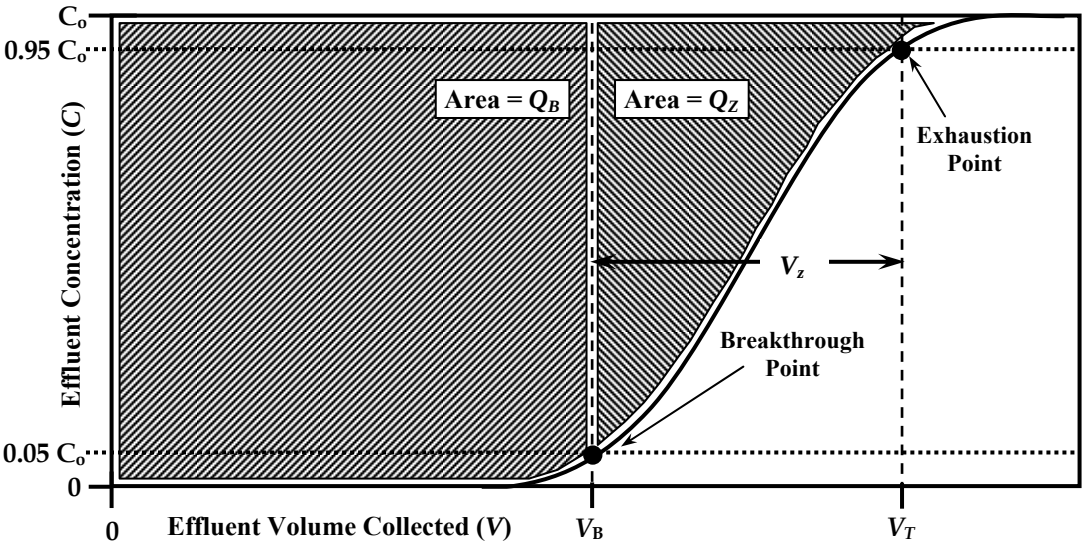

Figure 2.8. Idealized Effluent Concentration vs. Effluent Volume Collected for Ion Exchange Column (the Breakthrough Curve) (Michaels, 1952)

The breakthrough curve is very useful in calculating the dynamic parameters affecting the ion exchange process such as the mass transfer zone height (h_z). The mass transfer zone height is a measure of the resistance of the exchanger to mass transfer, and also a measure of the exchanger's thermodynamic affinity to the exchangeable cations.

Referring to quantities related to mass transfer zone, the height of the exchange zone can be calculated from the following relationship:

$$h_z = U_z\, t_z = h_T \left[\frac{t_z}{t_T - t_f} \right] \qquad 2.3$$

where (h_z) is the exchange zone height, (h_T) is the is the mean height of the packed bed, (U_z) is the descent rate of the mass transfer zone, (t_z) is the time required for the

zone to move its own height, (t_f) is the time of formatoin of transfer zone, (t_T) is the time required for exhaustion of the bed.

The time, (t_z), required for the exchange zone to move its own height down through the bed under steady-state conditions is proportional to the volume of effluent (V_z) Figure 2.8; so that;

$$t_z = \frac{V_z}{U_f A_{c.s}} \qquad 2.4$$

where (U_f) is the fluid velocity, and ($A_{c.s}$) is the cross-sectional area of the exchange column.

Acknowledging that:

$$V_z = V_T - V_B \qquad 2.5$$

where (V_B) is the effluent volume collected up to the breakthrough point, (V_T) is the effluent volume collected up to the exhaustion point of the bed.

Similarly, the time, (t_T), required for the zone to establish itself at the top of the bed and to move downward out of the bed is proportional to the total volume of the effluent collected (V_T); so that;

$$t_T = \frac{V_T}{U_f A_{c.s}} \qquad 2.6$$

The mass transfer zone height (h_z), except for the period of time during which the exchange zone being formed at the beginning of the process (t_f), is descending through the bed at a constant rate, and can be determined by:

$$U_z = \frac{h_T}{t_T - t_f} \qquad 2.7$$

The mass zone formation time (t_f), is a function of the time required for the transfer zone to move its own height (t_z), and its value depends on the shape (S-Shape) of the breakthrough curve (Michael, 1952). In general, it has been shown that:

$$t_f = (1 - F) t_z \qquad 2.8$$

where (F) is the fraction residual capacity of the exchange zone

Equation 2.8 shows that the lower average metallic cation content of the exchanger in the mass transfer zone (after steady state is attained), the shorter the time required to form the zone initially. In many cases the S-shaped curves are found to be symmetrical, so that $F = 0.50$, and $t_f = 0.5\ t_z$ (Michael, 1952). However, the fraction residual capacity of the exchange zone (F) can be evaluated by:

$$F = \frac{G_z}{G_{z,\,max}} \qquad 2.9$$

The amount of the total cations removed by the exchange zone (G_z) from the breakthrough point up to the exhaustion point of the bed can be evaluated graphically from the breakthrough curve utilizing the relationship follows;

$$G_z = \int_{V_B}^{V_T} (C_o - C) dV \qquad 2.10$$

where (C) is the component ion concentration in the effluent solution

Assuming that the clinoptilolite bed in the exchange zone is completely in the sodium form, this same region of the bed would have removed a maximum quantity of exchanged ions equal to:

$$G_{z,\,max} = C_o\ (V_t - V_B) \qquad 2.11$$

Accordingly, substituting Equation 2.10 and Equation 2.11 in Equation 2.9 will yield;

$$F = \frac{\int_{V_B}^{V_T} (C_o - C)dV}{C_o(V_t - V_B)} \qquad 2.12$$

If $F = 0$, so that the exchanger within the exchange zone at steady state is in essence saturated with the ions being removed, the time of formation, t_f, of the exchange zone at the top of the bed would be anticipated to be almost equal to the time required for the zone to descend a distance equal to its own height, t_z, after steady state is reached. In opposition, if $F = 1.0$, so that the exchanger within the exchange zone at steady state is basically free of the ions being detached, the time of formation, t_f, of the exchange zone would be very short.

Finally, by combining Equations 2.4, 2.6, and Equation 2.8 in Equation 2.3, the height of the exchange zone (h_z) can be obtained as follows:

$$h_z = h_T \left[\frac{V_z}{V_t - (1 - F) V_z} \right] \qquad 2.13$$

or, for symmetrical curves;

$$h_z = h_T \left[\frac{V_z}{V_t - 0.5 V_z} \right] \qquad 2.14$$

The term breakthrough capacity (Q_B), also known as the work exchange capacity (Fanfan et al, 2006), refers to the ion exchange capacity of a particular type of zeolite utilized in column operations and it is not constant but depends on the experimental conditions (Inglezakis, 2004).

According to the International Union of Pure and Applied Chemistry (IUPAC) and Helfferich, the breakthrough capacity (Q_B) is the loading of the ion exchanger material in a fixed bed column when the incoming ion is first detected in the effluent or when the concentration in the effluent reaches some arbitrary value. In practical use of ion exchangers, it is suitable to use certain breakthrough levels such as 1-10% (Lehto and Harjula, 1995) and mean value of 5% of the initial effluent concentration is recommended. The breakthrough capacity depends on the specific ion exchanger system and on the experimental conditions used for its determination. Such experimental conditions are the volumetric flow rate, breakpoint concentration, and temperature and normality of the solution (Inglezakis, 2005).

The breakthrough capacity (Q_B) of the fixed bed (the zeolite bed) is expressed by the mass of the zeolite (M_z), and can be determined by evaluation of the area above the S-shaped curve, shown in Figure 2.8, up to the breakthrough point by the graphical integration of the relationship;

$$Q_B = \frac{\int_0^{V_B} (C_o - C)\, dV}{M_z} \qquad 2.15$$

where (C_o) is the initial ion concentration in the influent solution, (C) is the component ion concentration in the effluent solution, (V) is volume of effluent solution collected, and (V_B) is the effluent volume collected up to the breakthrough point.

The mass of the zeolite clinoptilolite (M_z), can be expressed as:

$$M_z = \rho_b\, h_T\, A_{c.s} \qquad 2.16$$

where (ρ_b) is the packed bed density.

Finally, by substituting equation 2.16 in Equation 2.15, we will yield:

$$Q_B = \frac{\int_0^{V_B} (C_o - C)\, dV}{\rho_b\, h_T\, A_{c.s}} \qquad 2.17$$

The total exchange capacity (Q_T), also known as the operating capacity, represents the total amount of cations (of pollutant) trapped over the material (zeolite) until complete saturation is reached at the exhaustion point of the breakthrough curve (Fanafan et al, 2006). It is theoretically independent of the flow rate (Helfferich, 1962). However, experimentally it has been found that it is influenced by the operational conditions, which are the liquid flow rate (or contact time), and flow quality (Ingelzakis, 2005).

The total exchange capacity (Q_T) can be shown in Figure 2. as the total area above the curve, and is given by;

$$Q_T = Q_B + Q_Z \qquad 2.18$$

Where (Q_z) is area above the breakthrough curve between breakthrough and exhaustion point (Figure 2.8.).

However, the total exchange capacity of the bed (Q_T) can be evaluated by taking the integral of the area above the breakthrough curve up to the exhaustion point and can be expressed by the mass of the zeolite (M_z) as;

$$Q_T = \frac{\int_0^{V_T} (C_o - C)\, dV}{\rho_b\, h_T\, A_{c.s}} \qquad 2.19$$

where (V_T) is the effluent volume collected up to the exhaustion point.

The Column Efficiency (η_c), or the degree of column saturation or utilization, is the fraction of the exchange capacity utilized, and can be demonstrated as:

$$\eta_c = Q_B / Q_T \qquad 2.20$$

In summary, the different types of exchange capacities discussed previously can be arranged as follows: TEC ≥ IEC ≥ REC ≥ Q_T ≥ Q_B (Inglezakis, 2005).

2.3.3 Factors Effecting on Ion Exchange on Clinoptilolite Zeolite

Generally, there are several aspects that affect the dynamics of the cation uptake by zeolite, such factors are mainly solution and solid specific factors. Solution specific factors include temperature, pH, the flow rate, the initial cation concentration being removed by zeolite, the pretreatment solution, the presence of other competing ions in the solution, and the characteristics of the heavy metal being removed by the zeolite. On the other hand, the solid specific factors include, particle size, surface dust, impurities found in the zeolite sample, and the pretreatment procedure type applied to the zeolite (Moralı, 2006).

In addition, it should be emphasized that the cation exchange capacity of the clinoptilolite is distinctly dependent on its original cationic composition, because not all the cationic sites in the clinoptilolite structure are available for cation exchange. Therefore, before any practical ion exchange application, specific studies on representative clinoptilolite samples from the deposit, being examined for its exploitation potential, should be carried out (Langella et al., 2000).

2.3.3.1 Effect of Pretreatment

The zeolite contains several exchangeable cations that reside at the internal channels of its framework, such cations are calcium, sodium, magnesium, and potassium; and these cations have different exchange properties for every environment. In practice, prior to any ion exchange application of the zeolite, the zeolite is conditioned to the increase of the content of a single (more easily detachable) cation so that it becomes homoionic in order to enhance the zeolite effective exchange capacity (EEC) and its performance in ion exchange applications (Inglezakis et al., 2001). It is stated that the pretreatment give rise to new accessible and available sites for exchange, resulting in higher distribution coefficient and selectivity (Inglezakis et al., 2004). It's even stated that the pretreatment process brings about a slight increase in the surface area of clinoptilolite (Gedik and Imamoglu, 2008).

Generally, the final homoionic or near-homoionic state of the zeolites is found to enhance their effective exchange capacity (EEC), which can be defined as the amounts of cations of the zeolite contained in a specific amount of the material, which are exchangeable under specific experimental conditions (Kesraoul-Oukl et al., 1993; Hellferich, 1995). On the other hand, since the theoretical exchange capacity (TEC) is characteristic of a specific type of zeolite; not the pretreatment and nor any modification application has any effect on it. That is because some of the zeolite cations cannot be detached easily due to low mobility and strong bonding forces within the structure of the zeolite (Jama and Yücel, 1990).

Throughout literature, different chemicals have been utilized in the pretreatment (or conditioning) of zeolites, such as Sodium Chloride (NaCl), Sodium Hydroxide (NaOH), Calcium Chloride ($CaCl_2$), Potassium Chloride (KCl), Ammonium Chloride (NH_4Cl), Magnesium Chloride ($MgCl_2$), Hydrochloric Acid (HCl), Nitric Acid (HNO_3), Sulfuric Acid (H_2SO_4), and Sodium Acetate ($C_2H_3NaO_2$).

However, among theses chemicals, NaCl is most common and effective one used in the pretreatment of zeolite both in batch and column mode (Milan et al., 1997). Inglezakis et al. (2001) showed that the pretreatment with NaCl almost doubled the effective exchange capacity (EEC) of clinoptilolite when removing lead in column mode. The reason of that is related to the bonding strength between the cations and the zeolite framework, in which: the sodium bonds into two framework oxygen atoms and five water molecules, the calcium is coordinated with three framework oxygen atoms and five water molecules, potassium is coordinated with six framework oxygen atoms and three water molecules, and finally magnesium is coordinated with six water molecules (Jama and Yücel, 1990). By comparing, sodium has the weakest cation bonding with zeolite making it more mobile and more exchangeable ion, whereas calcium is more tightly bonded and potassium is the least mobile ion in the zeolite framework.

Upon using NaCl, one should consider using high concentration of NaCl solution (1-1.5M) when using little volume of the solution, and lower concentration when more volume of pretreatment solution is used (Rahmani et al., 2004). A thorough study conducted by Vassilis J. Inglezakis (2001), in which NaCl solution was used, investigated other factors affecting the pretreatment process itself. The effect of pH of the NaCl solution was examined and the best working pH was found to be around 7.5. The low pH means high concentration of H^+ that leads to simultaneous uptake of hydrogen ion by the zeolite, and the high pH means high concentrations of OH^- in the solution leading to the entrapment of hydroxide ion in the structure of zeolite leading to partial destruction of zeolite structure. Also, the washing of pretreated samples with ionized water was studied, since it is a necessity to avoid excess of sodium ions to be entrapped in the zeolite structure. Aside from pretreatment, NaCl is also used in many studies regarding the regeneration of the zeolite after ion exchange process is completed, and levels around 95 to 98 % of regenerations are achieved (Rahmani et al., 2004).

2.3.3.2 Effect of Particle Size

Generally, for column mode ion exchange processes, the particle size of the zeolite has a momentous effect on the whole ion exchange process. It is generally measured according to the average particle diameter (D_p) of the zeolite. Large particle size results in low contact time between the zeolite and the solution flowing through the column, leading to low cation exchange probability. In contrast, smaller particle size results in high flow resistance, high pressure drop, and channeling in the column (Leif and Terry, 1982; Czárán et al, 1988).

Therefore, an optimum particle size should be utilized depending on the hydrodynamic properties of the exchange column such as column diameter, column height, and other factors. In column operations, high rates of ion exchange performance can be achieved when utilizing relatively small particle sizes of clinoptilolite, if particle diffusion is rate controlling (Güray, 1997).

In his study to remove ammonium from wastewater, Ames (1960) concluded that grain sizes bigger than 1.0 mm radically decreased the ammonium exchange capacity. However, the head loss increases with smaller grain sizes. Others suggested grain sizes of 0.4 - 0.5 mm in ammonium removal (Hlavay et al., 1982; Leung et al., 2007). The higher ammonium exchange capacity when using smaller particle sizes is explained to be caused by a higher mass transfer into the zeolite (Hedström, 2001).

To sum up, in order for the ion exchange in the column mode to be enhanced, long contact time as possible is required between the zeolite particles and the solution surrounding it. In addition, as the zeolite ion exchange mechanism takes place within its cavities and not on its surface, washing the zeolite particles, no matter what size is it, plays a significant rule in making the majority of its internal surface area accessible.

2.3.3.3 Effect of Flow Rate

The flow rate in column operations is a core factor for practical application and it is credited to the optimal selection of experimental conditions, such as the ratio of particle to column diameters, and the ratio of bed depth to column diameter (Inglezakis et al., 2003).

Any volume element of the solution will be in contact with a given layer of zeolite bed for only a limited time, and the flow rate is controlling this contact time. The limited period of contact time is usually insufficient in continuous mode operations for equilibrium to be attained, and thus resulting in low uptake of cations from the feed solution (Inglezakis et al., 2002).

Medvidović et al. (2007) stated that in continuous mode operations, the breakthrough capacity (Q_B), and the total exchange capacity (Q_T) do not depend on the flow rate of the solution in the column. However, the difference between these two capacities increases with increasing the flow rate, and by which negligibly decreases the column efficiency (η_c). In addition, as the flow rate increases, the height of the mass transfer zone (h_z) increases. However, Inglezakis et al. (2002) and Dyer (2007) showed that the total exchange capacity (Q_T) is dependent on the flow rate, and the saturation in the column is also dependent on the flow rate and is favored by low flow rates.

Law et al. (2004) showed that oscillations, when applied to the bulk fluid flowing upwards through a column packed with zeolite, enhance the liquid phase adsorption column performance. The use of oscillatory flow in the liquid phase had shown to delay the breakthrough time, increase the average bed loading up to breakthrough point, reduce the length of unused bed zone (UBZ), and reduce the length of mass transfer zone (MTZ).

2.3.3.4 Effect of Feed Concentration

The initial feed concentration (C_o) of the solution passing through the zeolite bed is also an important factor affecting the zeolite uptake for metal cations in the ion exchange process. Among set of experiments for the removal of the same metal by clinoptilolite, it is stated that a decrease in breakthrough capacity (Q_B) is occurred when removing initially high concentration influents compared to low ones (Güray, 1997). That is because the ion exchange service cycle takes relatively short time resulting in limited contact time between the clinoptilolite and the metal in which, from industrial view, is not practical (Tufan, 2002).

However, when the ion exchange system is multicomponent, the selectivity factor will also play a role in the removal of metals. The zeolite selectivity and efficiency for the different metal cations engaged in the exchange system are proportional to their initial concentration in the solution, where the higher the concentration of heavy metals, the higher the efficiency of the zeolite tuff (Ibrahim and Akashah, 2004). For example, studies in batch process mode, for a single component, indicated that the removal of lead and ammonium with clinoptilolite has increased with the increase in initial ammonium concentration (Günay et al., 2006; Wang et al., 2006).

2.3.3.5 Effect of pH

The removal of the metal cations from solutions by the zeolite is affected by pH of the aqueous environment to a great extent. That is because pH influences both the surface charges of zeolite and the character of the exchanging metal specie (Martinez et al., 2004). Heavy metals, such as lead, may form complexes with inorganic legands present in the solution like OH^- (Ouki and Kavannagh, 1997). As a result, complex formation might occur, leading to the reduction of the cation exchange capacity of the zeolite for a given contact time and thus affecting adversely the kinetics of the removal process (Semmens and Seyfarth, 1978).

The ion exchange adsorption of the metals is stated to be directly proportional to pH values of aqueous solutions. In acidic solutions, the hydrogen ions compete with other cations in the solution for the exchange sites in the zeolite (Sprynskyy, 2006). Accordingly, the cation uptake decreases with decreasing pH due to the less availability of the accessible sites (Inglezakis et al., 2001). During acidic processing of clinoptilolite, it is stated that the clinoptilolite structure does not change; however, the pores and the channels change because of the cation exchanging process (Korkuna et al., 2006).

The clinoptilolite surface in water has a negative charge at natural pH and preserves its negative charge even in very acidic condition low to pH=2 (Ersoy and Çelik, 2002). Therefore, clinoptilolite have the ability to neutralize the aqueous environment, acting as proton acceptor or as a proton donor, as a result of its amphoteric nature (Rivera et al., 2000). This behavior is dependent on the other metal cations' concentrations which are present in the ion exchange system, and it is minimal for high metal concentration. Thus, the competitive uptake of H^+ cations is believed to be the cause of the lower uptake of metals in more acidic environment (El-Bishtawi and Ali,2001; Inglezakis et al., 2003).

In general, applications of clinoptilolite for metal cation removal require pH values between 3 and 11 (Payne and Abdel-Fattah, 2004). However, as H^+ cations act as a competitive cation in ion exchange processes, the ion exchange of heavy metals is favored at high acidity values (Inglezakis et al., 2003). For lead removal, Llanes-Monter (2007) stated that ideal exchange is found at initial pH of 3, while others showed that optimal removal is achieved at pH range of 4 and 5 (Ouki and Kavannagh, 1997; Ali and El-Bishtawi, 1997). In order to achieve optimum ion exchange in removing ammonium from aqueous medium, the pH of the aqueous solution should be kept below 7 (Koon and Kaufmann, 1975; Rahmani et al., 2004).

2.3.3.6 Effect of Temperature

The temperature independence of employing ion exchange method in the treatment of wastewater is an advantage in this method (Atkins and Scherger, 1997). Generally, increasing temperature will lead to the increase metal uptake by zeolite. Clinoptilolite shows a linear increase in adsorption and ion exchange performance with increasing temperature, since both of the processes are strongly spontaneous and endothermic (Lin and Wu, 1996; Günay et al., 2006). That is because the temperature increase assists the adsorption process through the activation of adsorption sites in clinoptilolite (Payne and Abdel-Fattah, 2004). For example, Ćurković et al. (1996) demonstrated that the lead removal clinoptilolite has increased with increasing temperature.

At high temperatures, the higher diffusion coefficients, resulting in a rapid movement of cations, boost the metal uptake by the zeolite. The reason of that is the weakening of electrostatic interactions and the hydrated radii of the ions getting smaller with increasing temperature (Inglezakis et al., 2004).

2.3.3.7 Effect of Competing Ions

In the presence of competing ions, the clinoptilolite adsorption performance and eventually the cation uptake by the zeolite turn down. That is because the zeolite attraction for the heavy metal is electrostatic and thus influenced strongly by competing ions (Payne and Abdel-Fattah, 2004). For instance, calcium is a major competing cation for ion exchange with clinoptilolite (Ouki and Kavannagh, 1997).

In general, the subtraction of heavy metals in the company of inorganic and organic ligands is affected by direct or indirect mechanisms. The ligands that are existed in

the aqueous environment influence the metal ion behavior and the surface properties of the sorbents (Inglezakis, 2004).

The ion exchange performance is decreased in the case of the formation of surface complexes with ligands compared to a ligand-free system (Semmens and Seyfarth, 1978). In addition, the ligands favor the metal removal by changing the surface electrical properties or by adsorbing sturdily to the zeolite surface, weigh against to the case where either one is present unaccompanied in the solution (Doula and Ioannou, 2003).

When present together, the competition between different metal species for exchangeable sites in zeolite structure depend on their ionic characteristics. Therefore, when the zeolite is used to remove different cations from the solution simultaneously (multicomponent system), the exchange selectivity of zeolite for the different cations will become the touching factor.

The preference of the zeolite for one cation rather than another (zeolite exchange selectivity), in a multicomponent system, depends on several factors, such as the Si/Al ratio, the exchangeable cation of the zeolite, distance between anionic sites, cationic radii, hydrated cationic radii, and cationic hydration energy (of the co-ion and the in-going ions), as well as temperature and the three-dimensional zeolite framework (Barros et al., 2003; Oter and Akcay, 2007).

The zeolite clinoptilolite has a high Si/Al ratio, therefore it has a low structural charge density and as a result, divalent cations, like lead, with low hydration energies are sorbed preferably compared to cations with high hydration energy (Wingenfelder et al., 2005). So, the selectivity is mostly determined by the free energies of the cations; the cation with the largest hydration energy prefers the solution phase, whereas the cation with the least hydration energy prefers the zeolite phase (Semmens and Seyfarth, 1978).

To illustrate, let's consider the following data for three different cations: Pb^{2+}, Zn^{2+}, and Cu^{2+} which have ionic radii of (1.21, 0.74, and 0.80 Å), respectively; hydrated ionic radii of (4.01, 4.30, and 4.19 Å), respectively; enthalpy of hydration of (-1481, -2046, and -2100 kj/mol), respectively (Kesraoui-Ouki et al., 1994). Considering these data and the dimensions of the channel system of clinoptilolite, it is obvious that the unhydrated ions can pass through the channels of clinoptilolite channels, however; the hydrated ions may exchange only with obscurity. Therefore, lead has the smallest hydrated cationic radius and can pass easily through the channels. Also, lead has the lower hydration energy and that means it can lose its hydration shell more easily than the other ions (Inglezakis et al., 2003). So, the clinoptilolite will have higher affinity and selectivity for lead and the metals selectivity can be ordered as: $Pb^{2+} > Zn^{2+} > Cu^{2+}$ (Oter and Akcay, 2007).

The typical cations rank for clinoptilolite according to their affinity to, considering different studies conducted regarding the subject (Ames, 1960; Howery and Thomas, 1965), can be ordered as:

$Cs^{+} > Rb^{+} > K^{+} > NH_4^{+} > Ba^{2+} > Sr^{2+} > Pb^{2+} > Ag^{2+} > Cd^{2+} > Zn^{2+} > Cu^{2+} > Na^{+} > Ca^{2+} > Fe^{3+} > Al^{3+} > Mg^{2+} > Li^{+}$

For instance, the selectivity series indicates that potassium cations are the most vital competing ions compared to ammonium for ion exchange by clinoptilolites. Thus, the content of potassium cations in aqueous solutions will influence the ammonium removal by ion exchange (Langwaldt, 2008). Nevertheless, the selectivity of the zeolite upon such ions, when present in mediums containing polar organic solvents influencing the surface charge density of mobile ions within zeolite, can be totally changed (Inglezakis and Loizidou, 2007; Jorgensen and Weatherley, 2008).

2.3.3.8 Effect of Impurities

In nature, zeolites do not exist in pure form, but they found as zeolite ores (tuffs) containing several impurities, such as feldspars, quartz, clays, volcanic glass, and other zeolites as well as to other several inorganic compounds, such as the calcium and magnesium carbonates calcite, dolomite, and magnesite (Payra and Dutta, 2003). These impurities effect both on the theoretical exchange capacity (TEC) and on the real exchange capacity (REC) of the zeolite (Townsend and Coker, 2001).

Feldspars, which are anhydrous aluminosilicates of potassium, sodium and calcium, have interlinked tetrahedra connect at each corner to other tetrahedra forming a three dimensional, intricate, negatively charged framework. Feldspars having the cations, potassium, sodium, and calcium, which sit within the voids in its structure, can exchange theses cations with others surrounding it.

Clays are mostly chemically and structurally analogues to other phyllosilicates; however, they contain varying amounts of water and allow more substitution of their cations which are exchangeable. It is stated that clays exhibit high cation exchange capacity that effect on the overall cation exchange capacity of the zeolite containing it. The most significant clay minerals related to zeolite ore are kaolinite, smectites (vermiculite and montmorillonite), and illite (Li et al., 2002).

The zeolite clinoptilolite is also found along with the quartz in zeolite tuffs. Even though quartz is a neutrally charged inert mineral, not having the capacity for cation exchange; it is stated that sandy soils which contain large amounts of quartz have low cation exchange capacity. As a result, it might interfere with the ion exchange capacity of the zeolite resulting in unpredictable exchange capacity (Inglezakis, 2005).

2.3.3.9 Effect of Surface Dust

Surface dust occurs throughout the grinding processes of the zeolite and may deter the metal uptake capacity of zeolites. It is a clogging element of the particle pore opening in zeolite structure, leading to slower ion exchange kinetics (Inglezakis et al., 1999; Zorpas et al., 2002). As a result, it might lead to the slower uptake of Na^+ ions during the pretreatment process of zeolite with NaCl solution. Inglezakis et al. (2001) stated that the percentage of dust increases with decreasing particle size since decreasing particle size results into higher area-to-volume ratios, and thus, resulting in higher surface available for dust attachment.

Moreover, surface dust might have other influences on the ion exchange process in column mode, such as the clogging of the packed bed leading to high pressure loss, consequent overflow and leakage. Also, surface dust of the zeolites might result in difficulties in bed unloading since zeolite fragments are mound together (Inglezakis et al., 2001). Therefore, washing the sorbent material (the zeolite) prior to metal removal studies is recommended in order to enhance the ion exchange performance in column.

CHAPTER 3

LITERATURE SURVEY

Mercer et al. (1970) studied the removal of ammonia in column (up-flow) mode using natural clinoptilolite mined in California-USA both in laboratory and pilot-plant scale. In the experimental studies, influents were adjusted at pH of 6.5 and greater than 99% of ammonia removal was achieved when using two zeolite columns in series. The regeneration of clinoptilolite was studied and most economical approach was found when using a mixture of 0.03N NaCl, and 0.07N $CaCl_2$, and the spent clinoptilolite was reused after exhausting the ammonia into atmosphere by air stripping.

Koon and Kaufmann (1975) studied the practical ammonia removal from municipal wastewaters using clinoptilolite mined in California-USA with grain sizes of 0.3-0.84 mm in column mode. In all tests, the bed depth was 0.9 m and flow rate was 15BV/h. They also studied the regeneration of clinoptilolite after exhaustion in column in upflow mode and effects of competing ions, pH and flow rate. They observed that the removal of ammonium decreased sharply with increasing competing cation concentrations. Also, they found optimum ammonium removal in pH range of 4 to 8. In regeneration process, they concluded that when using NaCl or NaOH as the regenerant rather than $CaCl_2$ or $Ca(OH)_2$, the breakthrough capacity (Q_B) was doubled while the total exchange capacity (Q_T) was almost the same.

Suzuki and Ha (1984) studied the establishment of fundamental relations in removing ammonium from wastewater in batch and column mode using natural

Korean clinoptilolite with particle size range of (0.25-0.3, 0.84-1.19, and 3.36-4.76 mm). In column studies, influent ammonium concentration (C_o) used were 17 and 34 ppm, and the breakthrough curves were determined using Carter's numerical calculation method based on solid phase diffusion kinetics, and mass transfer coefficients were evaluated using Wilson's equation. Consequently, the predicted lines and experimental curves show good agreement in both cases suggesting that both equilibrium relation and coefficient obtained by batch method are applicable to the design of fixed bed adsorption for ammonium removal.

El Akrami (1991) examined ammonium removal by ion exchange process in column mode using natural Turkish clinoptilolite mined in Bigadiç with particle size ranges of (0.3-.06, 0.6-1.18, 1.8-3.35 mm). The effects of feed composition, particle size, flow rate, and accompanying cation concentration on the ion exchange process were studied. Flow rates throughout the column were in the range of 22-78 BV/h. An optimum condition for ion exchange was found when using 0.3-.06 particles size and loading flow rate of 30 BV/h. The breakthrough capacities (Q_B) were varied from 0.085 to 0.891 meq NH_4^+/g of clinoptilolite depending on the influent ammonium ion concentration in the range of 23-178 mg/L.

Abusafa (1995) investigated the performance for ammonium and cesium removal in continuous mode using natural Turkish clinoptilolite mined in Bigadiç. In the study, the breakthrough capacity (Q_B) ranged from 0.036 to 1.08 meq NH_4^+/g of clinoptilolite. Also, an optimum particle size for ion exchange application was estimated while using clinoptilolite with particle size range of (0.3-0.6mm).

Milan et al. (1997) compared different homoionic forms of natural clinoptilolite from Spain with particle size of 5 mm, when used in the removal of ammonium from piggery manure wastewater in column mode. They used clinoptilolites pretreated with NaCl, KCl, $CaCl_2$, and $MgCl_2$ and the best result was obtained with Na-Zeolite form, with the exchange capacity rank of: Na-Zeolite > Ca-Zeolite > K-Zeolite > Mg-Zeolite. They explained that the exchange of K^+-NH_4^+ was affected by the low

mobility of K^+ in zeolite structure, the exchanges of Ca^{2+}-NH_4^+ and Mg^{2+}-NH_4^+ were affected by the high concentration of suspended solids and the viscosity of the influent, which resulted in low mobility of these cations in the liquid phase.

Nguyen and Tanner (1998) investigated the ammonium removal from wastewaters using natural New Zealand zeolites (clinoptilolite and mordenite) under both batch and column conditions. Effects of two types of zeolite and of particle size ranges (0.25-0.50, and 2.0-2.83 mm) were explored. In the study, mordenite showed more effective ammonium removal than clinoptilolite for wastewaters solutions containing high NH_4^+ concentrations particularly in the presence of competing Na^+ ions. In continuous mode operations, for both types of zeolite, the fine zeolites were more efficient than the coarse zeolites in removing ammonium ions (95% and 55% removal, respectively) which is equivalent to 5.8 - 6.5 g of NH_4^+/kg of zeolite. In contrast, by increasing flow rate, coarse zeolites were not as effective as fine zeolites in removing NH_4^+ ions since the ammonium breakthrough for coarse zeolites occurred quickly and they explained it by probable result of the insufficient contact time for NH_4^+ ions adsorption and diffusion into zeolites.

Petruzzelli et al. (1999) made a practical study for lead ion removal and recovery from battery manufacturing wastewater using natural clinoptilolite mined in California-USA with particle size range of (0.2-0.5mm) in column mode operation. For optimum practical use, they suggested the conditioning of clinoptilolite with 2M NaCl with 10 BV and the adjustment of pH (5.5-6) is required to minimize degradation of clinoptilolite. In the absence of competing ions (aluminium and ferric species), they achieved quantitative removal and recovery of lead (≈90%) from wastewater after elution from clinoptilolite. The best clinoptilolite performance was observed at almost neutral solution (pH=6) and moderate loading flow rate (10 BV/h). They also performed a regeneration process for the clinoptilolite used with NaCl solution, and more than 30 exhaustion-regeneration cycles were made without major lead leakage from column.

Abd El-hady et al. (2001) studied the removal of ammonia from drinking water using natural Slovakian clinoptilolite with large particle sizes range (3-5mm) in column mode. The effect of thermal pretreatment of clinoptilolite and the concentration of regenerant solution (2, 5, and 10% NaCl) on the breakthrough capacity were studied. Their findings were that the repeated pretreatment process on clinoptilolite improved its removal capacity while the structure of clinoptilolite remained unchanged throughout loading and regeneration cycles. However, there was no difference between the regenerates for 5% and 10% NaCl solutions. Also, they observed that ammonium removal capacity was increased by the range of 20%-40% when heat-treating the clinoptilolite compared to the non treated samples. Therefore, it was revealed that the thermal activation increases the clinoptilolite selectivity for ammonium ions.

Cincotti et al. (2001) investigated the uptake of lead, ammonium, copper, zinc, and cadmium from wastewater in batch and column modes using natural and pretreated Sardinian clinoptilolite. In column mode experiments, the bed volume for the natural zeolite - lead, and Na-zeolite - lead systems corresponding to the breakthrough point were equal to 250 and 700 BV, respectively, illustrating the extreme effect of the pretreatment process on zeolite. The ion selectivity scale for clinoptilolite was found as: $NH_4^+ > Pb^{2+} > Cd^{2+} > Cu^{2+} > Zn^{2+}$.

Demir et al. (2002) studied the removal of ammonium ion from aqueous solution both in batch and column mode using clinoptilolite mined from Bigadiç-Turkey with particle sizes range of (0.875-1.0, and 1.0-2.0 mm). They investigated the impact of particle size and flow rate on the ammonium exchange capacity in clinoptilolite. The column studies were done with flow rates of 10, 25, 50, and 75 BV/h and optimum loading rate was found around 25 to 50 BV/h. They observed higher exchange capacity for smaller particle size (0.57 meq/g of zeolite) compared to larger particle size (0.38 meq/ g of zeolite), and they explained that the smaller particles had higher exchange capacity due to greater available surface area.

Inglezakis et al. (2002) investigated the ion exchange of Pb^{2+}, Cr^{3+}, Fe^{3+} and Cu^{2+} on natural Greek clinoptilolite with particle size range of (1.14-1.18 mm) at 27°C and initial concentration of 10meq/L. They investigated the effect of flow rate (5, 10, and 15 BV/h) on the breakthrough point and the total exchange capacity (Q_B) in column processes, and evaluated both of their values as 12.3 BV and 0.433 meq Pb^{2+}/g of clinoptilolite, respectively, at flow rate of 5 BV/h. Consequently, they were able to determine the selectivity series of the elements as: $Pb^{2+} > Cr^{3+} \approx Cu^{2+} > Fe^{3+}$.

Park et al. (2002) performed both batch and column tests in removing ammonium, lead, and copper from polluted groundwater utilizing natural Greek clinoptilolite in size range of (0-0.15, 0.42-0.85, and 0-1 mm). Their experiments were focused on the design factors for permeable reactive barriers (PRBs) against the contaminated wastewater when using clinoptilolite as the reactive material. In continuous mode, high removal efficiency (above 82% except copper ions) was observed when using (0.42-0.85 mm) particle size fraction of clinoptilolite.

Bolan et al. (2003) conducted experiments regarding the commercial removal of ammonium ions from fellmongery wastewater stream using HCl-pretreated New Zealand clinoptilolite with particle size of 2mm. They observed that the clinoptilolite samples can hold a potential cation exchange capacity of 18.7 to 20.1 g of NH_4^+/kg of zeolite, and the adsorption of ammonium ions increases with the increase in ammonium concentration in wastewater stream. However, the presence of other competing ions in the fellmongery wastewater interfered with ammonium removal. They also studied the regeneration of cation-loaded clinoptilolite with 0.5 M of HCl, and found that even after 12 cycles of regeneration, the amount of NH_4^+ adsorbed remained unaffected.

Inglezakis and Grigoropoulou (2003) investigated the modeling of lead ion exchange in both batch and column (upflow) mode operations using natural Greek clinoptilolite with particle size range of (1.14-1.18 mm). The operations made under ambient temperature and initial concentration of lead of 0.01N at pH of 4, and the

effect of flow rate was studied (5, 10, and 15 BV/h). They determined both the total exchange capacity (Q_T) of clinoptilolite in column and the solid-phase diffusion coefficient of lead to clinoptilolite, in which values of (0.21-0.43 meq Pb^{2+}/g of clinoptilolite) and ($1.08x10^{-12}$-$5.45x10^{-12}$ m^2/s), respectively, were estimated. They concluded that the capacity and diffusion coefficient are flow dependent. They stated that ion exchange and adsorption in fixed bed operations are susceptible to the contact time where increasing the contact time will lead to a higher ion exchange capacity and a lower solid diffusion coefficient.

Turan and Celik (2003) studied the removal of ammonia from drinking water and the regenerability of the zeolite used in batch and column applications, employing natural Turkish clinoptilolite mined in Gördes-Manisa with particle range of (1-2, and 2-2.8 mm). The finer particles exhibit greater exchange capacity than the coarse ones, and the authors attributed it to higher specific surface area of fine particles. The regeneration of clinoptilolite was made using solution consisting of 30g/L NaCl and 1.5g/L NaOH at pH value of 11.5, and twice-regenerated clinoptilolite showed the best performance compared to others. They explained the reason as the specific surface area of clinoptilolite increased in the first and second regeneration, and began to decrease in third regeneration.

Rahmani et al. (2004) studied the factors effecting on the efficiency of ammonia removal from wastewater using pretreated Iranian clinoptilolite of particle size range of (0.42-0.589, 0.589-0.84 mm) both in batch and column mode. They found that the average ion exchange breakthrough capacity of clinoptilolite in continuous system were between 16.31 and 19.5 mgNH_4^+/g of zeolite, and the selectivity of cations were ranked as: $K^+ > NH_4^+ > Na^+ > Ca^{2+} > Mg^{2+}$. They also studied the regeneration of the clinoptilolite after usage in removal of ammonium and observed high level of regeneration (95-98%) with NaCl solution.

Sarioglu (2005) investigated the removal of ammonium ions from municipal wastewater in both batch and column mode using natural Turkish clinoptilolite

mined from Dogantepe-Amasya with particle size range of (1-2 mm). In column studies, the effects of flow rate, pH, initial ammonium concentration (C_o), washing with acid and regeneration on the ammonium adsorption capacity of clinoptilolite were verified. He found that increasing initial ammonium nitrogen concentration from 5.0 to 12.0 mg/L, increased the total adsorption capacity from 0.70 to 1.08 mg NH_4^+-N/g. Highest adsorption capacities were obtained at flow rate of (0.5ml/min) and pH of 4, as (1.08 mg NH_4^+-N/g), and highest adsorption capacity attained with acid-washed sample was determined to be (1.32 mg NH_4^+-N/g) and cation exchange capacity of Dogantepe zeolite was found to be (1.646 meq/g of zeolite).

Aşiroğlu (2006) studied the simultaneous removal of lead and ammonium ions in batch and column mode using natural Turkish clinoptilolite mined in Gördes-Manisa with particle size range of (0.25-0.5 mm). In column mode experiments, the binary and ternary studies were made under total initial feed concentration of 0.01 N, under pH range of (4-6) with different flow rates of (8, 15, and 30 mL/min). The experiments revealed the total capacity, in binary column experiment, for Pb^{2+} and NH^{4+} as 1.09 and 1.16 (meq/g of zeolite) respectively. The results showed that clinoptilolite had more affinity to Pb^{2+} ion than NH^{4+} ion when they were together in column ternary system, and yielded the order of clinoptilolite cation selectivity sequence as: $Pb^{2+} > NH^{4+} > Na^+$. In addition, he concluded that removal efficiency of Gördes clinoptilolite for both lead and ammonium decreased with increasing flow rate in ternary column operations.

Cincotti et al. (2006) studied the performance for heavy metals: lead, cadmium, copper, and zinc, removal from wastewater, both in batch and column mode, utilizing Na-pretreated natural Italian clinoptilolite. In column mode experiments, breakthrough curves obtained were compared with different ion-exchange rate laws (equilibrium model, linear driving force (LDF), film model rate approximations, and Nernst-Planck model), and results showed that LDF and film model approximations better described the breakthrough behavior. The

selectivity scale of $Pb^{2+} > Cu^{2+} > Cd^{2+} \approx Zn$ based on maximum metal removal in terms of meq/L was proposed. The system for Pb^{2+} removal from aqueous solutions using clinoptilolite was selected as a potentially competitive low-cost adsorption application, from the thermodynamic point of view as well as in terms of bed volumes at breakthrough point.

Stylianou et al. (2006) studied the removal of lead, copper, and zinc from aqueous solutions in fixed column mode using fine particles (2-5 mm) of natural zeolite clinoptilolite. They used different volumetric flow rates; 5, 7, and 10 BV/h under constant normality of 0.01N and constant room temperature. They observed that the removal efficiency increased with decreasing the flow rate and found a selectivity series of: $Pb^{2+} > Zn^{2+} \geq Cu^{2+}$. Also, they performed a conductivity measurement and proved that lead removal by clinoptilolite followed mainly ion exchange mechanism.

Karadag et al. (2006) and Salatali et al. (2007) studied the removal of ammonium in aqueous solution using Turkish natural zeolite clinoptilolite. In both studies, the effect of temperature on the removal was examined, and it was shown that increasing temperature resulted in a decrease of ammonium removal efficiency concluding that the uptake of ammonium onto clinoptilolite is controlled by an exothermic process with a negative $\Delta H°$ and $\Delta S°$ values. In addition, they stated that ion exchange process is spontaneous with a negative $\Delta G°$ value.

Inglezakis et al. (2007) studied the effect of temperature and pH of the aqueous solution on the removal of lead using natural Greek clinoptilolite in size range of (1.4-1.7 mm). They observed an increase in lead removal with increasing temperature. Also, they stated that the adsorption of lead increased with an increase in pH value of the solution from 1 to 4.

Medvidović et al. (2007) investigated the effect of flow rate (down-flow) in column mode when removing lead ions from aqueous solutions utilizing natural Serbian clinoptilolite with particle size range of (0.6-0.8 mm). Experiments were made with

initial influent concentration of 1.024 mmol/L of Pb^{2+}, under isothermal conditions (20°C), constant bed depth of 40 mm (2.9 g = 4.5 cm^3 of the clinoptilolite), and the effect of different flow rates (1, 2 and 3 mL/min) were examined. Maximum values of column efficiency (η_c = 0.78) and breakthrough capacity (Q_B = 0.433 mmol Pb^{2+}/g of clinoptilolite) were found at flow rate of 1.0 mL/min; and maximum values of height of the exchange zone (h_z = 2.42 cm), and total exchange capacity (Q_T = 0.594 mmol Pb^{2+}/g of clinoptilolite) were found at flow rate of 3 mL/min. Results showed that the capacities of the breakthrough and exhaustion points do not change significantly with the increase of the flow rate, while the time needed for reaching the breakthrough point decreased with higher values of the flow rate, and consequently, at higher flow rates, the same volume of the lead ions solution can be treated in a significantly shorter time. Also, the difference between Q_B and Q_T increases with increasing flow rate, and thus negligibly decreases the column efficiency η_c. Finally, the parameters of the Yoon-Nelson model have been used for scaling up the bed depth of the column system, and a reasonable agreement of experimental and predicted breakthrough curves was been obtained.

Miladinovic and Weatherley (2007) studied the removal of ammonium from wastewater in which colonies of nitrifying bacteria are cultivated, by combining nitrification and ion exchange in column system using Na-pretreated natural New Zealand clinoptilolite and mordenite with particles size range of (0.5-0.71, 0.71-1, and 1-1.4 mm). In the study, the ion-exchange breakthrough behavior of the natural zeolites, clinoptilolite and mordenite, in the presence of nitrifying bacteria was compared. They observed that in the presence of nitrifying bacteria, the breakthrough capacities of columns for both mordenite and clinoptilolite were enhanced and the fractional enhancement of breakthrough capacity for clinoptilolite was greater than in the case of the mordenite: 50% for clinoptilolite and 36% for mordenite.

Stylianou et al. (2007) investigated the removal of lead, copper, and zinc from aqueous solutions using natural Greek clinoptilolite with particle size range of (2-5

mm). Column experiments were done with different flow rates of (5, 7, and 10 BV/h), under a total normality of 0.01N, at initial pH of 4 and ambient temperature. Results showed that the removal efficiency increased when decreasing the flow rate and the selectivity order for removal was obtained as: $Pb^{2+} > Zn^{2+} \geq Cu^{2+}$. The authors performed a conductivity measurement and concluded that lead removal followed mostly ion exchange mechanism, whereas copper and zinc removal followed ion exchange and sorption mechanism as well.

Hedström and Amofah (2008) investigated ammonium removal from on-site sanitation system wastewater in column mode using natural Turkish clinoptilolite mined in Manisa-Gördes with large particle size range of (4-8, and 7-15 mm). The pH of experiments was adjusted between 7 and 7.5; the initial ammonium concentrations in influents were 20, 21.6, and 27.6 mg NH_4^+-N/L; and flow rates were 8, and 11.5 mL/h. It was shown that ammonium adsorption on clinoptilolite increased with decreasing grain size, and highest adsorption capacity was (2.7 NH_4^+-N/g of clinoptilolite) when using (4-8 mm) grain size, (8 mL/min) flow rate, and (20 mg NH_4^+-N/L). In all experiments, breakthrough capacity occurred immediately due to relatively high flow rate and grain size. The clogging in the column was extensive cause by particles in effluent wastewater and by microbiological growth on the clinoptilolite.

Jorgensen1 and Weatherley (2008) studied the continuous removal of ammonium ions and other ionic pollutants from wastewater in column mode using natural clinoptilolite mined in California with particle size range of (0.5-1.0 mm). The effects of interfering species in wastewater, including: the organic compounds citric acid, phenol, hexane, glucose, natural sunflower oil and whey protein, upon the column breakthrough behavior were studied. Also, the effect of regeneration on the ion-exchange performance over a number of uptake/regeneration cycles was examined. The experiment results show that the presence of citric acid had only a minute effect on column breakthrough capacity, and the column performance in the

presence of whey protein is slightly enhanced. Moreover, the column uptake performance is significantly enhanced after regeneration over the first four to five cycles of regeneration until a stable exchange performance is achieved.

Karadag et al. (2008) studied the removal of ammonium from sanitary landfill leachate both in batch and column using Na-pretreated natural Turkish clinoptilolite mined in Gördes-Manisa, with size range of (0.6-1.2 mm). The effects of pH (6.5, 7.5, and 8.3), flow rate (6.8, 11, and 21 mL/min), ammonium concentration (100, 200, and 400 mg/L) and competitive cations on the elimination efficiency were investigated. Maximum ammonium exchange capacity (16.32 mg NH_4^+/g of clinoptilolite) was achieved at pH=7.5, and high removal efficiency was observed utilizing low flow rate and low initial ammonium concentration. Analyzing the breakthrough data was made using Thomas model, and the fitting of column data was examined using nonlinear least square method. Also, the authors concluded that ammonium capacity obtained in column was higher than in batch system, and the competitive cation effect was more obvious lower ammonium concentration and higher cation concentrations.

Karadag et al. (2008) explored the removal of high concentration ammonium ions from municipal landfill leachate in column (up-flow and fluidized-bed) mode by the exploit of natural Turkish clinoptilolite mined in Gördes-Manisa, with size range of (0.6-1.2 mm). All experiments were conducted at room temperature and influents at pH of 7.5 and effects of different flow rates (6.8, 11, and 21 mL/min) and different influent initial ammonium concentrations (100, 200, and 400 mg/L) on breakthrough curves were examined. The results showed that lower flow rates resulted in higher removal performance (49.61%), and lower ammonium concentrations resulted in higher effluent volumes and removal rates (60.12%). In addition, the models of Yoon-Nelson and Clark (models developed to describe the breakthrough curves in column method) were used to question the breakthrough behavior of the fixed and fluidized beds and the outcome show that the Clark model is better for modeling the

experimental data. As the results revealed that individual ion exchange is insufficient to decrease high ammonium concentrations to desirable levels, air stripping was performed as a pretreatment step prior to ammonia exchange decreasing the leachate ammonium concentration from 3000 to 400 mg/L. Accordingly, authors reveled that combining ammonia stripping and an upflow fixed-bed system is practical in reducing higher ammonium concentrations to acceptable levels.

Medvidović et al. (2008) conducted a study regarding the kinetics for the removal of lead ions from aqueous solutions in column mode using natural Serbian clinoptilolite with particle size range of (0.6-0.8 mm). They compared the breakthrough curves obtained from experimental results with the results obtained from the kinetic equation developed by Clark via means of linear and non-linear regression analysis. The total lead removal of lead (for all examined initial concentrations) was estimated as (89.50-95.66%), and testing these experimental results with Clark kinetic equation sowed excellent fitting both in linear and nonlinear methods of solving. They concluded that Clark equation can be used for predicting of the shape of breakthrough curves for a restricted examined interval of experimental conditions.

Perić et al. (2009) studied the effect of zeolite fixed bed depth on the removal of lead from aqueous solutions in column (down-flow) mode method using natural Serbian clinoptilolite with particle size range of (0.6–0.8 mm). The experiment were made under isothermal temperature (23°C) with clinoptilolite bed depth of (40, 80, and 120mm) and flow rates of (1, 2, and 3 mL/min) with constant initial lead concentration (C_o=1.026 mmol/L). Experiments' outcome showed that increasing bed depth delay the breakthrough point and exhaustion point, and increase the contact time of the clinoptilolite-lead solution, and the height of the mass transfer exchange zone height (h_z). The results gained from experiment were tested using the bed depth-service time (BDST) kinetic model (derived by Bohart and Adams) in order to predict the time needed for exceeding the defined effluent concentration for

a constant bed depth. Equation derived from the breakthrough curves gave modeled linear equations used for calculation of (h_z). Authors found that increasing the flow rate increased (h_z), indicating that the zeolite–solution contact time is not sufficient as a result of the affect of axial dispersion on mass transfer on the solid-liquid interface.

Mažeikienė et al. (2010) investigated experimental ammonium ion removal from drinking water using natural clinoptilolite with size range of (0.3-0.6, and 0.6-1.5 mm). Initial influent ammonium concentration was 2 mg/L and initial pH was 7.5. The solution was filtrated through an experimental filter column packed with clinoptilolite. The results indicated that the removal of ammonium was more efficient using a finer fraction (0.3-0.6 mm) of clinoptilolite.

Šiljeg et al. (2010) studied the removal of ammonium from ground water using Na-pretreated form of natural clinoptilolite samples from Croatia and Serbia. The complete ammonium removal, with the use of both clinoptilolite types was achieved during 20 h. The clinoptilolite samples were regenerated with the use of 2 mol/L NaCl, and reused for calculation of ammonium sorption efficiency and the regenerated samples showed to be still very efficient for ammonium removal in which the ammonium removal increased and reached nearly 100%. Moreover, the Serbian clinoptilolite was shown as superior for ammonium removal in comparison to the Croatian clinoptilolite and therefore be effectively used for efficient ammonia removal from ground waters.

Tao et al. (2010) compared the capability of Na-form of natural Chinese clinoptilolite (52-61 μm particle size) to selectively remove Pb^{2+} ions from aqueous solutions containing salt, glycine, and nitrosamines; with other porous materials such as zeolite NaZSM-5 and activated carbon. Clinoptilolite revealed the highest potential in adsorbing lead ion in the solution at temperature of 37°C achieving the capacity of 7 mg Pb^{2+}/g of clinoptilolite, two times more than that by zeolite NaZSM-5 and six times over that by activated carbon.

CHAPTER 4

EXPERIMENTAL WORK

4.1 Characterization of Clinoptilolite

The clinoptilolite samples which are used throughout the studies is originated from Gördes-Manisa in Western Anatolia region of Turkey and obtained from Mineral Research and Exploration Institute (MTA) in Ankara.

The clinoptilolite samples as received were crushed and sieved into the desired 0.25-0.5 mm (or 60-35 ASTM E-11) using an Octagon 200 shaker instrument. The selection of the particle size range relied on previous different ion exchange studies (Abusafa, 1995; Tufan, 2002; Gül, 2003; Aşiroğlu, 2006). Afterwards, the samples were washed with deionized water to remove surface dust, and then dried in an oven for 24 hours at 70°C to be followed with the pretreatment procedure.

In order to verify the clinoptilolite mineral identity, Scanning Electron Microscopy (SEM) analysis was performed via Scanning Electron Microscopy (SEM) instrument for morphology in Central lab of METU. In addition to that, X-ray diffraction (XRD), thin section analysis, thermal gravimetric analysis (TGA), the specific surface area of clinoptilolite by BET area analysis, and pore size distribution by mercury porosimetry of the clinoptilolite sample of studies of Tufan (2002) were considered, given that clinoptilolite samples and clinoptilolite particle size range used in this study were from the same batch of Tufan's study (Tufan, 2002). The chemical composition of original and Na form of clinoptilolite was determined with

X-ray Fluorescence analysis performed at Central Lab of METU. Founded on chemical composition, theoretical cation exchange capacity (TEC) and Si/Al ratio of Gördes clinoptilolite were also calculated.

4.2 Reagents

All chemicals used in the experiments were analytical grade reagents and obtained from J.T.Baker and Acros. The aqueous solutions of Pb^{2+}, NH_4^+ and Na^+ ions were prepared by dissolving pure $Pb(NO_3)_2$, NH_4Cl and NaCl in doubly deionized water having a conductivity of 18 μS/cm.

4.3 Pretreatment of Clinoptilolite

Prior to the ion exchange process, the pretreatment process was done in order to improve the effective exchange capacity (EEC) of the clinoptilolite, and by doing that, improving the performance of the ion exchange process.

The original form of Gördes clinoptilolite contains exchangeable cations such as K^+, Na^+, Mg^{2+}, and Ca^{2+}. It was attempted to replace these cations by Na^+ ion to prepare a near homoionic form of clinoptilolite and to improve the effective ion exchange capacity (EEC).

A common pretreatment procedure is the use of ion exchange packed beds. The modus operandi consisted of the following steps:

1. The homoionic sodium for of clinoptilolite was obtained by passing a certain volume of sodium chloride solution (V_{NaCl} = 150 BV), with a concentration of (C_{NaCl} = 1.5 mol/L), through a column of height of (h_c = 60 cm) and diameter of ($Ø$ = 2.0 cm), over a certain amount of packed clinoptilolite with mass (M_z = 10 gm) forming a bed height of (h_T = 3.0 cm) in the column in which the

bed volume (BV) was equal to 9.425 mL. The NaCl solution was pumped with volumetric flow rate of ($\hat{O}$ = 25 BV/h), from a feed reservoir in down flow current mode. The process was done at regular ambient temperature (25°C).

2. Samples were taken from the effluent at different time intervals in order to measure the concentrations of the exchangeable cations released by the clinoptilolite in the solution and the analysis were done using atomic absorption spectrophotometer (AAS) and flame photometer.

3. A certain volume of de-ionized water (V_w = 20 BV) was passed through the column in order to remove the excess of sodium chloride from the clinoptilolite structure. The washing process continued till no chloride ion was detected when a drop of 1% $AgNO_3$ was introduced to the effluent.

4. The clinoptilolite sample was then dried in a furnace at 70°C for time period of 24 hours.

5. Clinoptilolite samples were sieved again to avoid the presence of any broken particles with smaller sizes resulted during the pretreatment process.

6. Finally, the treated clinoptilolite was kept in a desiccator containing saturated NaCl solution in order to ensure constant moisture content, being ready for further use.

These mentioned values used in the pretreatment process were achieved through considering many studies in literature and many different experimental trials until the most optimized values were achieved (Czárán et al, 1988; Milan et al., 1997; Inglezakis et al., 2001; Zorpas et al., 2002; Rahmani et al., 2004; Inglezakis et al., 2004; Sprynskyy, 2006).

4.4 Column Studies

Column studies included both binary and ternary studies. In both studies, the ion exchange experiments were conducted using a column of 1.0 cm in diameter ($\emptyset$) and 15.0 cm in height (h_c). The column was loaded with 5 g of clinoptilolite (M_z), with 0.25-0.5 mm particle size diameter range (D_p) of near homoionic Na form of clinoptilolite sample. The packed bed height (h_T) was 8.3 cm with bed volume (BV) of 6.52 mL. The feed solution was pumped from a feed tank throughout the clinoptilolite loaded column in down flow mode at different flow rates, using a Cole Parmer Masterflex L/S model peristaltic pump. Effluent samples from the column were collected at periodic volume intervals corresponding to the discharge of certain volumes of treated solution in order to determine the concentration of ions in the effluent.

In all studies, the ion exchange process was stopped when the cation concentration in the effluent (C) became equal to the initial concentration in the influent (C_o) in which the exhaustion of clinoptilolite bed is reached (C/C_o=1.0) and breakthrough curves were established. During breakthrough analysis, the breakthrough concentration for the exchanged cations studied was taken as 5 % of the initial influent concentration.

A schematic of the equipments employed in the ion exchange experiments is presented in Figure 4.1. The column and the clinoptilolite bed specifications are given in Table 4.1.

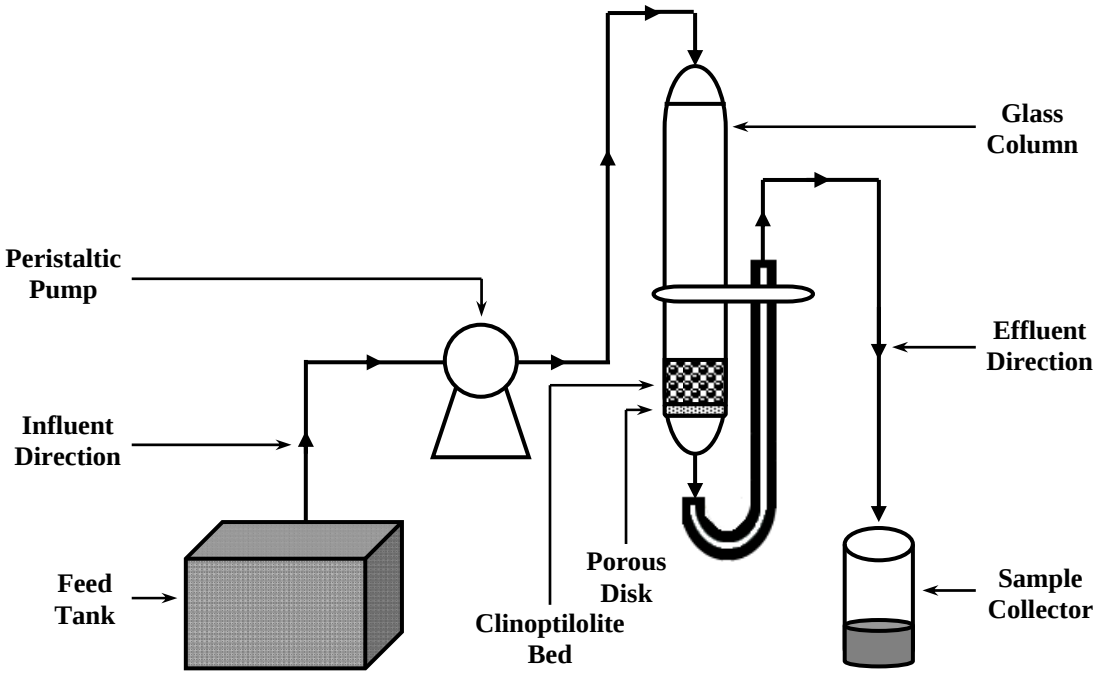

Figure 4.1. Schematic Representation of Experimental Setup

Table 4.1. The Column and the Clinoptilolite Bed Specifications Used in Experiments

Column height (h_c)	15.0 *cm*
Column diameter ($Ø$)	1.0 *cm*
Mass of clinoptilolite packed in column (M_z)	5.0 *gm*
Mean clinoptilolite bed height in column (h_T)	8.3 *cm*
Clinoptilolite particle diameter range (D_p)	0.25 - 0.5 *mm*
Clinoptilolite bed volume in column (BV)	6.52 *mL*

4.4.1 Binary Studies

In binary studies, the inspection of Pb^{2+} and NH_4^+ removal on Na-form of clinoptilolite was carried out on the Pb^{2+} and NH_4^+ cation containing solutions. The solutions used in the experiments were prepared by dissolving $Pb(NO_3)_2$ and NH_4Cl salts in doubly deionized water. A set of experiments were carried out with different flow rates ($\hat{O}$) of 8, 16, and 32 mL/min (corresponding to 73.6, 147.3, and 294.5 *BV/h*) through the column to investigate the effect of flow rate in column for the Pb^{2+}-Na^+ and NH_4^+-Na^+ binary systems.

Another set of experiments were done with different influent concentrations of 0.005, 0.01, and 0.02 total normality for both cations (corresponding to: 518, 1036, and 2072 ppm for Pb^{2+} cations; 90, 180, and 360 ppm for NH_4^+ cations), in order to examine the effect of the initial feed concentration on the breakthrough curve behavior. The flow rate during all these experiments was 8 mL/min as this loading flow was found to be giving the highest exchanging results based on binary flow rate examining studies.

All experiments were carried out at isothermal conditions (T=25 ± 2° C), and the initial pH value throughout the studies was adjusted between 4 and 6, using HNO_3 and NaOH solutions.

4.4.2 Ternary Studies

Ternary column experiments were carried out similar to experiments conducted in binary column experiments. Nevertheless, foremost difference between binary and ternary column experiments is that feed solution used in ternary system included two species: Pb^{2+} and NH_4^+. Therefore, the studies involved the simultaneous ion exchange for Pb^{2+}-NH_4^+-Na^+ to observe the effect of flow rate and initial feed solution concentration on the breakthrough capacity.

To observe the effect of flow rate, a set of experiments was carried out with different flow rates ($\hat{O}$) of 8, 16, and 32 mL/min (corresponding to 73.6, 147.3, and 294.5 *BV/hr*) through the column for Pb^{2+}-NH_4^+-Na^+ ternary system. The total normality of the solutions used was 0.01 N, i.e. 0.05 N of Pb^{2+} and 0.05 N of NH_4^+ corresponding to 518 ppm of Pb^{2+}, and 90 ppm of NH_4^+.

Another set of experiments were done with different influent concentrations of Pb^{2+} and NH_4^+ cations in order to examine the effect of initial feed concentration on the breakthrough curve behavior; however, the total normality of the solutions was kept at 0.01 N. The influent concentration of cations in these studies changed between 0.0025, 0.005, and 0.0075 N (corresponding to: 259, 518, and 777 ppm of Pb^{2+}; 45, 90, and 135 ppm of NH_4^+). In these experiments, the ratio of Pb^{2+}/NH_4^+ concentrations where: 1/3, 1, and 3. The flow rate during all these experiments was 8 mL/min as this loading flow was found to be giving optimum exchanging results based on ternary flow rate examining studies.

All experiments were carried out at isothermal conditions (T=25 ± 1° C), and the initial pH value throughout the studies was adjusted between 4 and 6 using HNO_3 and NaOH solutions.

The experimental parameters examined ion exchange process for both binary and ternary studies are summarized in Table 4.2. and Table 4.3.

Table 4.2. Experimental Parameters for Binary Studies

Observation	**Pb^{2+} Concentration in Feed (*N*)**	**NH_4^+ Concentration in Feed (*N*)**	**Flow Rate (*mL/min*)**
Effect of Flow Rate	0.01	0.00	8
	0.01	0.00	16
	0.01	0.00	32
	0.00	0.01	8
	0.00	0.01	16
	0.00	0.01	32
Effect of Feed Concentration	0.005	0.00	8
	0.01	0.00	8
	0.02	0.00	8
	0.00	0.005	8
	0.00	0.01	8
	0.00	0.02	8

Table 4.3. Experimental Parameters for Ternary Studies

Observation	**Pb^{2+} Concentration in Feed (*N*)**	**NH_4^+ Concentration in Feed (*N*)**	**Flow Rate (*mL/min*)**
Effect of Flow Rate	0.0050	0.0050	8
	0.0050	0.0050	16
	0.0050	0.0050	32
Effect of Feed Concentration	0.0025	0.0075	8
	0.0050	0.0050	8
	0.0075	0.0025	8

4.4 Analysis

The analysis of the samples examined throughout the experiments was made through different instruments. The concentration of Na^+ and K^+ were determined using a flame photometer (Janway Model PFP7). The concentration of Ca^{2+}, Mg^{2+} and Pb^{2+} were determined using flame atomic absorption spectrophotometer (Shimadzu AAS Model: AA-6300 - P/N 206-51800). The absorption of each solution using AAS were measured at the wavelength that corresponds; Ca^{2+}: 422.7nm, Mg^{2+}: 285.2 nm and Pb^{2+}: 283.3 nm. For lead analysis, extra pure $Pb(NO_3)_2$ was used to prepare the stock solutions for lead and the instrument was calibrated by measuring the absorbance of four standard solutions in the concentration range of 2 mg/L to 10 mg/L. For ammonium concentration determinations, combination ammonium ion selective electrode (Sentek Model: 3051) was used. The calibration for ammonium electrode is given in Appendix A. All measurements were estimated out in duplicates and mean values were used in the analysis of data.

CHAPTER 5

RESULTS AND DISCUSSION

5.1 Characterization of Clinoptilolite

The original clinoptilolite batch samples were crushed, washed, dried, and sieved into the desired particle size range (0.25 - 0.50 mm) as it is shown in Figure 5.1. Afterwards, the samples were washed again to remove the surface dust and pretreated with NaCl solution to be converted to the Na-form then, and finally dried and preserved in a desiccator filled with saturated NaCl solution for further use. All experiments during this study were performed using the selected size range of clinoptilolite mentioned above.

(i) **(ii)**

Figure 5.1. Clinoptilolite Zeolite: i) Larger Particle Size (>1 mm), ii) Smaller Particle Size (0.25-0.50 mm).

Different thesis studies related to the ion exchange process in clinoptilolite were made previously using the same clinoptilolite sample used in this study; hence, the mineralogical characterization of the zeolite has already been done.

X-ray diffraction (XRD) pattern for Gördes clinoptilolite sample given by Tufan (Tufan, 2002) is shown in Figure 5.2. As seen in the figure, characteristic clinoptilolite peaks in the XRD pattern are indicated. The data were compared with International Center for Diffraction Data and the clinoptilolite peaks were recognized (Tufan, 2002; Aşiroğlu, 2006).

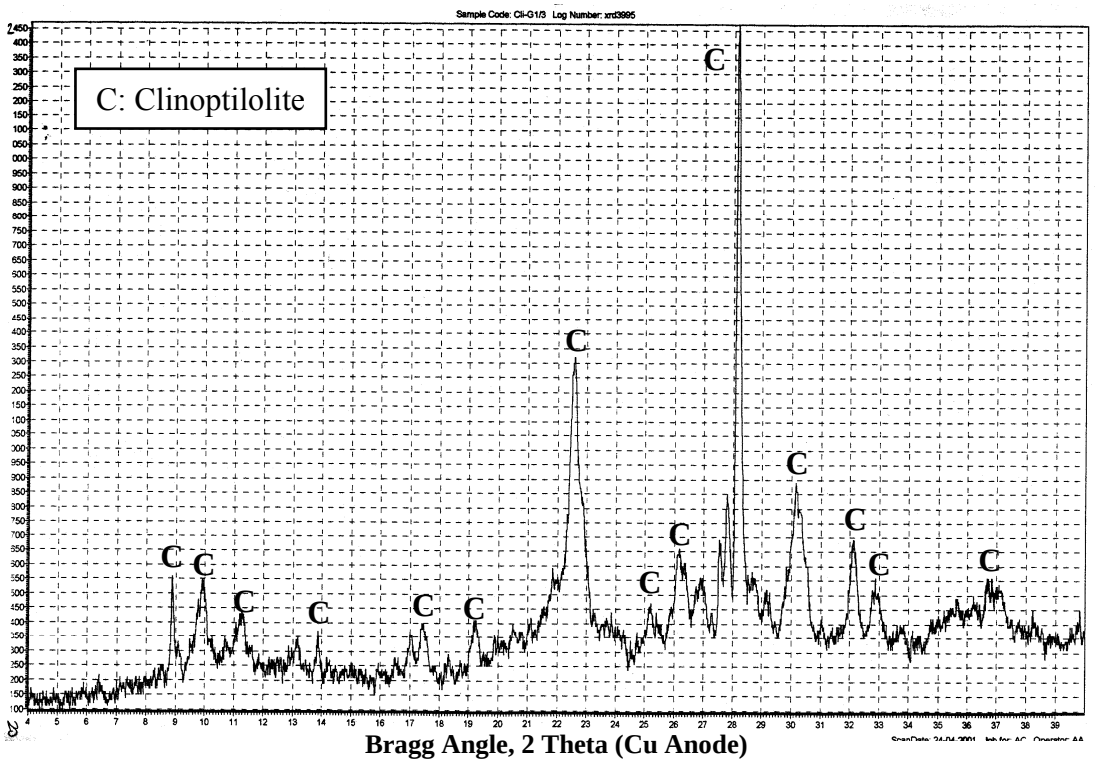

Figure 5.2. X-Ray Diffraction Patterns of Gördes Clinoptilolite for 0.25-0.5 mm (Tufan, 2002)

According to X-ray pattern (Figure 5.2.) even though there are some crystalline impurities, the zeolite consisted mainly of clinoptilolite. The approximate percentages of these species were determined by thin section analysis and found that 95±1 % of the sample is composed of clinoptilolite, and the rest is small amounts of quartz, feldspar, biotite and rock fragments (quartz: 3±0.3 %, feldspar: 2±0.2 %, biotite: 0.4±0.3 %, and rock fragments: 0.25±0.5 %) (Tufan, 2002; Gül, 2003).

In addition to X-ray diffraction, SEM analysis was also performed to analyze the morphology of clinoptilolite sample. As a result, typical coffin-shaped crystal structure was observed. Scanning electron micrograph of original Gördes clinoptilolite is given in Figure 5.3.

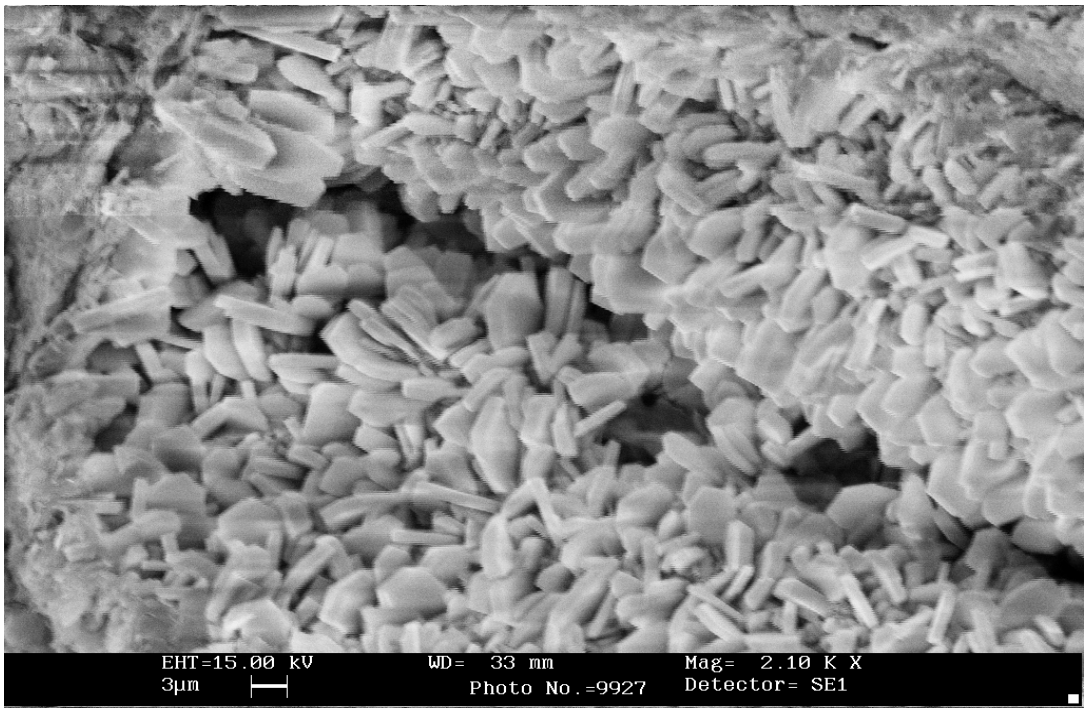

Figure 5.3. Scanning Electron Micrograph (SEM)
of Original Clinoptilolite Sample (Aşiroğlu, 2006)

Thermal gravimetric analysis on Gördes Clinoptilolite sample according to Tufan (2002), showed that during the heating of the sample up to 1000° C, clinoptilolite loses its water till 400° C, and after that, the clinoptilolite sample weight maintains almost constant.

By BET area analysis, the surface area (a_s) of clinoptilolite was estimated approximately as 38.3 m^2/g (Tufan, 2002).

In addition, according to the result of pore size distribution, the solid density (ρ_s), and the porosity (ε) of clinoptilolite were estimated as 2.21 g/L, and 36%;

respectively (Tufan, 2002). Gedik and Imamoglu (2008) estimated the specific surface area, the porosity, and the average pore diameter of original Gördes clinoptilolite as 36.9 m^2/g, 2.27 g/L, and 17.5 Å; respectively.

Chemical composition of original clinoptilolite sample obtained with Lithium Metaborate Fusion Dissolution Method analysis is presented in Table 5.1. According to the table, Si/Al ratio of original sample was calculated as 5.2, which is in the typical range of 4 to 5.5 given for clinoptilolite zeolite (Tsitsishvili et al., 1992). The theoretical exchange capacity (TEC) of the clinoptilolite sample based on aluminum content, which is the total sum of the zeolite free cations, measured according to equation 2.1 as stated in ion exchange theory section, was calculated as 2.3 meq/g of zeolite. This value agrees with the results obtained in previous studies utilized the same clinoptilolite sample used in this study (Tufan, 2002; Moralı, 2006; Aşiroğlu, 2006, Bayraktaroğlu, 2006)

Table 5.1. Chemical Composition of Original Clinoptilolite Sample

Component	**% Weight**	**Mole/100 g**	**Exchangeable Cations (*meq/g*)**
SiO_2	68.21	1.1352	
Al_2O_3	11.22	0.1078	
Fe_2O_3	2.39	0.0149	
MgO	0.90	0.0223	0.4466
CaO	2.10	0.0374	0.7490
Na_2O	0.60	0.0096	0.1936
K_2O	4.30	0.0456	0.9129
MnO	0.08	0.0011	
TiO_2	0.10	0.0012	
P_2O_5	0.02	0.0001	
H_2O	7.25	0.4028	
LOI*	10.02		

(*) Loss of ignition

5.2 Effect of Pretreatment on Clinoptilolite Sample

Chemical composition of sodium form of clinoptilolite sample obtained with Lithium Metaborate Fusion Dissolution Method analysis is presented in Table 5.2. According to the table, Si/Al ratio of Na form of clinoptilolite was determined as 5.3. This means that Si/Al ratios of original and pretreated samples are in typical ranges (4-5.5) for clinoptilolite zeolite. Theoretical exchange capacity of Na clinoptilolite samples based on aluminium content was also calculated as 2.1 meq/g of zeolite.

Table 5.2. Chemical Composition of Na-form of Clinoptilolite Sample

Component	**% Weight**	**Mole/100 g**	**Exchangeable Cations (*meq/g*)**
SiO_2	68.22	1.1354	
Al_2O_3	11.19	0.1097	
Fe_2O_3	2.38	0.0149	
MgO	0.80	0.0198	0.3969
CaO	0.48	0.0085	0.1712
Na_2O	3.28	0.0529	1.1604
K_2O	2.43	0.0257	0.5159
MnO	0.08	0.0011	
TiO_2	0.10	0.0012	
P_2O_5	0.02	0.0001	
H_2O	8.70	0.4833	
LOI*	10.64		

(*) Loss of ignition

The contribution of exchangeable cations calculated from Tables 5.1, and 5.2. for original and sodium-form clinoptilolite samples are given in Table 5.3.

Table 5.3. Contribution of Exchangeable Ions to Theoretical Exchange Capacity

Clinoptilolite	**Na^+ (*eq/eq%*)**	**K^+ (*eq/eq%*)**	**Ca^{2+} (*eq/eq%*)**	**Mg^{2+} (*eq/eq%*)**	**TEC (*meq/g*)**
Original	8.90	35.69	30.01	21.70	2.3021
Na-form	48.66	20.17	6.86	19.29	2.1424

From the results shown in Table 5.3., the increase of Na^+ ion content of the clinoptilolite by rearranging other exchangeable cations (K^+, Ca^{2+}, Mg^{2+}) from zeolite structure was apparent. Semmens and Martin (1988) stated that after conditioning the clinoptilolite with NaCl, although the total exchange capacity remained unaltered; the sodium content of the pretreated samples was increased. Additionally, results verify that although Ca^{2+} was exchanged fruitfully, it was difficult to replace K^+ and Mg^{2+} ions. This can be explained as Mg^{2+} ions are robustly bonded to the clinoptilolite structure. It is proposed that K^+ is located at a site which is located in an eight-membered ring of clinoptilolite structure and has the highest coordination (six framework oxygen and three water molecules) among all the other cation sites in the unit cell (Yücel and Jama, 1990). As a result of this location and robust bonding to the clinoptilolite structure, potassium ion has low ion exchange ability.

The real exchange capacity (REC) of the clinoptilolite sample which is the amount of actual exchangeable cations of the zeolite was calculated by performing ion exchange process (batch or column mode) in which the zeolite negative charge should be totally and fully balanced by any equivalent amount of incoming cations.

Utilizing the same clinoptilolite sample, Aşiroğlu (2006) previously calculated the real exchange capacity (REC) for clinoptilolite by batch experiments as 1.16 meq/g of zeolite with respect to sodium cations. Aside from batch mode, the chemical analysis and column mode experiments in this study resulted in exchange capacity values of 1.16 meq/g of zeolite with respect to sodium cations.

In order to further investigate the effect of conditioning the clinoptilolite sample with NaCl solution, two ion exchange experiments were made using original form and Na-form of clinoptilolite. The exchange of ammonium NH_4^+ ions on both clinoptilolite samples were investigated in column mode using 5 g of clinoptilolite in each experiment. The NH_4^+ feed concentration was 0.01 N (corresponding to 180 ppm), and the flow rate of the solution passing through the column was kept as 12 mL/min (corresponding to 110.4 BV/hr).

The effect of conditioning the clinoptilolite sample on the breakthrough behavior is given in Figure 5.4. The corresponding raw data for the analysis are given in Appendix D.

It is shown in the figure that the ion exchange process when using the original form of clinoptilolite resulted in the absence of S-shaped curve; whereas the S-shaped curve is obvious when using the Na-form sample. In addition, when using the virgin form of clinoptilolite, the breakthrough point occurred immediately (4.2 BV), while the onset of the breakthrough point when using Na-form of clinoptilolite was observed after treating 50.23 BV of the ammonium solution. Furthermore, the exhaustion point of the clinoptilolite raised from 86.27 BV into 136.9 BV when using the sodium conditioned form of clinoptilolite, giving the outcome that the ion exchange process in the latter case was more effective than using the original form of clinoptilolite.

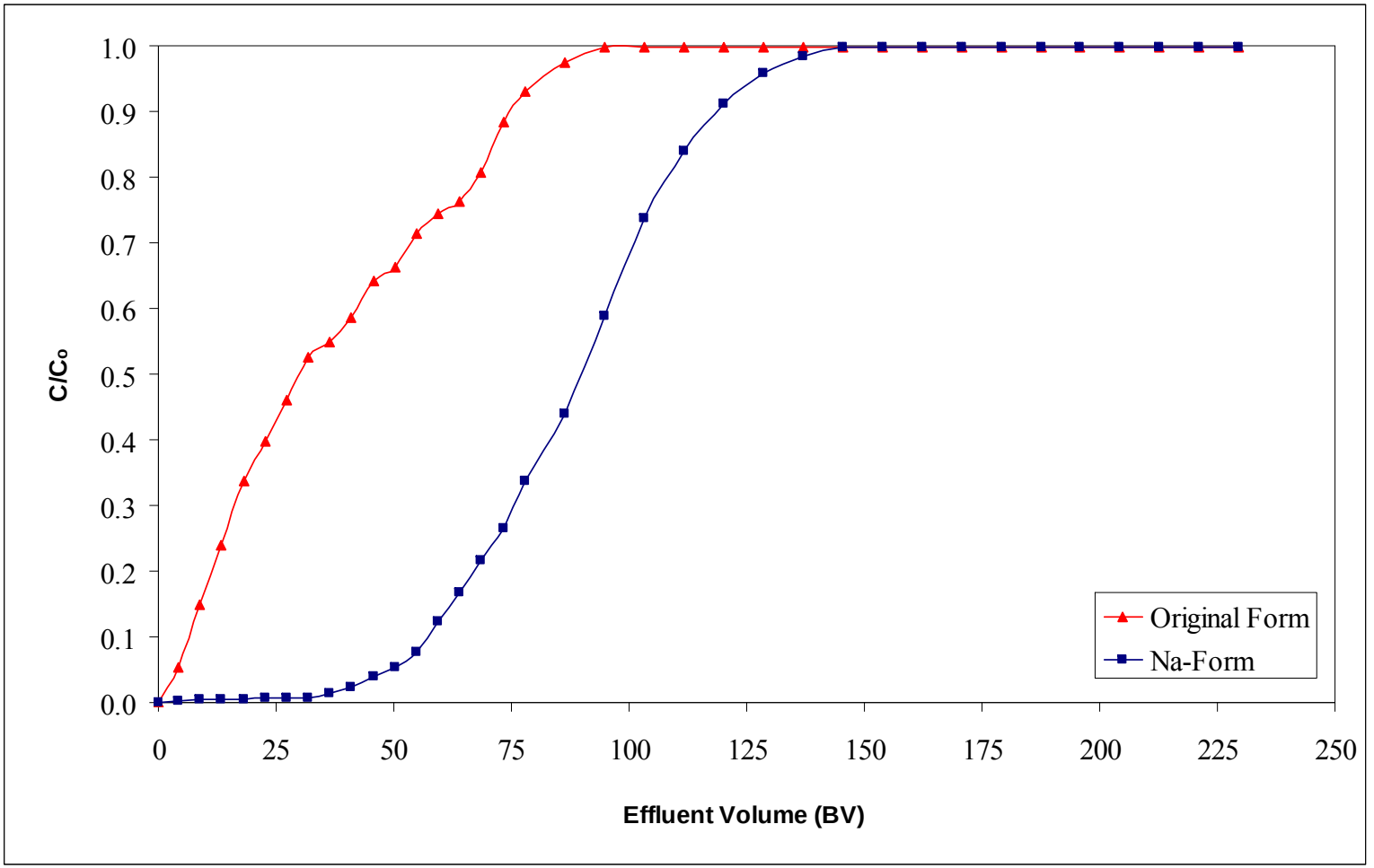

Figure 5.4. The Breakthrough Curves of NH_4^+-Na^+ System - The Effect of Pretreatment (Original and Na-Form Clinoptilolite) (C_o = 0.01 N, $\hat{O}$ = 12

The ion exchange capacities and column efficiencies for both experiments are given in Table 5.4. By comparing the results gained when utilizing the original form and the Na-form of clinoptilolite, the breakthrough capacity (Q_B) was raised from 0.054 to 0.648 meq/g of zeolite, and the total capacity (Q_T) was raised from 0.57 to 1.162 meq/g of zeolite, and the column efficiency (η_c) increased from 9.47 into 55.76 %.

Güray (1997) found that pre-treating the clinoptilolite with NaCl solution increases the performance of the clinoptilolite bed. Under the condition of influent lead concentration of 311 ppm, 250-300 mm range particle size and flow rate of 8 ml/min, she found that the breakthrough capacity (Q_B) was 0.94 meq/g of zeolite when the clinoptilolite bed in the sodium form was used, while the breakthrough capacity of the unconditioned clinoptilolite was found to be only 0.11 meq/g of zeolite.

The results show that the amount of the exchangeable ions increased with conditioning the clinoptilolite with sodium solution, and therefore enhanced the effective exchange capacity (EEC) of the clinoptilolite. Kesraoui-Ouki et al. (1993) stated that converting the clinoptilolite into sodium form improves its exchange capacity. Therefore, converting the clinoptilolite into the homoionic Na form is a vital procedure in enhancing the effective exchange capacity (EEC) of the clinoptilolite to a great extent.

Table 5.4. Results of Ion Exchange Experiments Using Original Form and Na-form of Clinoptilolite

Clinoptilolite	Q_B ***(meq/g of zeolite)***	Q_T ***(meq/g of zeolite)***	Q_z ***(BV)***	V_B ***(BV)***	η_c **(%)**
Original	0.054	0.57	82.05	4.21	9.47
Na-form	0.648	1.162	86.66	50.23	55.76

The cation exchange process between a clinoptilolite particle and the surrounding solution (for example: the exchange of NH_4^+ and Na^+ cations) is depicted schematically in Figure 5.5.

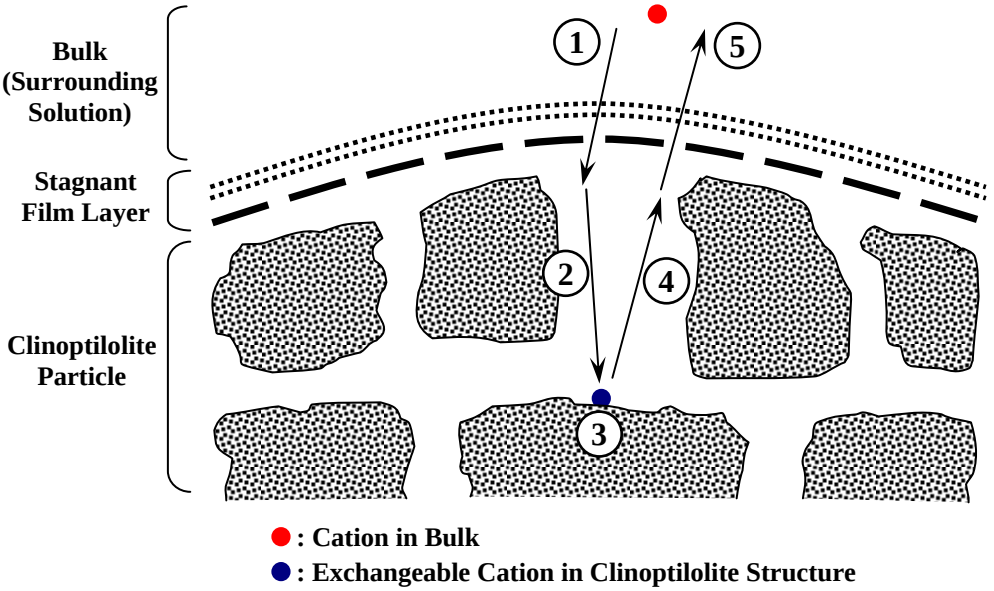

Figure 5.5. Schematic Representation of the Various Steps of the Exchange of Cations between Bulk Solution and the Clinoptilolite Particle.

The steps that may limit the exchange rate during the ion exchange process are as follows (Tufan, 2002):

1. The cation in bulk solution (i.e. NH_4^+ cation) moves towards a stagnant water layer surrounding the clinoptilolite particle, in which the NH_4^+ will face a film mass transfer resistance. The thickness of this stagnant water film depends on the prevailing hydraulic conditions of the system.

2. Intra-particle transport of NH_4^+ cations into the clinoptilolite particle. After the NH_4^+ cation moves across the stagnant film layer by molecular diffusion, it then diffuses into an exchange site inside the pores of the clinoptilolite.

3. The ion exchange process between NH_4^+ and Na^+ cations at the exchanging positions in the interior pores inside the clinoptilolite particle. This step is considered a very rapid step.

4. Diffusion of the displaced cation (i.e. Na^+ cation) out of the interior of the clinoptilolite particle (reverse of step 2).

5. Transport of Na^+ cations from the liquid-solid interface towards the bulk liquid stream (reverse of step 1).

The speed of overall process is limited by the slowest step. Usually, the slowest step of the ion exchange process in clinoptilolite is the ionic diffusion step within the clinoptilolite structure, i.e. step 2 (Tufan, 2002).

5.3 Effect of Particle Size

The selection of appropriate particle size range of clinoptilolite while conducting column ion exchange experiments is an important parameter as achieving long contact time as possible is required between the zeolite particles and the solution surrounding it is essential point. However, large particle size results in low contact time between the zeolite and the solution flowing through the column, leading to low cation exchange probability. In contrast, smaller particle size results in high flow resistance, high pressure drop, and channeling in the column (Leif and Terry, 1982; Czárán et al, 1988).

In earlier thesis studies, Abusafa (1995) and Tufan (2002) determined the most proper particle size range while performing ion exchange experiments to be in the range of 0.50 to 0.25 mm (35/60 mesh size ASTM E-11), for column systems, hence; this particle size range of clinoptilolite was chosen and used in all of the column

experiments of this study. Table 5.5. summarizes the particle size selection of previous thesis studies.

Table 5.5. The Particle Size Selection of Previous Thesis Studies

Author	Year	Particle Size Range (mesh size ASTM E-11)
Abusafa A.	1995	20 - 140
Güray Ş.	1997	30 - 60
Tufan E.Ö.	2002	35 - 60
Gül Ö.	2003	35 - 60
Moralı N.	2006	20 - 100
Aşiroğlu S.	2006	35 - 60
Bayraktaroğlu K.	2006	35 - 60

5.4 Binary Studies

In conducting ion exchange experiments in binary studies, the performance of sodium pretreated Gördes clinoptilolite for the removal of lead and ammonium cations was investigated. A particular number of column experiments were conducted to examine Gördes clinoptilolite ion exchange features for each of lead Pb^{2+} and ammonium NH_4^+ cations with sodium Na^+ cations, individually. The effects of solution flow rate and the initial concentration on the breakthrough behavior were studied for both cations.

The reproducibility of the experiments was checked for a specific run in order to determine whether the experimental results are reliable or not, and almost the same results were obtained and these are presented in Appendix C.

5.4.1 Effect of Flow Rate

The effect of flow rate (with constant feed concentration at 0.01 N) on the breakthrough curve behavior in ion exchange experiments for the exchange of lead by Na-form Gördes clinoptilolite is shown Figure 5.6, and for the ammonium exchange, is shown in Figure 5.7. The results for both systems: Pb^{2+}-Na^{+}, and NH_4^{+}-Na^{+} exchanges, are summarized in Table 5.6. The corresponding raw data for the analysis are given in Appendix D.

For lead removal, Figure 5.6. shows that by decreasing the flow rate from 32 mL/min into 8 mL/min, the breakthrough capacity (Q_B) increased by 73.7%, and the column efficiency (η_c) increased by 68.7%, while the total exchange capacity (Q_T) almost remained constant. Furthermore, the volume of effluent collected up to the breakthrough point (V_B) increased from 22.62BV to 50.23BV. The maximum capacities for both (Q_B) and (Q_T) were found at flow rate of 8 mL/min as 0.655, and 1.030 meq/g of zeolite; respectively.

For ammonium removal, Figure 5.7. shows that by decreasing the flow rate from 32 mL/min into 8 mL/min, the breakthrough capacity (Q_B) increased by 56.2%, and the column efficiency (η_c) increased by 47.6%, while the total exchange capacity (Q_T) almost remained constant. In addition, the volume of effluent collected up to the breakthrough point (V_B) increased from 13.42BV into 73.24BV. The maximum capacities for both (Q_B) and (Q_T) were found at flow rate of 8 mL/min as 0.667, and 1.164 meq/g of zeolite; respectively.

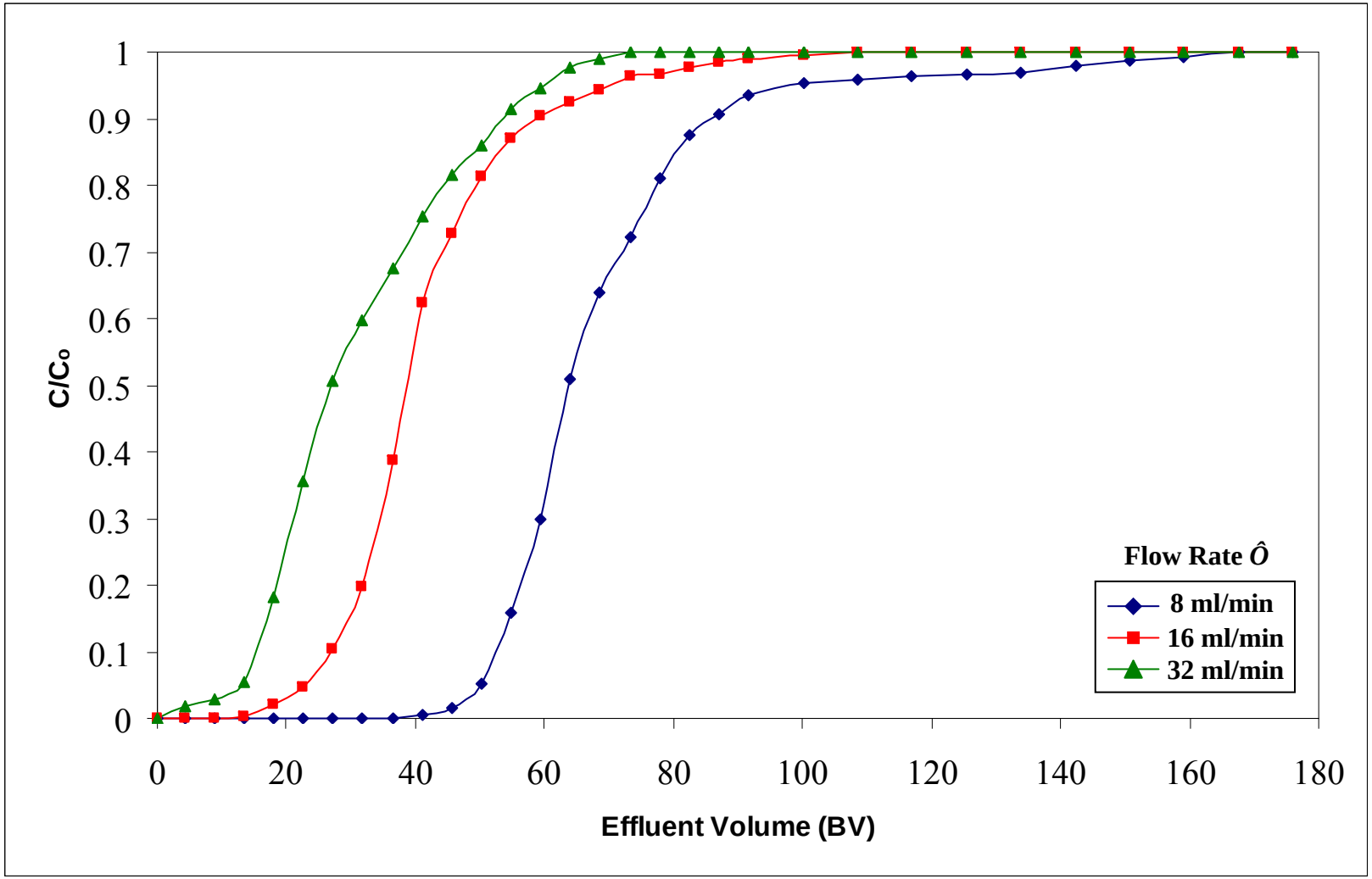

Figure 5.6. The Breakthrough Curves of Pb^{2+}-Na^{+} System - The Effect of Flow Rate (C_o = 0.01 N)

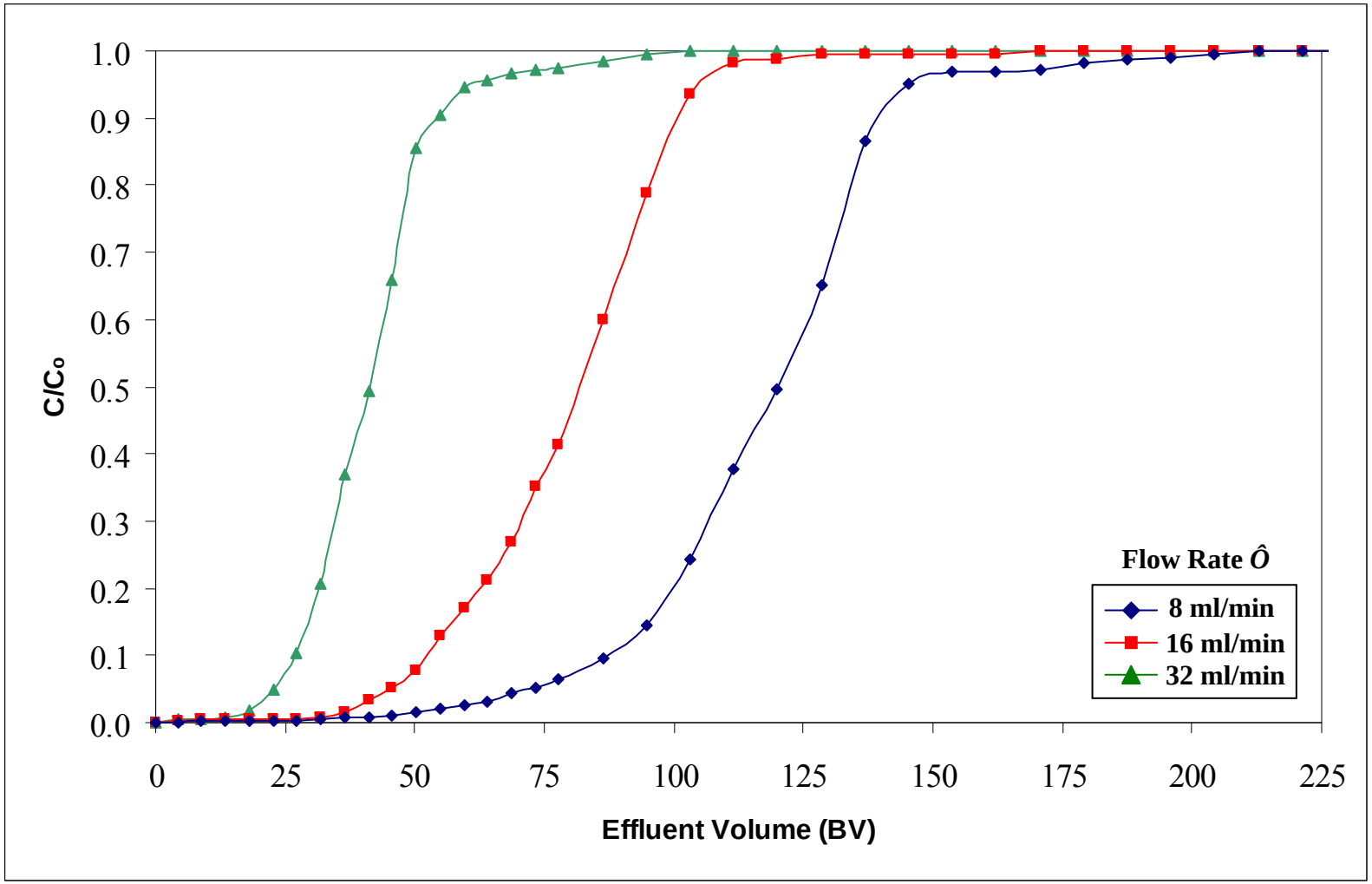

Figure 5.7. The Breakthrough Curves of NH_4^+-Na^+ System - The Effect of Flow Rate (C_o = 0.01 N)

While investigating the ammonium removal by clinoptilolite, Rahmani et al. (2004) found a breakthrough capacity of 0.62 meq/g of zeolite utilizing column mode experiments with clinoptilolite particles of 30-40 Mesh size and initial ammonium concentration of 101 ppm.

In the study conducted by Bayraktaroğlu (2006), the estimated breakthrough capacity was 0.895 meq/g of zeolite when working in column mode under the flow rate of 8 mL/min and initial ammonium concentration of 0.01 N. Aşiroğlu (2006) found breakthrough capacity of 0.888 meq/g of zeolite when working in column mode under the flow rate of 8 mL/min and initial ammonium concentration of 0.01 N. The experimental parameters of Bayraktaroğlu (2006) and Aşiroğlu (2006) were similar to this study except that their clinoptilolite conditioning with NaCl procedure was made using batch mode and not column mode.

The results of binary lead-sodium and ammonium-sodium exchange systems shows that Pb^{2+} and NH_4^+ is less strongly preferred over Na^+ by the clinoptilolite as the zeolite is progressively converted to the lead or the ammonium form. This result yields the selectivity sequence of $Pb^{2+} > Na^+$ and $NH_4^+ > Na^+$ which confirms the outcome of other studies in literature (Ames, 1960; Howery and Thomas, 1965; Hulbert, 1987; Rahmani et al., 2004; Aşiroğlu, 2006).

In all binary experiments made to investigate the effect of flow rate on the breakthrough behavior of clinoptilolite, the results summarized in Table 5.6. shows that when the loading volumetric flow rate ($\hat{O}$) is increased (keeping the influent concentration and the temperature constant), the breakthrough capacity (Q_B), and the column efficiency (η_c) values were decreased, while the total exchange capacity (Q_T) remained almost constant.

Other observations obtained in the binary studies were: the difference between the two capacities (Q_B, and Q_T) increased with increasing the flow rate, the volume of

the effluent collected up to the breakthrough point (V_B) increased with decreasing the flow rate, indicating that the time needed to reach the breakthrough point decreases with incresing flow rate; therefore, more solution was treated when working under low flow rate before the breakthrough concentration was reached.

Consequently, it can be seen from the results (under the specified conditions) that increasing the loading flow rate in column operations will lead to a decrease in lead and ammonium removal efficiency by Na-form Gördes clinoptilolite.

Table 5.6. Binary Ion Exchange Experiments Result - The Effect of Flow Rate (C_o = 0.01 N, $\hat{O}$ = 8, 16, 32 mL/min)

System	$\hat{O}$ *(mL/min)*	Q_B *(meq/g of zeolite)*	Q_T *(meq/g of zeolite)*	Q_z *(BV)*	V_B *(BV)*	η_c **(%)**
Pb^{2+}-Na^+	8	0.633	1.030	31.11	50.23	61.4
	16	0.293	0.982	27.77	22.62	29.8
	32	0.172	0.893	22.09	13.42	19.2
NH_4^+-Na^+	8	0.667	1.164	43.65	73.24	57.3
	16	0.634	1.160	37.93	45.63	54.6
	32	0.292	0.973	24.97	22.62	30.0

5.4.2 Effect of Feed Concentration

The effect of feed concentration (with constant flow rate of 8 mL/min) on the breakthrough curve behavior in column ion exchange experiments for the exchange of lead by Na-form Gördes clinoptilolite is shown Figure 5.8, and for the ammonium exchange, is shown in Figures 5.9. The results for both systems: Pb^{2+}-Na^{+}, and NH_4^{+}-Na^{+}, are summarized in Table 5.7. The corresponding raw data for the analysis are given in Appendix D.

For lead removal, Figure 5.8. shows that by decreasing the influent concentration (keeping the flow rate constant), from 0.02 to 0.005 N, the breakthrough capacity (Q_B) increased by 16.4%, and column efficiency (η_c) increased by 12%, and the volume of effluent collected up to the breakthrough point (V_B) increased from 27.22 *BV* into 87.04 *BV*, while the total exchange capacity (Q_T) remained almost constant. Also, the area above the breakthrough curve between breakthrough and exhaustion points (Q_z) increased with decreasing influent concentration.

For ammonium removal, Figure 5.9. shows that by decreasing the influent concentration (keeping the flow rate constant), from 0.02 to 0.005 N, the breakthrough capacity (Q_B) increased by 40.2%, the column efficiency (η_c) increased by 39.7%, and the volume of effluent collected up to the breakthrough point (V_B) increased from 18.02 *BV* into 120.02 *BV*. Also, the area above the breakthrough curve between breakthrough and exhaustion points (Q_z) increased with decreasing influent concentration.

In all experiments, the volume of the effluent collected up to the breakthrough point (V_B) is shown to increase with decreasing feed concentration, indicating that the time needed to reach the breakthrough point decreased with incresing influent concentration.

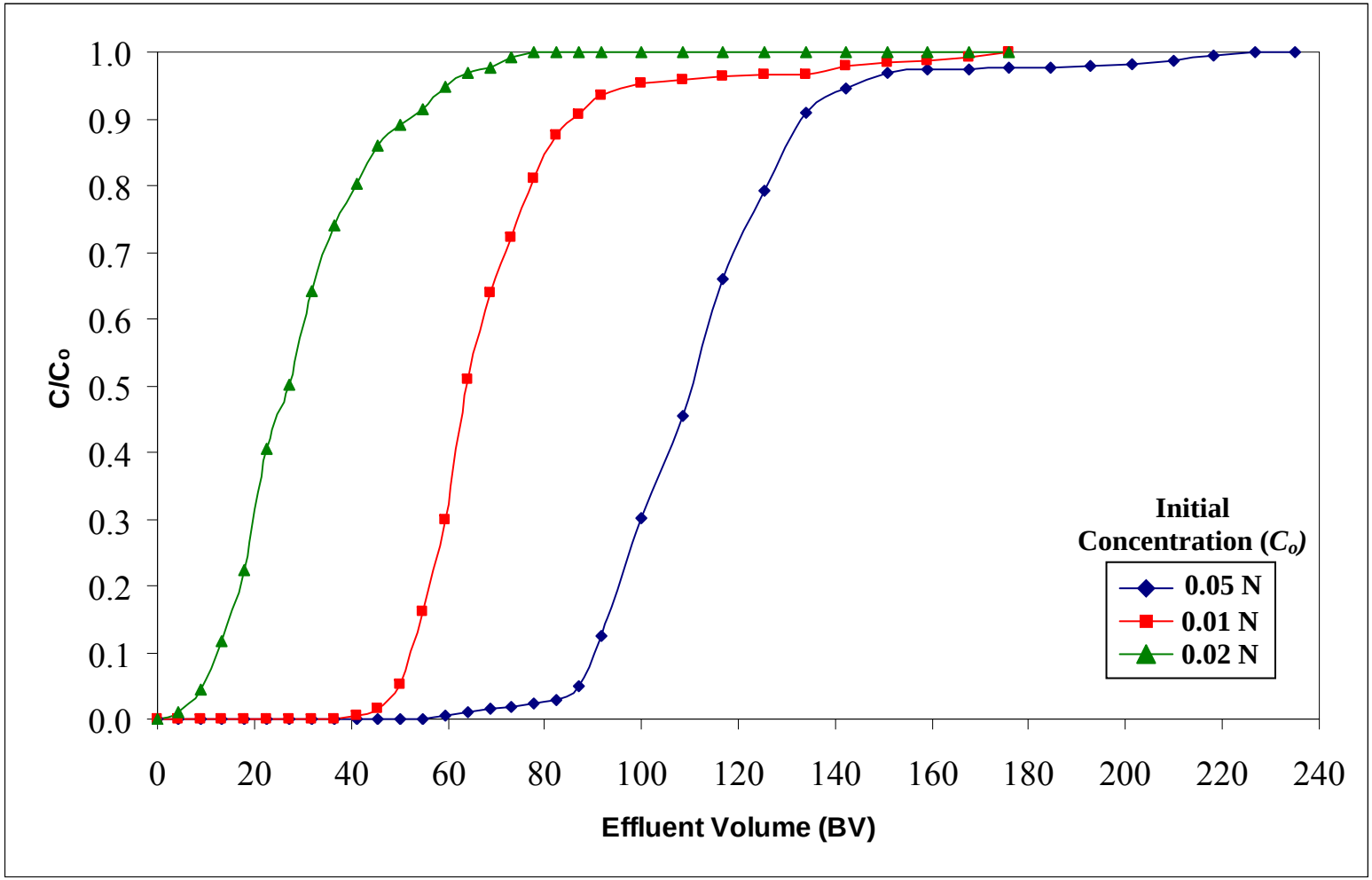

Figure 5.8. The Breakthrough Curves of Pb^{2+}-Na^{+} System - The Effect of Feed Concentration ($\hat{O}$ = 8 ml/min)

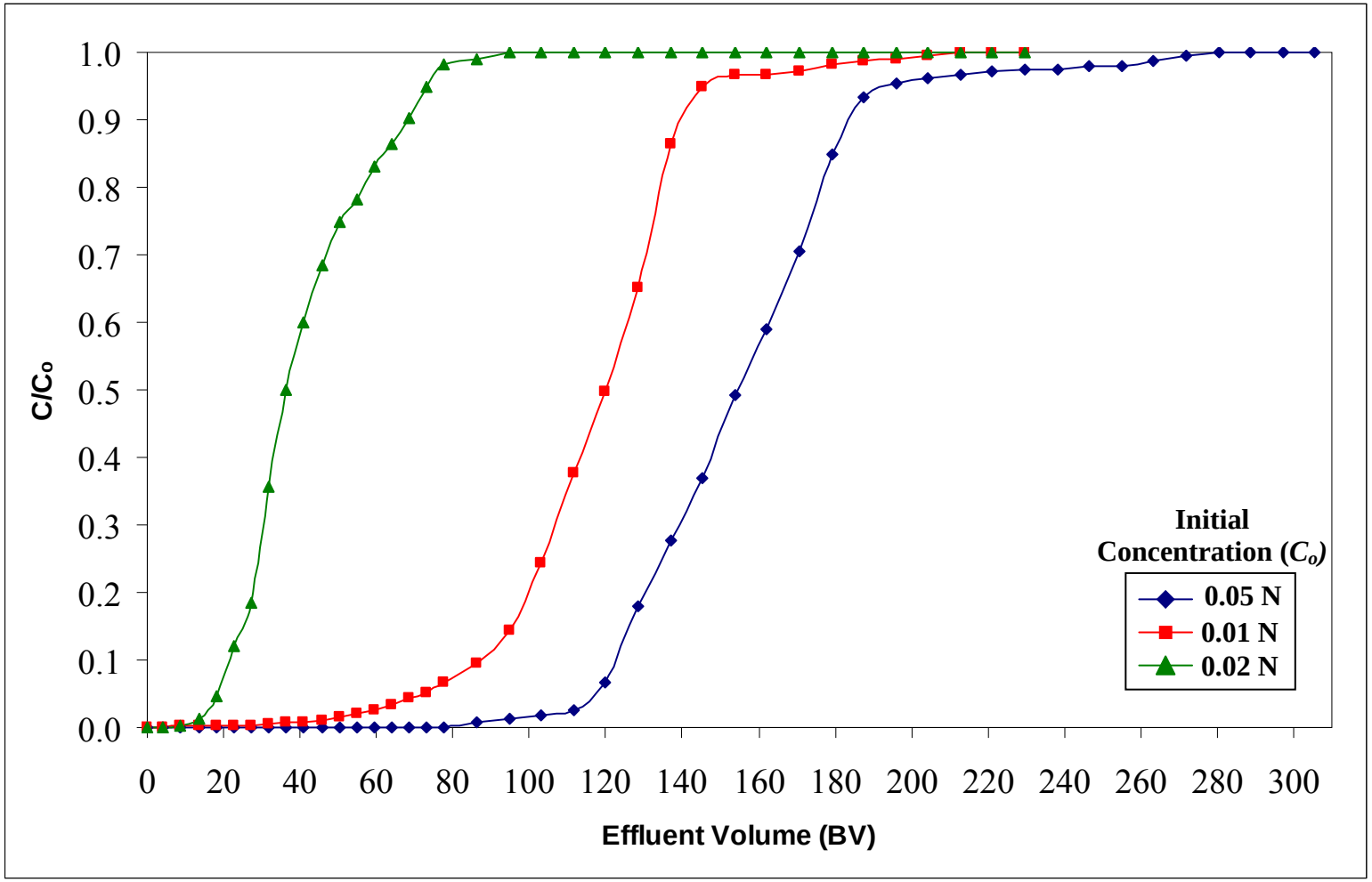

Figure 5.9. The Breakthrough Curves of NH_4^+-Na^+ System - The Effect of Feed Concentration ($\hat{O}$ = 8 ml/min)

Table 5.7. Binary Ion Exchange Experiments Result - The Effect of Feed Concentration ($\hat{O}$ = 8 mL/min, C_o = 0.005, 0.01, and 0.02 N)

System	C_o (*N*)	Q_B *(meq/g of zeolite)*	Q_T *(meq/g of zeolite)*	Q_z (*BV*)	V_B (*BV*)	η_c (%)
Pb^{2+}-Na^+	0.005	0.665	1.101	36.65	87.04	60.4
	0.010	0.601	1.030	29.21	50.23	58.3
	0.020	0.547	1.029	15.00	27.22	53.1
NH_4^+-Na^+	0.005	0.780	1.160	47.57	120.02	67.2
	0.010	0.667	1.151	37.92	73.24	57.9
	0.020	0.466	1.149	26.9	18.02	40.5

For binary studies, regarding the ammonium and lead removal, it was concluded that by decreasing the volumetric flow rate, and the pollutant influent concentration, the contaminant removal efficiency of local clinoptilolite increases under the specified conditions. These achieved capacity results of this study is in the range of results attained by authors that have examined similar systems and agree with relevant work found in literature (Milan et al., 1997; Cincotti et al., 2001; Demir et al., 2002; Rahmani et al., 2004; Aşiroğlu, 2006; Inglezakis et al., 2007; Medvidović et al., 2007; Stylianou et al., 2007).

By comparing the breakthrough capacities (Q_B) for Pb^{2+}-Na^+ and NH_4^+-Na^+systems, for one particular experiment parameter, whether in flow rate or concentration examination, it was observed that the breakthrough capacities of ammonium is higher than that of lead. Also, the total exchange capacity (Q_T) shows the same behavior. For instance, in experiments made under 8 mL/min flow rate and constant initial concentration of 0.01 N, the breakthrough capacities (Q_B) for Pb^{2+}-Na^+ system was 0.633 meq/g of zeolite, while for NH_4^+-Na^+system it was 0.667. Also, the total exchange capacity (Q_T) for Pb^{2+}-Na^+ system was 1.03 meq/g of zeolite, while for

NH_4^+-Na^+system it was 1.16. In addition, it was calculated by the chemical analysis of the pretreated clinoptilolite, that the sodium content ion exchange capacity was found as 1.16 meq/g of zeolite. These results indicate that almost all of the sodium cations are replaced with the lead and ammonium cations due to the high affinity of clinoptilolite for these cations. Therefore, the results indicate that nearly all the available exchange channels presented in the structure of clinoptilolite were occupied by NH_4^+ and Pb^{2+} cations.

Consequently, the cations selectivity sequence for Gördes clinoptilolite according to their affinity was found as: $NH_4^+ > Pb^{2+} > Na^+$ and this result is consistent with the results found in relevant column mode studies regarding the removal of lead and ammonium using clinoptilolite (Ames, 1960; Howery and Thomas, 1965; Langella et al., 2000; Cincotti et al., 2001; Aşiroğlu, 2006). Table 5.8. summarizes the results of different cation selectivity sequence of clinoptilolite in some relevant studies.

Table 5.8. Examples of Cation Selectivity Ranks of Clinoptilolite from Some Studies

Author	Year	Selectivity Series
Howery and Thomas	1965	$Cs^+ > NH_4^+ > Na^+$
Blanchard et al.	1984	$Pb^{2+} > NH_4^+ \approx Ba^{2+} > Cu^{2+} \approx Zn^{2+} > Cd^{2+} > Co^{2+}$
Semmens and Martin	1988	$Pb^{2+} > K^+ > Ba^{2+} > NH_4^+ > Ca^{2+} > Cd^{2+} > Cu^{2+} > Na^+$
Langella et al.	2000	$NH_4^+ > Pb^{2+} > Na^+ > Cd^{2+} > Cu^{2+} \approx Zn^{2+}$
Cincotti et al.	2001	$NH_4^+ > Pb^{2+} > Cd^{2+} > Cu^{2+} \approx Zn^{2+}$
Watanabe et al.	2003	$NH_4^+ > K^+ > Ca^{2+} > Mg^{2+}$
Rahmani et al.	2004	$K^+ > NH_4^+ > Na^+ > Ca^{2+} > Mg^{2+}$
Aşiroğlu	2006	$NH_4^+ > Pb^{2+} > Na^+$
Bayraktaroğlu	2006	$NH_4^+ > Cd^{2+} > Na^+$

5.5 Ternary Studies

Generally, pollutants in wastewater do not exist individually but they rather present together with each other. Therefore, it is very important to study how to simultaneously remove more than one pollutant from the wastewater. The ion exchange process in industry application is a very common in removing pollutants from wastewater, and the use of clinoptilolite holds a great potential in this matter.

In the simultaneous (multicomponent) removal of lead and ammonium ions, the breakthrough curves become more complicated and the ions are exchanged with different strengths. The ion that clinoptilolite has more affinity will be detained more sturdily and will be exchanged more strongly than other ion. Therefore, at the outlet the weaker ion will breakthrough first. Hence, at the exit of the column, the ion that clinoptilolite has less affinity will break through first. Also, in capacity calculations, the breakthrough capacity and the breakthrough point were determined with respect to the ion that first emerged from column.

A particular number of column experiments were conducted to examine Gördes clinoptilolite ion exchange behavior for simultaneous exchange of lead Pb^{2+} and ammonium NH_4^+ cations with sodium Na^+ cations. The effects of the volumetric flow rate ($\hat{O}$) of the solution passing through the column, and the initial concentration (C_o) on the breakthrough behavior were investigated.

5.5.1 Effect of Flow rate

The effect of flow rate (with constant feed concentration at 0.01 total normality: 50% Pb^{2+}, 50% NH_4^+) on the breakthrough curve behavior in ion exchange experiments for the simultaneous exchange of lead and ammonium by Na-form Gördes clinoptilolite is shown in Figures 5.10. - 5.12. The experimental results for ternary

Pb^{2+}- NH_4^+-Na^+ system are summarized in Table 5.9. The corresponding raw data for the analysis are given in Appendix D.

For the ternary lead-ammonium-sodium system, it is observed from the corresponding figures that ammonium ion was first detected in the effluent; therefore, the breakthrough capacity (Q_B), and the breakthrough point were considered with respect to NH_4^+ ion. In the experiments, the corresponding results for the breakthrough capacity at flow rates of 8, 16, and 32 mL/min, were found as: 0.295, 0.206, and 0.176 meq/g of zeolite for Pb^{2+} ions; and 0.176, 0.146, and 0.145 meq/g of zeolite for NH_4^+ ions; respectively.

The results show that the removal of Pb^{2+} and NH_4^+ ions are dependent on the flow rate. At comparatively low flow rate, a higher ion exchange capacity is yielded. That can be explained as at higher flow rates, the retention time is insufficient for the ion exchange process to take place completely between clinoptilolite and lead and ammonium ions. Thus, a competition between Pb^{2+} and NH_4^+ ions for the exchange sites on clinoptilolite will arise, and this competition is favored for lead ions.

These results agree with the results obtained by Aşıroğlu (2006) in a similar study. The breakthrough capacities obtained in his study for the corresponding flow rates of 8, 15, and 30 mL/min, were 0.398 (Pb^{2+}), 0.337 (NH_4^+); 0.299 (Pb^{2+}), 0.297 (NH_4^+); and 0.197 (Pb^{2+}), 0.198 (NH_4^+) meq/g of zeolite; respectively.

Consequently, it is concluded that the affinity of clinoptilolite zeolite for lead ions is higher than that for ammonium ions in the ternary Pb^{2+}- NH_4^+-Na^+ multicomponent system. Therefore, the cations selectivity rank for clinoptilolite according to their affinity is determined as the following sequence: $NH_4^+ > Pb^{2+} > Na^+$.

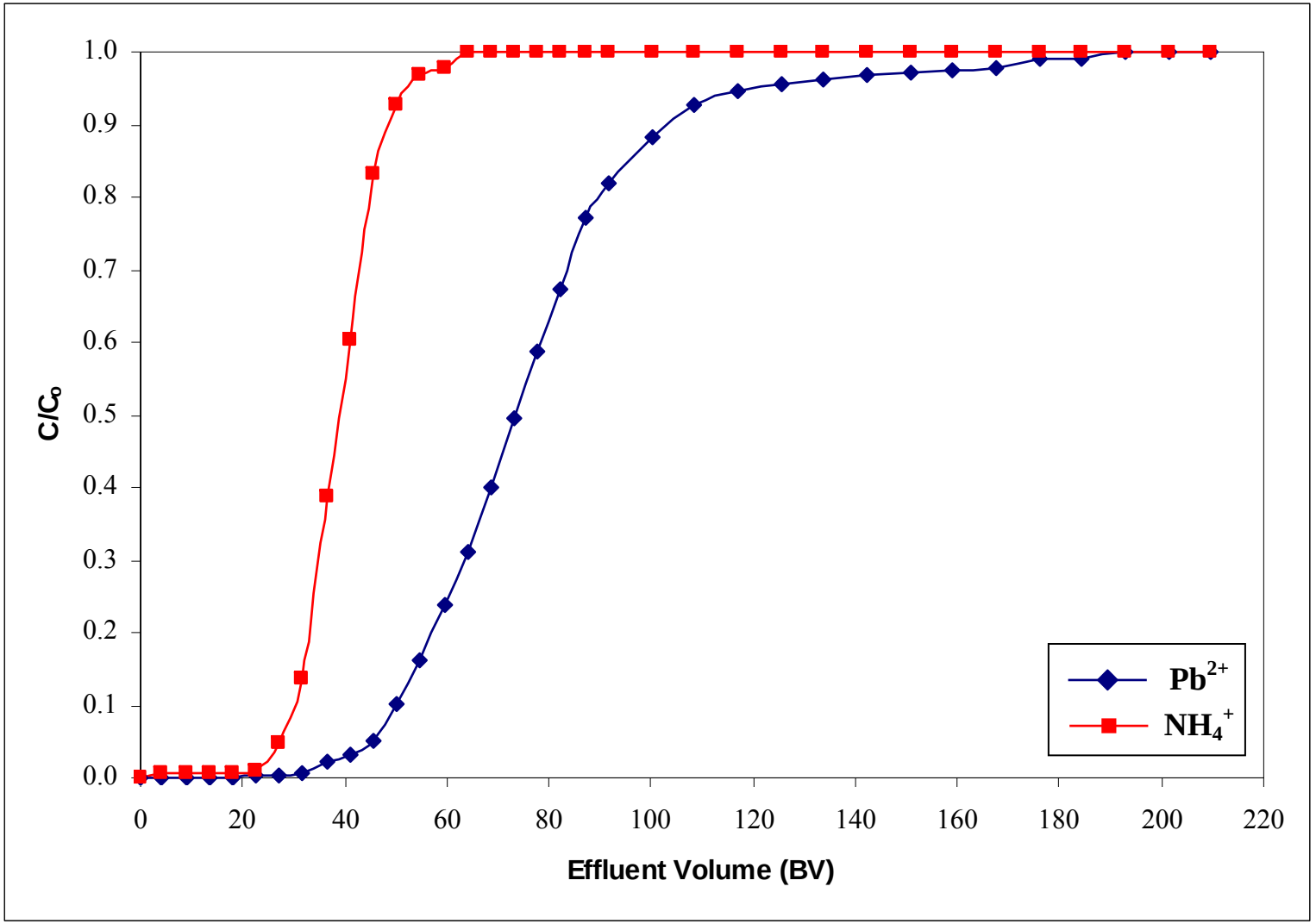

Figure 5.10. The Breakthrough Curves of Pb^{2+}-NH_4^+-Na^+ System ($\hat{O}$ = 8 mL/min, $C_o[Pb^{2+}]$= 0.005*N*, $C_o[NH_4^+]$= 0.005*N*)

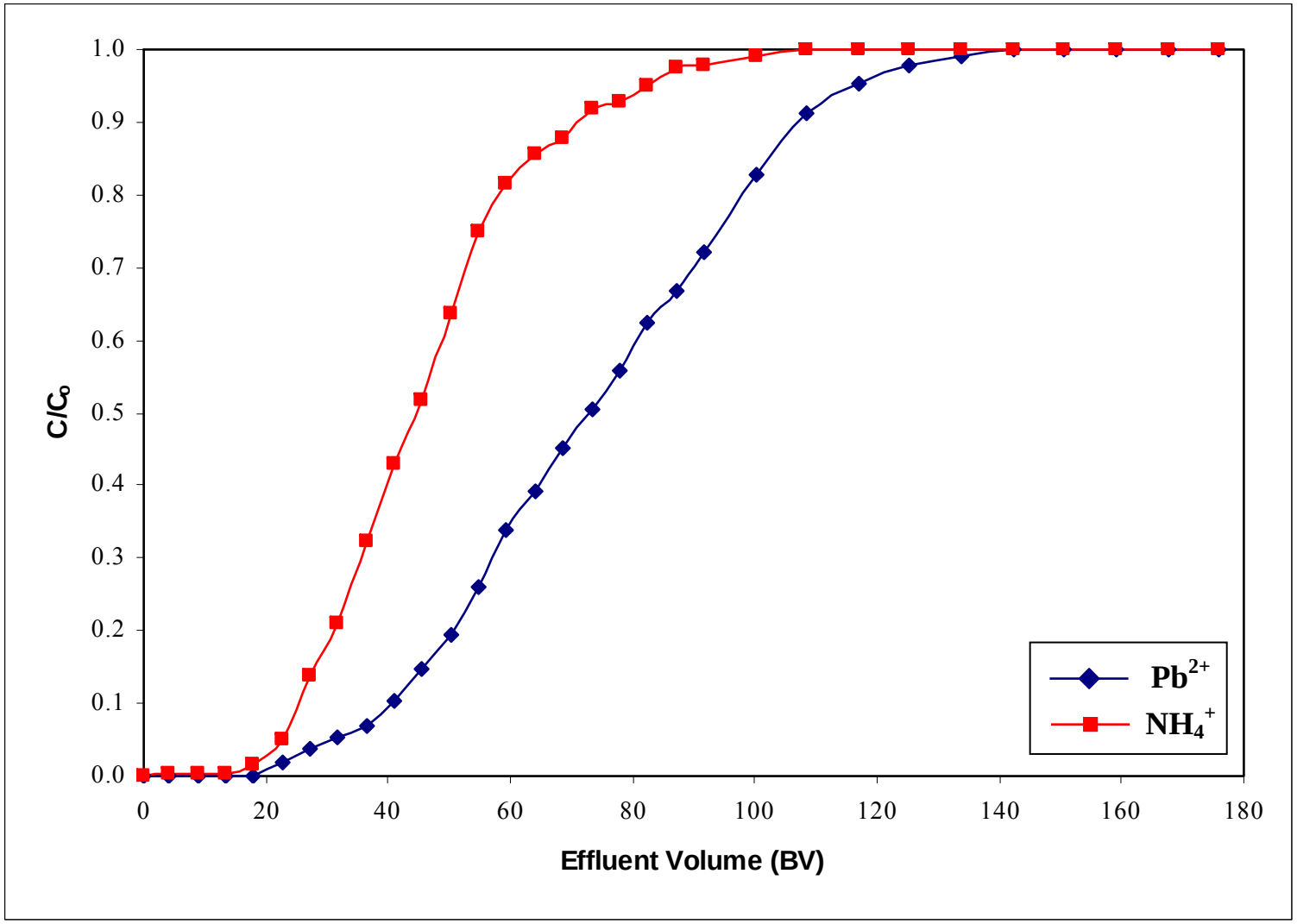

Figure 5.11. The Breakthrough Curves of Pb^{2+}-NH_4^+-Na^+ System ($\hat{O}$ = 16 *mL/min*, $C_o[Pb^{2+}]$= 0.005*N*, $C_o[NH_4^+]$= 0.005*N*)

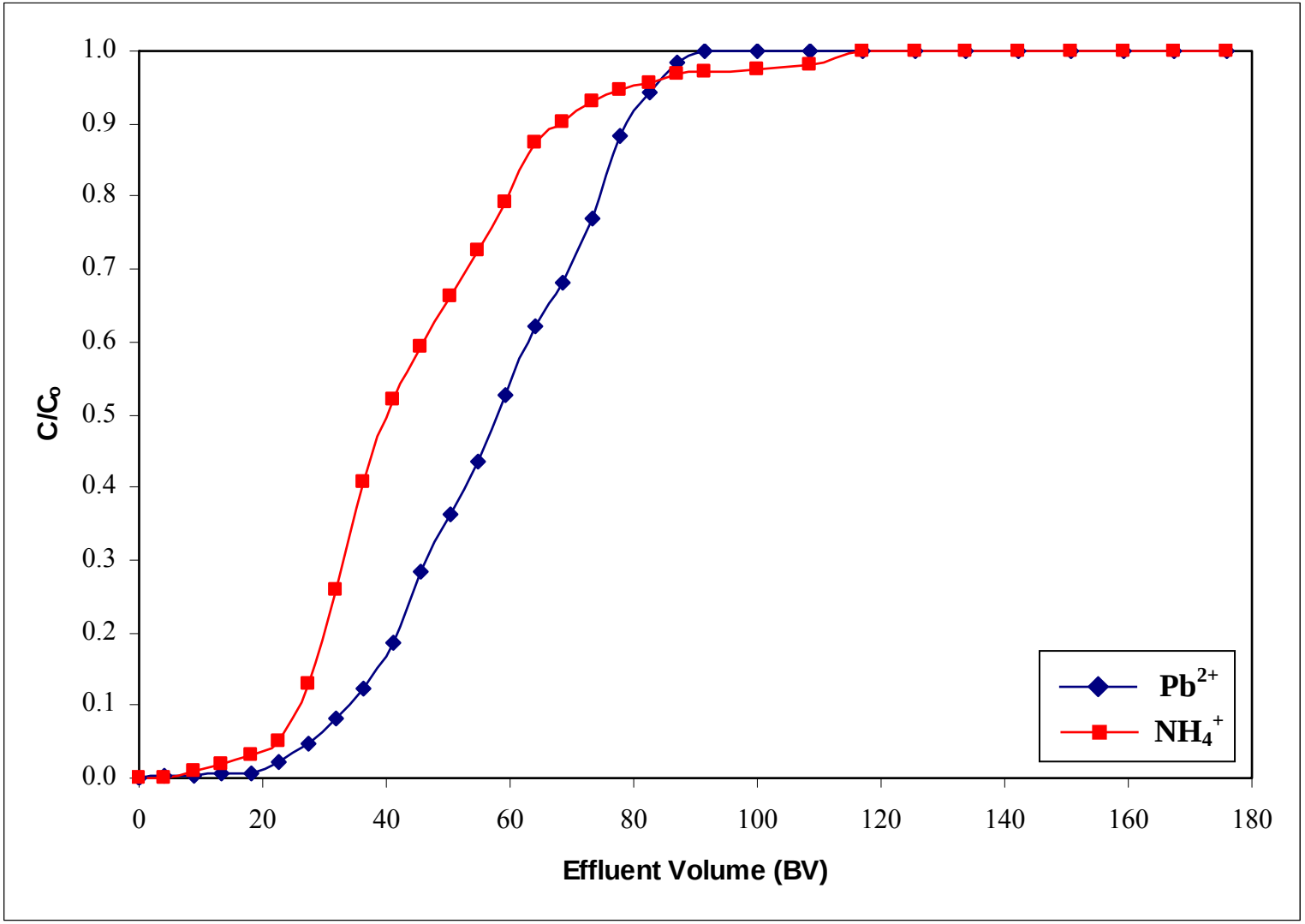

Figure 5.12. The Breakthrough Curves of Pb^{2+}-NH_4^+-Na^+ System ($\hat{O}$ = 32 *mL/min*, $C_o[Pb^{2+}]$= 0.005*N*, $C_o[NH_4^+]$= 0.005*N*)

Table 5.9. Ternary Ion Exchange Experiments Result - The Effect of Flow Rate (C_o, Pb^{2+} = 0.005 N, C_o, NH_4^+ = 0.005 N, $\hat{O}$ = 8, 16, 32 mL/min)

System	$\hat{O}$ (*mL/min*)	Q_B *(meq/g of zeolite)*		Q_T *(meq/g of zeolite)*		Q_z (*BV*)		V_B (*BV*)		η_c (%)	
		Pb^{2+}	NH_4^+	Pb^{2+}	NH_4^+	Pb^{2+}	NH_4^+	Pb^{2+}	NH_4^+	Pb^{2+}	NH_4^+
Pb^{2+}- NH_4^+-Na^+	8	0.295	0.176	0.601	0.281	46.960	16.184	45.63	27.22	49.1	62.6
	16	0.206	0.146	0.549	0.328	52.675	28.082	31.83	22.62	37.5	44.5
	32	0.176	0.145	0.504	0.339	50.256	29.805	27.22	22.62	35.0	42.9

5.5.2 Effect of Feed Concentration

The effect of initial concentration on the breakthrough curve behavior in ion exchange experiments for the simultaneous exchange of lead and ammonium by Na-form Gördes clinoptilolite is shown in Figure 5.10., Figure 5.13., and in Figure 5.14. The experimental results for ternary Pb^{2+}- NH_4^+-Na^+ system are summarized in Table 5.10. The corresponding raw data for the analysis are given in Appendix D.

The flow rate during all these experiments was 8 mL/min as this loading flow was found to be giving optimum exchanging results based on ternary flow rate examining studies. In these experiments, the total normality of the ammonium-lead solution was 0.01 N, and the ratio of Pb^{2+}/NH_4^+ concentrations where: 1/3, 1, and 3.

While observing effect of the influent concentration on the breakthrough behavior in the ternary lead-ammonium-sodium system, it was observed from the corresponding figures that ammonium ion was first detected in the effluent; therefore, the breakthrough capacity (Q_B), and the breakthrough point were considered with respect to NH_4^+ ion. In the experiments, the corresponding results for the breakthrough capacity for the ratio of Pb^{2+}/NH_4^+ concentrations of 1/3, 1, and 3, were found as: 0.379, 0.295, and 0.396 meq/g of zeolite for Pb^{2+} ions; and 0.442, 0.176, and 0.087 meq/g of zeolite for NH_4^+ ions; respectively.

The results show that by increasing the ratio of Pb^{2+}/NH_4^+ concentrations, the breakthrough capacity (Q_B) of ammonium decreased by 80.3%, and the column efficiency (η_c) with respect to ammonium ions decreased by 68.5. This is due to the fact that clinoptilolite has less affinity for ammonium ion than for lead ions. As a result of the clinoptilolite affinity towards these cations, a competition between Pb^{2+} and NH_4^+ ions for the exchange sites on clinoptilolite will arise, and this competition is favored for lead ions as it has a greater affinity.

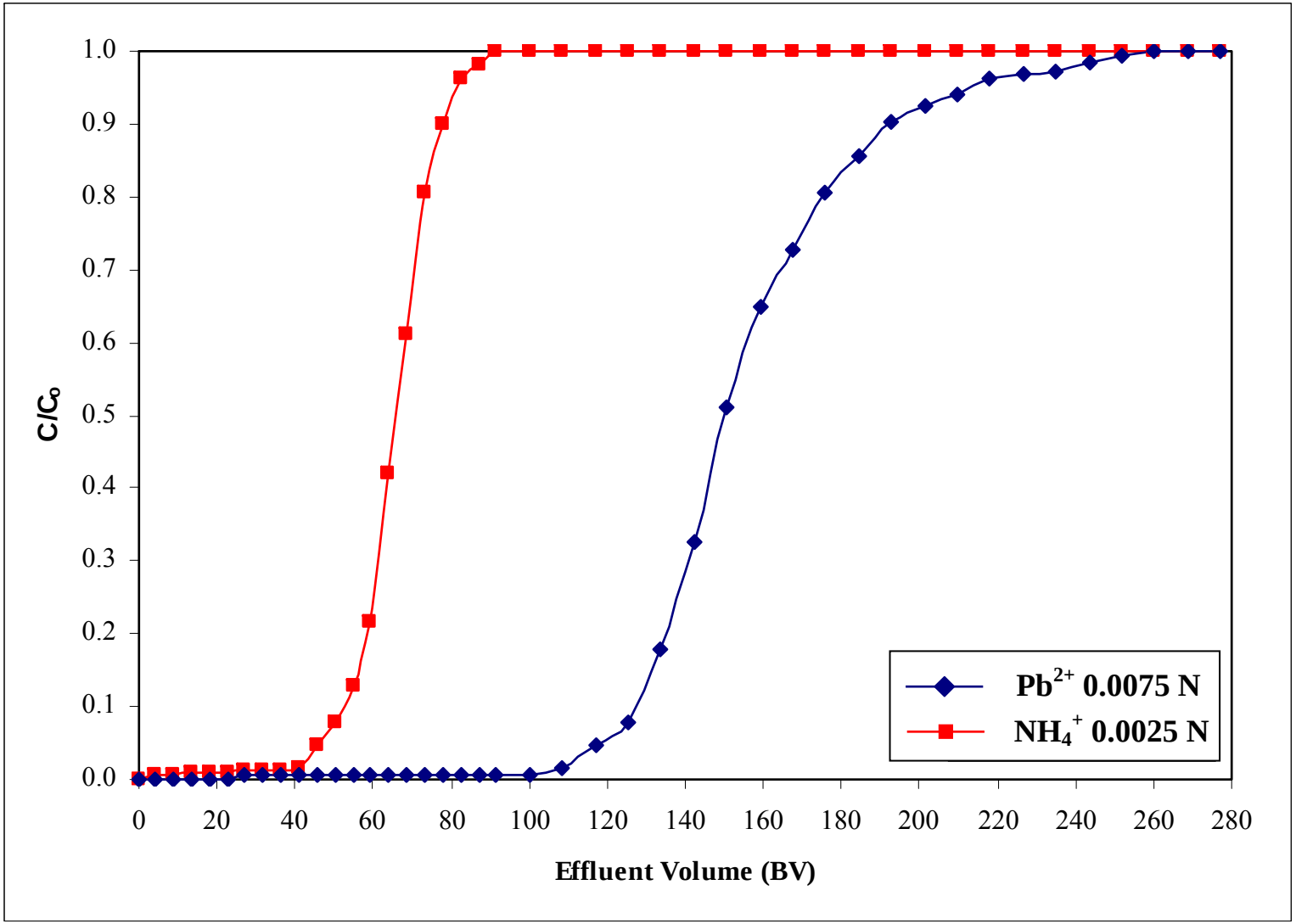

Figure 5.13. The Breakthrough Curves of Pb^{2+}-NH_4^+-Na^+ System ($\hat{O}$ = 8 mL/min, C_o [Pb^{2+}]/C_o [NH_4^+] = 1/3)

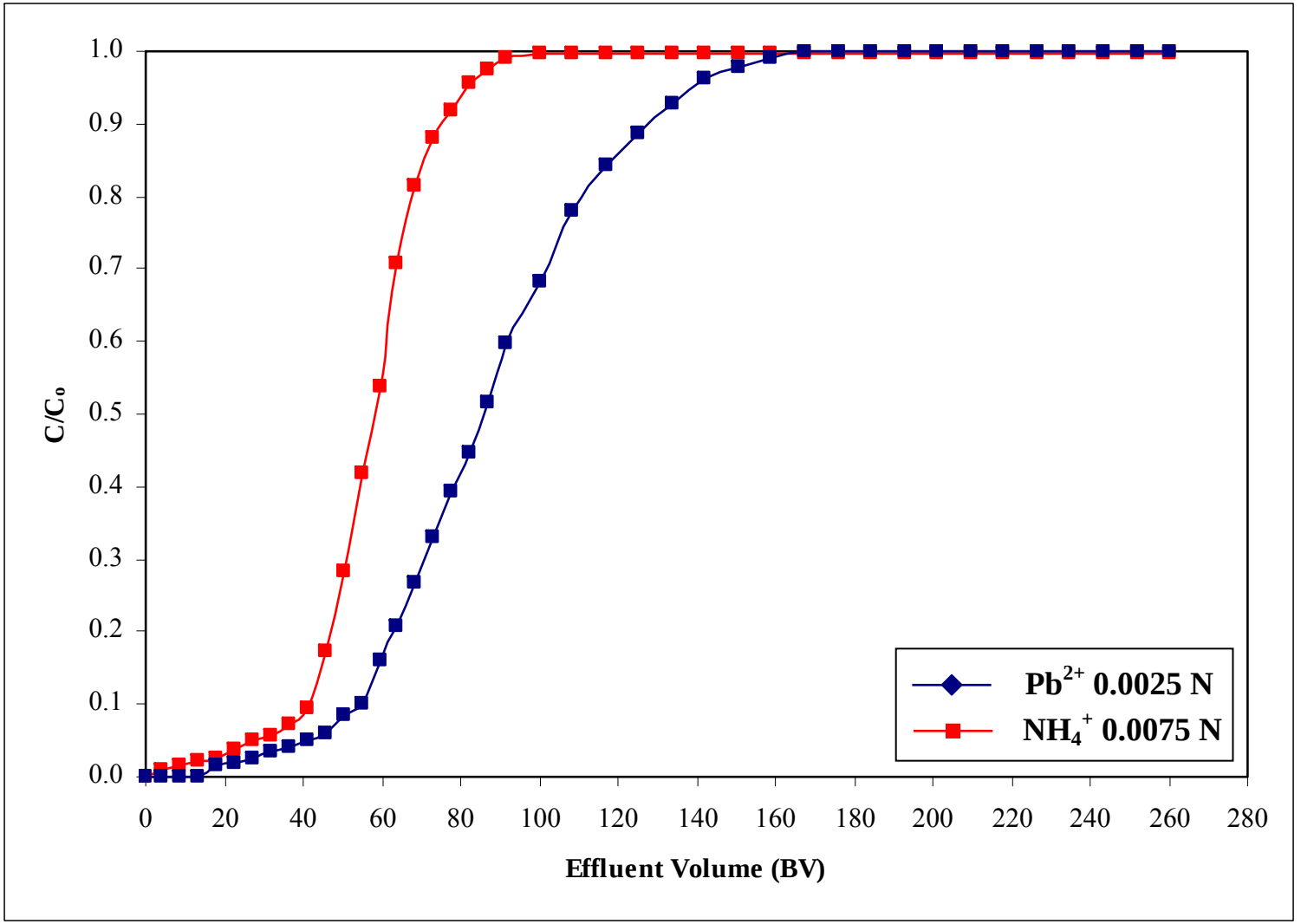

Figure 5.14. The Breakthrough Curves of Pb^{2+}-NH_4^+-Na^+ System ($\hat{O}$ = 8 mL/min, C_o [Pb^{2+}]/C_o [NH_4^+] = 3)

Table 5.10. Ternary Ion Exchange Experiments Result - The Effect of Initial Concentration (C_o [Pb^{2+}]/C_o [NH_4^+]: 1/3, 1, and 3, $\hat{O}$ = 8 mL/min)

System	$\frac{C_o(Pb^{2+})}{C_o(NH_4^+)}$	Q_B (meq/g of zeolite)		Q_T (meq/g of zeolite)		Q_z (BV)		V_B (BV)		η_c (%)	
		Pb^{2+}	NH_4^+	Pb^{2+}	NH_4^+	Pb^{2+}	NH_4^+	Pb^{2+}	NH_4^+	Pb^{2+}	NH_4^+
Pb^{2+}- NH_4^+-Na^+	1/3	0.379	0.442	0.536	0.632	48.137	24.061	116.95	45.63	70.7	69.9
	1	0.295	0.176	0.601	0.282	46.960	16.177	45.63	59.43	49.1	62.6
	3	0.396	0.087	0.682	0.398	64.152	34.232	41.03	27.22	58.0	21.8

By comparing the breakthrough capacities between the binary and ternary studies, it was observed that for each of ammonium and lead ions, the breakthrough capacity values were much smaller. The clarification for decreasing of the breakthrough capacity of each ion is due to the competition between lead and ammonium ions to diffuse into the exchange channels within the clinoptilolite structure. In addition, the little variation between breakthrough point of lead and ammonium (especially in flow rate effect examination) is an indication that the clinoptilolite affinities for lead and ammonium ions are approximately the same. Nevertheless, it was concluded from the breakthrough curves of the ternary Pb^{2+}-NH_4^+-Na^+ system that the competition for exchange sites between lead and ammonium ions is in favor of lead ions since it has the higher affinity towards clinoptilolite.

The observation of clinoptilolite affinity towards lead and ammonium ions in ternary systems support the results obtained in binary system examination. Also, the selectivity results are consistent with the batch and column mode results found by Aşıroğlu (2006) and Bayraktaroğlu (2006). Therefore, it was concluded that the selectivity sequence of clinoptilolite towards ammonium, lead, and sodium cations was determined as $NH_4^+ > Pb^{2+} > Na^+$.

CHAPTER 6

CONCLUSIONS

The laboratory characterization studies revealed some important properties of Gördes clinoptilolite zeolite in the removal of ammonium and lead ions from aqueous solutions by the selective ion exchange process in columns. Based on the results of the investigations made in this study, the following conclusions were achieved:

1. This study confirmed that the Na-form of Turkish Gördes clinoptilolite holds a great potential in the removal process of lead and ammonium ions from aqueous mediums individually or simultaneously by the means of ion exchange particularly at low influent concentrations and low flow rates. Moreover, this property of Gördes clinoptilolite makes it possible to be utilized in industrial applications rather than laboratory scales.

2. The column studies confirmed that the major factor affecting the breakthrough behavior of clinoptilolite is the pretreatment process since it has been emphasized that the cation exchange capacity of clinoptilolite was noticeably dependent on its original cationic composition. Therefore, in order to enhance the effective exchange capacity (EEC) of clinoptilolite, it should be converted into the homoionic sodium form.

3. The optimum concentration of NaCl solution used in the conditioning procedure was found to be as 1.5 mol/L according to the conditions of the pretreatment process used in this study.

4. The maximum total capacity (Q_T) was determined as 1.16 meq/g of zeolite for NH_4^+, and 1.1 meq/g of zeolite for Pb^{2+} in the binary column studies. Also, these values were close to each other and to the sodium content of Na-form of pretreated clinoptilolite (1.16 meq/g of zeolite).
5. In binary studies, it was concluded that by decreasing the volumetric flow rate ($\hat{O}$), and the pollutant influent concentration (C_o), the contaminant removal efficiency of local clinoptilolite increased under the specified conditions of this study.

6. In ternary studies, it was concluded that the removal of Pb^{2+} and NH_4^+ ions are dependent on the flow rate, were at comparatively low flow rate, higher removal efficiency was noticed since, as at higher flow rates the retention time is insufficient for the ion exchange process to take place completely between clinoptilolite and lead and ammonium ions. Thus, a competition between Pb^{2+} and NH_4^+ ions for the exchange sites on clinoptilolite was observed and this competition was in favor of lead ions.

7. Both binary and ternary studies exposed that the zeolite clinoptilolite had more affinity towards Pb^{2+} ions than that towards NH_4^+. Hence, it was concluded that the selectivity sequence for clinoptilolite towards the examined cations were as $NH_4^+ > Pb^{2+} > Na^+$.

8. By the comparison between binary and ternary column studies, it was observed that the breakthrough capacities for each of ammonium and lead ions were much smaller in ternary studies than those values obtained in binary studies. The reason behind this inspection was explained as the competition that took place in ternary studies between lead and ammonium ions to diffuse into the exchange channels within the clinoptilolite structure.

CHAPTER 7

RECOMENDATIONS

In this study, ion exchange behavior of natural zeolite clinoptilolite for lead and ammonium removal from synthetic wastewater was investigated in column mode utilizing ion exchange theory. Both binary and ternary systems were studied considering different parameters affecting the removal process: conditioning of clinoptilolite, solution flow rate in the column, and the initial feed concentration.

As a proceeding study, one can examine the exchange behavior when utilizing more than one column in parallel containing clinoptilolite on the removal process. Also, instead of the down-flow mode performed in this study, up-flow mode can be conducted for further contaminant removal investigation.

Also, regardless of the cations considered in this study for removal performance, other different heavy metals and/or organic substances can be investigated utilizing Gördes clinoptilolite. Moreover, it would be thoughtful to perform a quaternary ion exchange study including different cations and examining their removal behavior in the presence of each other both in batch and column operations, for a more realistic wastewater treatment process.

In addition, another study can be made based on the thermodynamic properties of lead-sodium and ammonium-sodium exchange systems. The thermodynamic models can be applied for the evaluation of activity coefficients of salts could be obtained for those exchange systems. The study can be made in both batch and column mode, and the existing isotherms can be used to compare the experimental results.

In order to facilitate the use of ion exchange theory with the advantageous use of clinoptilolite zeolite, pilot plant studies can be carried out so that fundamental and conceptual design of full-scale ion exchange column system can be established so it would be possible to shed the light on the applicability of the whole process on industrial scale. Also, the regeneration of the exhausted clinoptilolite and testing its removal performance would be a great topic for advance studies.

However, through the studies, it should be considered that despite of all attempts that will be applied to the clinoptilolite in order to convert it into the homoionic form, it in fact unattainable to remove all potassium or magnesium ions from the structure of clinoptilolite and replace it with sodium or calcium ions. Keeping this fact in mind, the clinoptilolite samples that will be used throughout the study should have the same conditioning treatment, and kept at constant humidity.

REFERENCES

Abd El-Hady H.M., Grünwald A., Vlčková K., Zeithammerová J. (2001). Clinoptilolite in Drinking Water Treatment for Ammonia Removal. *Acta Polytechnica*, 41(1), 41-45.

Abusafa A. (1995). Column Studies of Ammonium and Cesium Exchanges on Bigadic Clinoptilolite, MS. Thesis, METU, Ankara.

Abusafa A., Yücel H. (2002). Removal of ^{137}Cs from Aqueous Solutions Using Different Cationic Forms of a Natural Zeolite: Clinoptilolite. *Separation and Purification Technology*, 28(2), 103-116.

Ackley M.W., Yang R.T. (1991). Adsorption Characteristics of High-Exchange Clinoptilolites. *Industrial & Engineering Chemistry Research*, 30(12), 2523-2530.

Alberti A. (1972). On The Crystal Structure of the Zeolite Heulandite. *Mineralogy and Petrology*, 18(2), 129-146.

Ali A.A., El-Bishtawi R. (1997). Removal of Lead and Nickel Ions Using Zeolite Tuff. *Journal of Chemical Technology and Biotechnology*, 69(1), 27-34.

Ames L.L. (1960). The Cation Sieve Properties of Clinoptilolite. *The American Mineralogist*, 45(5-6), 689-700.

Armbruster T. (2008). Natural Zeolites: Cation Exchange, Cation Arrangement and Dehydration Behavior, in: Minerals as Advanced Materials, Volume I. Springer, Berlin, 1-6.

Armbruster T., Gunter M.E. (2001). Crystal Structures of Natural Zeolites. Natural Zeolites: Occurrence, Properties, Applications, in: Reviews in Mineralogy and Geochemistry, 45, 1-67.

Aşiroğlu S. (2006). Lead(II) and Ammonium Exchange on Na-Form of Gördes Clinoptilolite, MS. Thesis, METU, Ankara.

Atkins P.F., Scherger D.A. (1997). A Review of Physicalchemical Methods for Nitrogen Removal from Wastewaters. *Progress in Water Technology*, 8(4-5), 713-19.

Baerlocher Ch., McCusker L.B., Olson D.H., (2007). Atlas of Zeolite Framework Types, 6th Revised edition, Elsevier, Amsterdam.

Barrer R.M. (1949). Molecular-Sieve Action of Solids. *Quarterly Reviews of the Chemical Society*, 3(4), 293-320.

Barrer R.M., Papadopoulos R., Rees L.V.C. (1967). Exchange of Sodium in Clinoptilolite by Organic Cations. *Journal of Inorganic and Nuclear Chemistry*, 29(8), 2047-2063.

Barros M.A.S.D., Zola A.S., Arroyo P.A., Sousa-Aguiar E.F., Tavares C.R.G. (2003). Binary Ion Exchange of Metal Ions in Y and X Zeolites. *Brazilian Journal of Chemical Engineering*, 20(4), 413-421.

Bayraktaroğlu K. (2006). Multicomponent Ion Exchange on Clinoptilolite, MS. Thesis, METU, Ankara.

Blanchard G., Maunaye M., Martin G. (1984). Removal of Heavy Metals from Waters by Means of Natural Zeolites. *Water Research*, 18(12), 1501-1507.

Bolan N.S., Mowatt C., Adriano D.C., Blennerhassett J.D. (2003). Removal of Ammonium Ions from Fellmongery Effluent by Zeolite. *Communications in Soil Science and Plant Analysis*, 34(13-14), 1861-1872.

Boles J.R. (1972). Composition, Optical Properties, Cell Dimensions, and Thermal-Stability of Some Heulandite Group Zeolites. *American Mineralogist*, 57(9-10), 1463-1493.

Breck T.W. (1974). Zeolites Molecular Sieves: Structure, Chemistry and Use. John Wiley and Sons, New York.

Cincotti A., Lai N., Orrù R., Cao G. (2001). Sardinian Natural Clinoptilolites for Heavy Metals and Ammonium Removal: Experimental and Modeling. *Chemical Engineering Journal,* 84(3), 275-282.

Cincotti A., Mameli A., Locci A.M., Orru R., Cao G. (2006). Heavy Metals Uptake by Sardinian Natural Zeolites: Experiment and Modeling. *Industrial & Engineering Chemistry Research*, 45(3), 1074-1084.

Coombs D.S., Alberti A., Armbruster T., Artioli G., Colella C., Galli E., Grice J.D., Liebau F., Mandarino J.A., Minato H., Nickel E.H., Passaglia E., Peacor D.R., Quartieri S., Rinaldi R., Ross M., Sheppard R.A., Tillmanns E., Vezzalini G. (1998). Recommended Nomenclature for Zeolite Minerals: Report of the Subcommittee on Zeolites of the International Mineralogical Association, Commission on New Minerals and Mineral Names. *Mineralogical Magazine*, 62(4), 533-571.

Corbin D.R., Burgess Jr. B.F., Vega A.J., Farlee R.D. (1987). Comparison of Analytical Techniques for the Determination of Silicon and Aluminum Content In Zeolites. *Analytical Chemistry*, 59(22), 2722-2728.

Çulfaz M., Yağız M. (2004). Ion Exchange Properties of Natural Clinoptilolite: Lead-Sodium and Cadmium-Sodium Equilibria. *Separation and Purification Technology,* 37(2), 93-105.

Ćurković L., Cerjan-Stefanović Š., Filipan T. (1997). Metal Ion Exchange by Natural and Modified Zeolites. *Water Research,* 31(6), 1379-1382.

Czárán E., Mészáros-Kis Á., Domokos E., and Papp J. (1988). Separation of Ammonia from Wastewater Using Clinoptilolite as Ion Exchanger. *Nuclear and Chemical Waste Management*, 8(2), 107-113.

Demir A., Günay A., Debik E. (2002). Ammonium Removal from Aqueous Solution by Using Packed Bed Natural Zeolite. *Water SA*, 28(3), 329-336.

Doula M.K., Ioannou A. (2003). The Effect of Electrolyte Anion on Cu Adsorption-Desorption by Clinoptilolite. *Microporous and Mesoporous Materials*, 58(2), 115-130.

DPT (Devlet Planlama Teskilatı). (1996). Madencilik Özel (htisas Komisyonu Endüstriyel Hammaddeler Alt Komisyonu-Diger Endüstri Mineralleri Çalısma Grubu Raporu, http://ekutup.dpt.gov.tr/madencil/sanayiha/oik480c1.pdf (accessed date: June 24, 2010).

Duvarcı Ö.Ç., Akdeniz Y., Özmıhçı F., Ülkü S., Balköse D., Çiftçioğlu M. (2007). Thermal Behaviour of a Zeolitic Tuff. *Ceramics International*, 33(5), 795-801.

Dyer A. (2007). Ion-Exchange Properties of Zeolites. In: Studies in Surface Science and Catalysis. *Introduction to Zeolite Science and Practice*, 168, 13-37.

Dyer A., White K.J. (1999). Cation Diffusion in the Natural Zeolite Clinoptilolite. *Thermochimica Acta*, 341, 341-348.

EC (European Commission). (1991). European Council Directive No: 91/271/EEC of 21 May 1991 in Brussels, Concerning Urban Waste-Water Treatment. http://ec.europa.eu/environment/water/water-urbanwaste/index_en.html (accessed date: June 30, 2010).

El Akrami H.A. (1991). Column Studies of Ammonium Ion Exchange on Clinoptilolite, MS. Thesis, METU, Ankara.

El-Bishtawi R.F., Ali A.A. (2001). Sorption Kinetics of Lead Ions by Zeolite Tuff. *Journal of Environmental Science and Health*, 36(6), 1055-1072.

Ersoy B., Çelik M.S. (2002). Electrokinetic Properties of Clinoptilolite with Mono- and Multivalent Electrolytes. *Microporous and Mesoporous Materials*, 55(3), 305-312.

Fanfan P.N., Mabon N., Thonart P., Logancy G., Copin A., Barthélemy J. (2006). Investigations on Cationic Exchange Capacity and Unused Bed Zone according to Operational Conditions in a Fixed Bed Reactor for Water Lead Removal by a Natural Zeolite. *Biotechnology, Agronomy, Society and Environment*, 10(2), 03-99.

Fergusson J.E. (1991). The Heavy Elements: Chemistry, Environmental Impact and Health Effects, Pergamon Press, London.

Fogler H.S. (2005). Elements of Chemical Reaction Engineering, 4th edition, Prentice Hall PTR, New Jersey.

Gedik K., Imamoglu I. (2008). Removal of Cadmium from Aqueous Solutions Using Clinoptilolite: Influence of Pretreatment and Regeneration. *Journal of Hazardous Materials*, 155(1-2), 385-392.

Günay A., Arslankaya E., Tosun I. (2006). Lead Removal from Aqueous Solution by Natural and Pretreated Clinoptilolite: Adsorption Equilibrium and Kinetics. *Journal of Hazardous Materials*. 146(1-2), 362-371.

Gunter M.E., Armbruster T., Kohler T., Knowles C.R. (1994). Crystal-Structure and Optical-Properties of Na-Exchanged and Pb-Exchanged Heulandite-Group Zeolites. *American Mineralogist*, 79(7-8), 675-682.

Gül Ö. (2003). Exchanges of Strontium on Clinoptilolite Zeolite, MS. Thesis, METU, Ankara.

Güray Ş. (1997). Removal of Lead from Water by Natural Clinoptilolite, MS. Thesis, METU, Ankara.

Hedström A. (2001). Ion Exchange of Ammonium in Zeolites: A Literature Review. *Journal of Environmental Engineering*. 127(8), 673-681.

Hedström A., Amofah L.S. (2008). Adsorption and Desorption of Ammonium by Clinoptilolite Adsorbent in Municipal Wastewater Treatment Systems. *Journal of Environmental Engineering and Science*, 7(1), 53-61.

Helfferich F.G. (1962). Ion Exchange, McGraw-Hill, New York.

Hlavay J., Vigh G. Y., Olaszi V., Inczédy J. (1982). Investigations on Natural Hungarian Zeolite for Ammonia Removal. *Water Research*, 16(40), 417-420.

Howery D.G., Thomas H.C. (1965). Ion Exchange on the Mineral Clinoptilolite. *Journal of Physical Chemistry*, 69(2), 531-537.

Huang H., Xiao X., Yan B., Yang L. (2010). Ammonium Removal from Aqueous Solutions by Using Natural Chinese (Chende) Zeolite as Adsorbent. *Journal of Hazardous Materials*. 175, 247-252.

Hulbert M. H., (1987). Sodium, Calcium, and Ammonium Exchange on Clinoptilolite from the Fort Laclede Deposit, Sweetwater County, Wyoming. *Clays and Clay Minerals*, 35, 458-462.

Ibrahim K.M., Akashah T. (2004). Lead Removal from Wastewater Using Faujasite Tuff. *Environmental Geology*. 46(6-7), 865-870.

Inglezakis V.J. (2005). The Concept of "Capacity" in Zeolite Ion-Exchange Systems. *Journal of Colloid and Interface Science*, 281(1), 68-79.

Inglezakis V.J., Diamandis N.A., Loizidou M.D., Grigoropoulou H.P. (1999). Effect of Pore Clogging on Kinetics of Lead Uptake by Clinoptilolite. *Journal of Colloid and Interface Science*, 215(10), 54-57.

Inglezakis V.J., Girgoropoulou H.P. (2003). Modeling of Ion Exchange of Pb^{2+} in Fixed Beds of Clinoptilolite. *Microporous and Mesoporous Materials*, 61(1-3) 273-282.

Inglezakis V.J., Hadjiandreou K.J., Loizidou M.D., Girgoropoulou H.P. (2001). Pretreatment of Natural Clinoptilolite in a Laboratory-Scale Ion Exchange Packed Bed. *Water Research*, 35(9), 2161-2166.

Inglezakis V.J., Loizidou M.D. (2007) Ion Exchange of Some Heavy Metal Ions from Polar Organic Solvents into Zeolite. *Desalination*, 211(1-3), 238-248.

Inglezakis V.J., Loizidou M.D., Grigoropoulou H.P. (2002). Equilibrium and Kinetic Ion Exchange Studies of Pb^{2+}, Cr^{3+}, Fe^{3+} and Cu^{2+} on Natural Clinoptilolite. *Water Research*, 36(11), 2784-2792.

Inglezakis V.J., Loizidou M.D., Grigoropoulou H.P. (2003). Ion exchange of Pb^{2+}, Cu^{2+}, Fe^{3+}, and Cr^{3+} on Natural Clinoptilolite: Selectivity Determination and Influence of Acidity on Metal Uptake. *Journal of Colloid and Interface Science*, 261(1), 49-54.

Inglezakis V.J., Loizidou M.D., Grigoropoulou H.P. (2003). Short-Out Design of Ion Exchange and Adsorption Fixed Bed Operations for Wastewater Treatment. 8th International Conference on Environmental Science and Technology, Lemos Island, Greece.

Inglezakis V.J., Loizidou M.D., Grigoropoulou H.P. (2004). Ion Exchange Studies on Natural and Modified Zeolites and the Concept of Exchange Site Accessibility. *Journal of Colloid and Interface Science,* 275, 570 - 576.

Inglezakis V.J., Papadeas C.D., Loizidou M.D., Grigoropoulou H.P. (2001). Effects of Pretreatment on Physical and Ion Exchange Properties of Natural Clinoptilolite. *Environmental Technology*, 22(1), 75-82.

Inglezakis V.J., Stylianou M.A., Gkantzou D., Loizidou M.D. (2007). Removal of Pb(II) from Aqueous Solutions by Using Clinoptilolite and Bentonite as Adsorbents. *Desalination*, 210(1-3), 248-256.

Jama, M. A., Yücel, H. (1990). Equilibrium Studies of Sodium-Ammonium, Potassium-Ammonium, and Calcium-Ammonium Exchanges on Clinoptilolite Zeolite. *Separation Science and Technology*, 24(15), 1393-1416.

Jorgensen T.C., Weatherley L.R. (2008). Continuous Ion-Exchange Removal of Ammonium Ion onto Clinoptilolite in the Presence of Contaminants. *Asia-Pacific Journal of Chemical Engineering*, 3(1), 57-62.

Karadag D., Akkaya E., Demir A., Saral A., Turan M., Ozturk M. (2008). Ammonium Removal from Municipal Landfill Leachate by Clinoptilolite Bed Columns: Breakthrough Modeling and Error Analysis. *Industrial & Engineering Chemistry Research*, 47(23), 9552-9557.

Karadag D., Koc Y., Turan M., Armagan B. (2006). Removal of Ammonium Ion from Aqueous Solution Using Natural Turkish Clinoptilolite. *Journal of Hazardous Materials*, 136(3), 604-609.

Karadag D., Tok S., Akgul E., Turan M., Ozturk M., Demir A. (2008). Ammonium Removal from Sanitary Landfill Leachate Using Natural Gördes Clinoptilolite. *Journal of Hazardous Materials*, 153(1-2), 60-66.

Kesraoui-Ouki S., Cheeseman C., Perry R. (1993). Effects of Conditioning and Treatment of Chabazite and Clinoptilolite Prior to Lead and Cadmium Removal. *Environmental Science and Technology*, 27(6), 1108-1116.

Kesraoui-Ouki S., Cheeseman C., Perry R. (1994). Natural Zeolite Utilization in Pollution-Control - A Review of Applications to Metals' Effluents. *Journal of Chemical Technology and Biotechnology*, 59(2), 121-126.

Kocasoy G., Sahin V. (2007). Heavy Metal Removal from Industrial Wastewater by Clinoptilolite. *Journal of Environmental Science and Health Part A-Toxic/Hazardous Substances & Environmental Engineering*, 42(14), 2139-2146.

Koon J. H., Kaufmann W. J. (1975). Ammonia Removal from Municipal Wastewaters by Ion Exchange. *Journal Water Pollution Control Federation*, 47(3), 448-465.

Korkuna O., Leboda R., Skubiszewska-Zie ba J., Vrublevs'ka T., Gun'ko V.M., Ryczkowski J. (2006). Structural and Physicochemical Properties of Natural Zeolites Clinoptilolite and Mordenite. *Microporous and Mesoporous Materials*, 87(3) 243-254.

Koyama K., Takeuchi Y. (1977). Clinoptilolite: The Distribution of Potassium Atoms and Its Role in Thermal Stability. *Zeitschrift Für Kristallographie*, 145(3-4), 216-239.

Langella A., Pansini M., Cappelletti P., de Gennaro B., de' Gennaro M., Colella C. (2000). NH_4^+, Cu^{2+}, Zn^{2+}, Cd^{2+} and Pb^{2+} Exchange for Na^+ in a Sedimentary Clinoptilolite, North Sardinia, Italy. *Microporous and Mesoporous Materials,* 37(3), 337-343.

Langwaldt J. (2008). Ammonium Removal from Water by Eight Natural Zeolites: A Comparative Study. *Separation Science and Technology*, 43(8), 2166-2182.

Lau A., Crittenden B. D., Field R.W. (2004). Enhancement of Liquid Phase Adsorption Column Performance by Means of Oscillatory Flow: an Experimental Study. *Separation and Purification Technology*, 35(2), 113-124.

Lehto J., Harjula R., (1995). Experimentation in Ion Exchange Studies - The Problem of Getting Reliable and Comparable Results. *Reactive and Functional Polymers*, 27(2), 121-146.

Leung S., Barrington S., Wan Y., Zhao X., El-Husseini B. (2007). Zeolite (Clinoptilolite) As Feed Additive to Reduce Manure Mineral Content. *Bioresource Technology*, 98(17), 3309-3316.

Li Z., Alessi D., Allen L., (2002). Influence of Quaternary Ammonium on Sorption of Selected Metal Cations onto Clinoptilolite Zeolite. *Journal of Environmental Quality*, 31(4), 1106-1114.

Lin S.H., Wu C.L., (1996). Ammonia Removal from Aqueous Solution by Ion Exchange. *Industrial & Engineering Chemistry Research*, 35(2), 553-558.

Liu D.H.F., Lipták B.G. (1997). Environmental Engineers' Handbook, 2nd Edition, CRC Press, New Jersey.

Llanes-Monter M.M., Olguin M.T., Solache-Rios M.J. (2007). Lead Sorption by a Mexican, Clinoptilolite-Rich Tuff. *Environmental Science and Pollution Research*, 14(6), 397-403.

Lobo R.F. (2003). Introduction to the Structural Chemistry of Zeolites, in: Handbook of Zeolite Science and Technology. CRC Press, New Jersey.

Mažeikienė A., Valentukevičienė M., Jankauskas J. (2010). Laboratory Study of Ammonium Ion Removal by Using Zeolite (Clinoptilolite) to Treat Drinking Water. *Journal of Environmental Engineering and Landscape Management*, 18(1), 54-61.

McCusker L., Baerlocher C. (2007) Zeolite Structures, in: Studies in Surface Science and Catalysis, *Introduction to Zeolite Science and Practice*, 168, 13-37.

Medvidović N.V., Perić J., Trgo M. (2008). Testing of Breakthrough Curves for Removal of Lead Ions from Aqueous Solutions by Natural Zeolite-Clinoptilolite

According to the Clark Kinetic Equation. *Separation Science and Technology*, 43(4), 944-959.

Medvidović N.V., Perić J., Trgo M., Muzek M.N. (2007). Removal of Lead Ions by Fixed Bed of Clinoptilolite - The Effect of Flow Rate. *Microporous and Mesoporous Materials*, 105(3), 298-304.

Mercer B.W., Ames L.L., Touhill C.J., Van Slyke W.J., Dean R.B. (1970). Ammonia Removal from Secondary Effluents by Selective Ion Exchange. *Journal (Water Pollution Control Federation)*, 42(20), R95-R107

Merian E., Anke M., Ihnat M., Stoppler M. (2004). Elements and Their Compounds in the Environment: Occurrence, Analysis and Biological Relevance, Volume 2, Metals and their Compounds, 2nd Edition, Wiley-VCH, Germany.

Merkle A.B., Slaughter M. (1968). Determination and Refinement of the Structure of Heulandite. *The American Mineralogist*, 53(7-8), 1120-1138.

Michaels A.S. (1952). Simplified Method of Interpreting Kinetic Data in Fixed-Bed Ion Exchange. *Industrial and Engineering Chemistry*, 44(8), 1922-1930.

Miladinovic N., Weatherley L.R. (2007). Intensification of Ammonia Removal in a Combined Ion-Exchange and Nitrification Column. *Chemical Engineering Journal*, 135(1-20, 15-24.

Milan Z., Sénchez E., Weiland P., de Las Pozas C., Borja R., Mayari R., Rovirosa N. (1997). Ammonia Removal from Anaerobically Treated Piggery Manure by Ion Exchange in Columns Packed With Homoionic Zeolite. *Chemical Engineering Journal*, 66(1), 65-71.

Moralı N. (2006). Investigation of Zinc and Lead Removal from Aqueous Solutions Using Clinoptilolite, MS. Thesis, METU, Ankara.

Mumpton F.A. (1960). Clinoptilolite Redefined. *American Mineralogist,* 45(3-4), 351-369.

Mumpton F.A. (1999). La Roca Magica: Uses of Natural Zeolites in Agriculture and Industry. *Proc. Natl. Acad. Sci. USA,* 96, 3463-3470.

Nguyen M.L., Tanner C.C. (1998). Ammonium Removal from Wastewaters Using Natural New Zealand Zeolites. *New Zealand Journal of Agricultural Research*, 41(3), 427-446.

Ören A.H., Kaya A. (2006). Factors Affecting Adsorption Characteristics of Zn^{2+} on Two Natural Zeolites. *Journal of Hazardous Materials*, B131, 59-65.

Orhan Y., Kocaoba S. (2007). Adsorption of Toxic Metals by Natural and Modified Clinoptilolite. *Annali di Chimica*, 97(8), 781-790.

Oter O., Akcay H. (2007). Use of Natural Clinoptilolite to Improve, Water Quality: Sorption and Selectivity Studies of Lead(II), Copper(II), Zinc(II), and Nickel(II). *Water Environment Research*, 79(3), 329-335.

Ouki S.K., Kavannagh M. (1997). Performance of Natural Zeolites for the Treatment of Mixed Metal-Contaminated Effluents. *Waste Management & Research*, 15(4), 383-394.

Ozaydin S., Kocer G., Hepbasli A. (2006). Natural Zeolites in Energy Applications. *Energy Sources, Part A: Recovery, Utilization, and Environmental Effects*, 28(15), 1425-1431.

Park JB., Lee SH., Lee JW., Lee CY. (2002). Lab Scale Experiments for Permeable Reactive Barriers against Contaminated Groundwater with Ammonium and Heavy Metals Using Clinoptilolite (01-29B). *Journal of Hazardous Materials*, 95(1-2), Pages 65-79.

Passaglia E., Galli G. (1991). Natural Zeolites: Mineralogy and Applications. *European Journal of Mineralogy*, 3(4), 637-640.

Payne K.B., Abdel-Fattah T.M. (2004). Adsorption of Divalent Lead Ions by Zeolites and Activated Carbon: Effects of Ph, Temperature, and Ionic Strength. *Journal of Environmental Science and Health Part A-Toxic/Hazardous Substances & Environmental Engineering*, 39(9), 2275-2291.

Payra P., Dutta P.K. (2003). Zeolites: A Primer. In: Handbook of Zeolite Science and Technology, CRC Press, New Jersey.

Perić J., Trgo M., Medvidović N.V., Nuić I. (2009). The Effect of Zeolite Fixed Bed Depth on Lead Removal from Aqueous Solutions. *Separation Science and Technology*, 44(13), 3113-3127.

Petruzzelli D., Pagano M., Tiravanti G., Passino R. (1999). Lead Removal and Recovery from Battery Wastewaters by Natural Zeolite Clinoptilolite. *Solvent Extraction and Ion Exchange*, 17(3), 677-694.

Polat E., Karaca M., Demir H., Onus A. (2004). Use of Natural Zeolite (Clinoptilolite) In Agriculture. *Journal of Fruit and Ornamental Plant Research*, 12, 183-189.

Rahmani A.R., Mahvi A.H., Mesdaghinia A. R., Nasseri N. (2004). Investigation of Ammonia Removal from Polluted Waters by Clinoptilolite Zeolite. *International Journal of Environment Science and Technology*, 1(2), 125-133.

Saltalı K., Sarı A., Aydın M. (2007). Removal of Ammonium Ion from Aqueous Solution by Natural Turkish (Yildizeli) Zeolite for Environmental Quality. *Journal of Hazardous Materials*, 141(1) 258-263.

Sand L.B., Mumpton F.A. (1976). Natural Zeolites: Occurance, Properties, and Use, Pergamon Press, New York.

Sarioglu M. (2005). Removal of Ammonium from Municipal Wastewater Using Natural Turkish (Dogantepe) Zeolite. *Seperation and Purification Technology*, 41, 1-11.

Schaller W. T. (1923). The Mordenite-Ptilolite Group; Clinoptilolite, a New Species. *The America Mineralogist*, 17, 128-134.

Semmens M.J., Martin W.P. (1988). The Influence of Pretreatment on the Capacity and Selectivity of Clinoptilolite for Metal Ions. *Water Research*, 22(5), 537-542.

Semmens M.J., Seyfarth M. (1978). The Selectivity of Clinoptilolite for Certain heavy metals, in: Natural Zeolites, Occurrence, Properties and Use, Pergamon Press, New York.

Šiljeg M., Foglar L., Kukučka M. (2010). The Ground Water Ammonium Sorption onto Croatian and Serbian Clinoptilolite. *Journal of Hazardous Materials*, 178(1-3), 572-577.

Sprynskyy M., Buszewski B., Terzyk A.P., Namiesnik J. (2006). Study of the Selection Mechanism of Heavy Metal (Pb^{2+}, Cu^{2+}, Ni^{2+}, and Cd^{2+}) Adsorption on Clinoptilolite. *Journal of Colloid and Interface Science*, 304(1), 21-28.

Stylianou M.A., Hadjiconstantinou M.P., Inglezakis V.G., Moustakas K.G., Loizidou M.D. (2007). Use of Natural Clinoptilolite for the Removal of Lead, Copper and Zinc in Fixed Bed Column. *Journal of Hazardous Materials*, 143(1-2) 575-581.

Suzuki M., Ha K.S. (1984). Equilibrium and Rates of Ammonium Ion-Exchange by Clinoptilolite. *Journal of Chemical Engineering in Japan*. 17(2), 139-145.

Tao Y.F., Qiu Y., Fang S.Y., Liu Z.Y., Wang Y., Zhu J.H. (2010). Trapping the Lead Ion in Multi-Components Aqueous Solution by Natural Clinoptilolite. *Journal of Hazardous Materials*, 180(1-3), 282-288.

Tchobanoglous G., Schroeder E.D. (1985). Water Quality: Characteristics, Modeling Modification, Prentice Hall Press, Addison-Wesley.

Townsend R.P., Coker E.N. (2001). Ion Exchange in Zeolites. In: Studies in Surface Science and Catalysis. *Introduction to Zeolite Science and Practice*, 137, 467-524.

Tsitsishvili G.V., Andronikashvili T.G, Kirov G.N., Filizova L.D. (1992). Natural Zeolites, Ellis Horwood Limited, London.

Tufan E.Ö. (2002). Ion Exchange Properties of Gördes Clinoptilolite: Ammonium Exchange, MS. Thesis, METU, Ankara.

Turan M., Celik M.S. (2003). Regenerability of Turkish Clinoptilolite for Use in Ammonia Removal from Drinking Water. *Journal of Water Supply Research and Technology - AQUA*, 52(10), 59-66.

USEPA (United States Environmental Protection Agency). (2005). Lead in DC Drinking Water, http://epa.gov/dclead/ (accessed date: June 29, 2010).

USGS (United States Geological Survey). (2008). 2008 Minerals Yearbook, http://minerals.usgs.gov/minerals/pubs/commodity/zeolites/myb1-2008-zeoli.pdf (accessed date: June 20, 2010).

Watanabe Y., Yamuda H., Kokusen H., Tanaka J., Moriyoshi Y., Komatsu Y. (2003). Ion Exchange Behavior of Natural Zeolites in Distilled Water, Hydrochloric Acid, and Ammonium Chloride Solution. *Separation Science and Technology*, 38(7), 1519-1532.

Wang S., Peng Y. (2010). Natural Zeolites as Effective Adsorbents in Water and Wastewater Treatment. *Chemical Engineering Journal*, 156, 11-24.

Wang Y., Liu S., Xu Z., Han T., Chuan S., Zhu T. (2006). Ammonia Removal from Leachate Solution Using Natural Chinese Clinoptilolite. *Journal of Hazardous Materials*, 136(3), 735-740.

Widiastuti N., Wua H., Ang M., Zhang D. (2008). The Potential Application of Natural Zeolite for Greywater Treatment. *Desalination*, 218(1-3), 271-280.

Wingenfelder U., Hansen C., Furrer G., Schulin R. (2005). Removal of Heavy Metals from Mine Waters by Natural Zeolites. *Environmental Science & Technology*, 39(12), 4606-4613.

Zorpas A.A., Vassilis I., Loizidou M., Grigoropoulou H. (2002). Particle Size Effects on Uptake of Heavy Metals from Sewage Sludge Compost Using Natural Zeolite Clinoptilolite. *Journal of Colloid and Interface Science*, 250(1), 1-4.

APPENDIX A

CALIBRATION CURVE FOR AMMONIUM ION

The Ammonium Ion-Selective Electrode has a solid-state PVC polymer matrix membrane which is designed for the detection of ammonium ions (NH_4^+) in aqueous solutions and is suitable for both field and laboratory applications.

Instrument Used

Combination Ammonium ISE (Ion Selective Electrode)
Manufacture: Sentek - United Kingdom
Model: 3051
Membrane unit: liquid exchange material immobilized in a poly vinyl chloride matrix
Connection plug: BNC
Electrode slope: 56 ± 2 *mV/decade*
pH range: 1 - 8.5
Temperature using range: 0° to 50° *C*
Interfering ion: K^+ (Maximum allowable ratio: 1)
Ammonium NH_4^+ concentration range: (5.10^{-6} to 1 *M*) or (0.1 to 18,000 *ppm*)

Calibration

A series of standard solutions of 1, 10, 100, 500, and 1000 ppm NH_4^+ were prepared from NH_4Cl salt and doubly deionized water. The NH_4Cl salt was dried at 110°C for 24 hours in order to remove the humidity content and then kept in a desiccator containing silica gel until it was cooled and ready to be used. The solutions were prepared, kept and used for calibration at normal room temperature 25°C. The pH of (1000 ppm) NH_4Cl was measured and it was 5.5. All standards and samples were aqueous and do not contain any organic solvents.

Then, the electrode was connected to a pH meter having an ion strength reading ability in millivolt units and the function switch was set to *mV*. Magnetic stirrer was used throughout all measurements in order to insure well mixing. Afterwards, the electrode was immersed in the previously prepared standard ammonium solutions and after getting a stable reading, the reading of *mV* values for each standard concentration was recorded.

Finally, the calibration curve of *mV* readings against the corresponding standard solution concentration was plotted using semi-log graph paper. The electrode slop was checked by calculating the *mV* difference between two standard solutions whose concentrations are one decade apart. The corresponding data for electrode calibration are given in Table A.1., and the calibration curve is for ammonium is represented in Figure A.1.

Table A.1. Data for Calibration of Ammonium Selective Electrode

NH_4^+ Concentration (*ppm*)	Standard Reading (*mV*)
1000	201.4
500	187.6
100	153.9
10	107.4
1	63.3

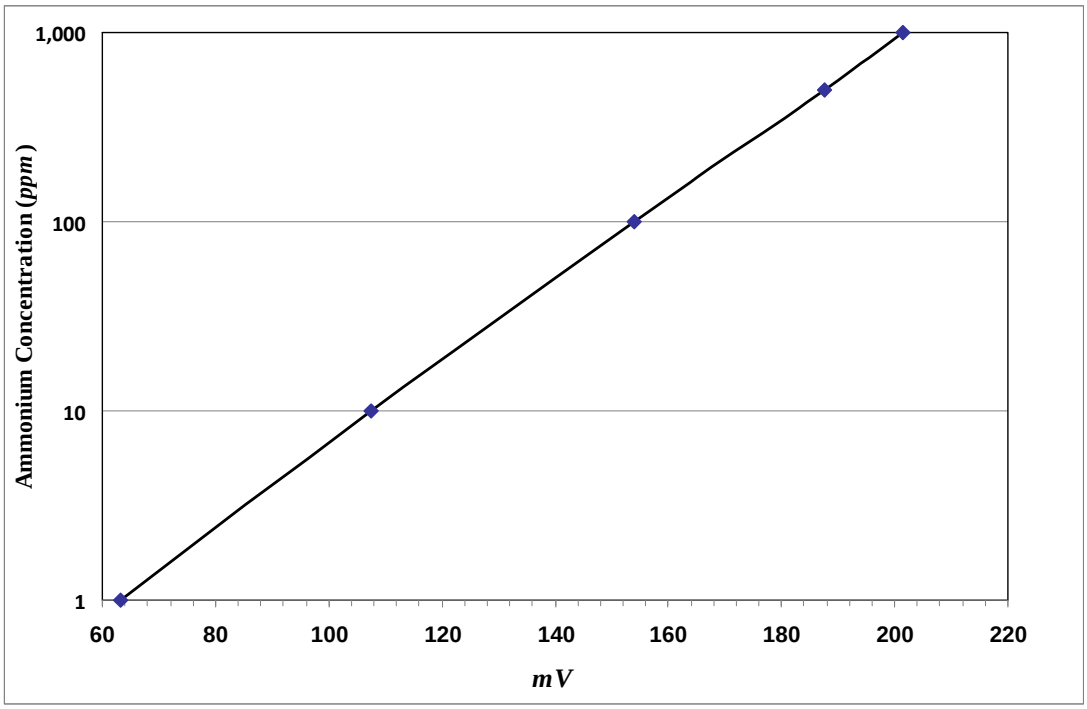

Figure A.1. Calibration Curve for Ammonium Selective Electrode

APPENDIX B

SAMPLE CALCULATION FOR THE DETERMINATION OF BREAKTHROUGH CAPACITY, TOTAL EXCHANGE CAPACITY, AND COLUMN EFFICIENCY FROM THE BREAKTHROUGH CURVE

Reagent Conditions

Influent Pb^{+2} Concentration (C_o) : 0.01N (1036 *ppm*)
Temperature (T) : 25°C
pH: 4.6

Column operation parameters

Clinoptilolite bed height in the column (h_T) = 8.3 *cm*
Diameter of the column ($\varnothing$) = 1 *cm*
One bed volume (BV) is equal to 6.52 *mL*
Flow rate ($\hat{O}$) = 8 *mL/min* (73.6 *BV/h*)

Samples

Samples were taken as follows:

1. For the first 20 samples, 5 mL of the effluent were taken every 25 mL.
2. After that, 5 mL were taken for every 50 mL for the rest of the effluent.

Results:

Table B.1. Data for Binary Pb^{2+}-Na^{+} Exchange System, $\hat{O}$ = 8 *mL/min*, C_o = 0.01 *N*

Sample No	Corrected Volume (*V*) (*mL*)	Bed Volume (*BV*)	Concentration (*C*) (*ppm*)	C/C_o
1	27.5	4.22	0.0	0.00
2	57.5	8.82	0.0	0.00
3	87.5	13.42	0.0	0.00
4	117.5	18.02	0.0	0.00
5	147.5	22.62	0.0	0.00
6	177.5	27.22	0.0	0.00
7	207.5	31.83	0.0	0.00
8	237.5	36.43	0.0	0.00
9	267.5	41.03	0.0	0.00
10	297.5	45.63	4.6	0.00
11	327.5	50.23	14.9	0.01
12	357.5	54.83	53.1	0.05
13	387.5	59.43	165.6	0.16
14	417.5	64.03	310.7	0.30
15	447.5	68.63	528.4	0.51
16	477.5	73.24	663.2	0.64
17	507.5	77.84	748.9	0.72
18	537.5	82.44	841.5	0.81
19	567.5	87.04	908.5	0.88
20	597.5	91.64	940.8	0.91
21	652.5	100.08	970.3	0.94
22	707.5	108.51	988.4	0.95
23	762.5	116.95	993.1	0.96
24	817.5	125.38	1000.5	0.96
25	872.5	133.82	1002.6	0.97
26	927.5	142.25	1003.8	0.97
27	982.5	150.69	1015.3	0.98
28	1037.5	159.13	1024.0	0.99
29	1092.5	167.56	1029.1	0.99
30	1147.5	176.00	1036.0	1.00

Finally, the concentration of the exchangeable ion in the effluent of the fixed bed exchange column is plotted as a function of total volume of the effluent collected, and the characteristic S-shaped curve is obtained.

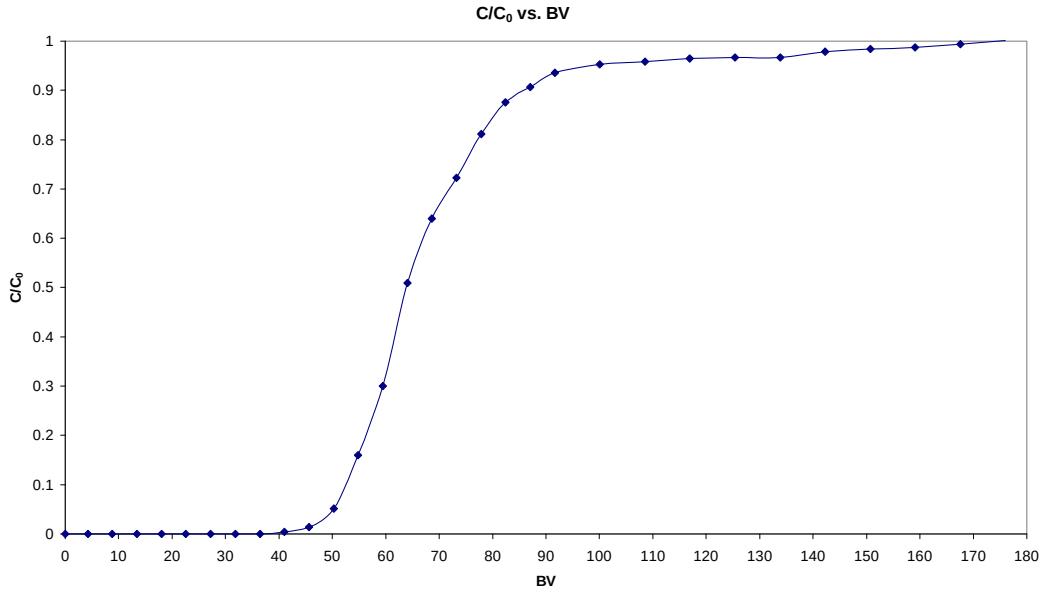

The Breakthrough Capacity (Q_B)

The quantity of cations exchanged up to the breakthrough point may be calculated graphically from equation 2.17:

$$Q_B = \frac{\int_0^{V_B} (C_o - C)dV}{\rho_b h_T A_{c.s}}$$

Equation 2.17 can be re-written in the form:

$$Q_B = \frac{C_o \int_0^{V_B} (1 - \frac{C}{C_o})dV}{\rho_b h_T A_{c.s}}$$

A_S is plainly seen, while A_B as it is shown in the next figure, can be calculated as:

$$A_B = \int_0^{V_B} (1 - \frac{C}{C_o})dV$$

where (A_B) is the area above the curve up to the breakthrough point. In order to estimate A_B, the area under the breakthrough curve (A_S) should be evaluated first by numerical techniques, and then it is subtracted from the total area up to this point, where: $A_T = A_B + A_S$.

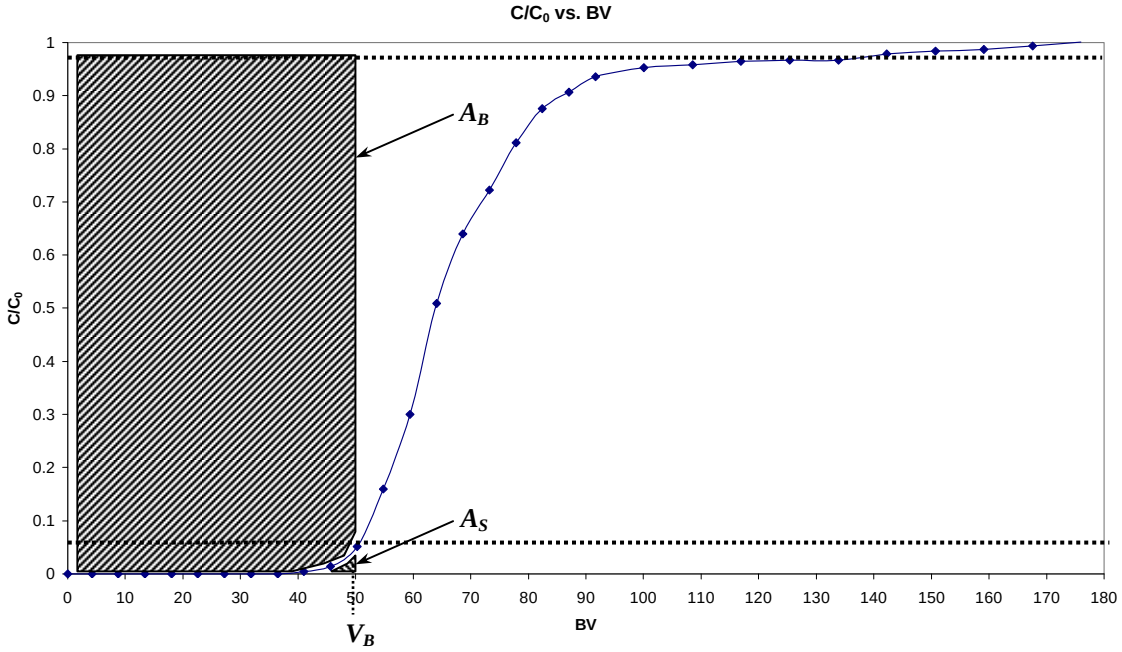

In this experiment, the volume of solution that is treated up to the breakthrough point (V_B) is 50.23 *BV*. The area under the curve up (A_S) to this value is found by using the multiple-segment Simpson's 1/3 Rule:

$$A_S \cong \int_0^{V_B} f(x)dx \cong \frac{h}{3}\left[f(x_o) + 4\sum_{\substack{i=1 \\ i=odd}}^{n-1} f(x_i) + 2\sum_{\substack{i=2 \\ i=even}}^{n-2} f(x_i) + f(x_n) \right]$$

where *n* is even, *f(x)* stands for *C/Co* values, and the segment width *h* is given by:

$$h = \frac{V_n - V_o}{n}$$

or

$$h = \frac{V_B - 0}{n}$$

$$h = \frac{50.23 - 0}{12} = 5.23BV$$

therefore;

$A_T = V_B - Vo = (50.23 - 0)\ BV * 1$

$A_T = 50.23\ BV$, (or 327.5 mL, where: 1 $BV = 6.52\ mL$)

so;

$$A_S \cong \frac{5.23}{3}\left[0 + 4(0 + 0 + 0 + 0 + 0) + 2(0 + 0 + 0 + 0.01) + 0.05\right]$$

$A_S = 1.636\ BV$, (or 10.67 mL)

Subtracting this value from the total area, A_T, gives:

$A_B = A_T - A_S$

$A_B = 50.23 - 1.636 = 48.59\ BV$, (or 316.82 mL)

then, since:

$$Q_B = \frac{C_o A_B}{\rho_b h_T A c._S}$$

therefore;

$$Q_B = \frac{(10\frac{meq}{L})(48.59\ BV)(6.52\times10^{-3}\ \frac{L}{BV})}{5 g_{zeolite}} = 0.633\frac{meq}{g_{zeolite}}$$

The Total Exchange Capacity (Q_T)

The total area is:

$A_T = A_B + A_S$, or;

$A_T = V_T - Vo = (142.25 - 0)\ BV * 1$

$A_T = 142.25\ BV$, (or 927.5 mL)

The area under the curve between (V_T) and (V_B) can be determined using the multiple-segment Simpson's 1/3 Rule:

$$\int_{V_B}^{V_T} f(x)dx \cong \frac{h}{3}\left[f(x_o) + 4\sum_{\substack{i=1 \\ i=odd}}^{n-1} f(x_i) + 2\sum_{\substack{i=2 \\ i=even}}^{n-2} f(x_i) + f(x_n) \right]$$

Where n is even and the segment width, h, is given by:

$$h = \frac{V_T - V_B}{n}$$

$$h = \frac{142.25 - 50.23}{16} = 5.75 BV$$

$$A_S \cong \frac{5.75}{3}\left[\begin{array}{l} 0.05 + 4(0.16 + 0.51 + 0.72 + 0.88 + 0.94 + 0.96 + 0.97) + \\ 2(0.3 + 0.64 + 0.81 + 0.91 + 0.95 + 0.96 + 0.97) + 0.98 \end{array} \right]$$

$As = 62.55\ BV$, (or 407.85 mL)

Subtracting this value from the total area, A_T, gives:

$A_B = A_T - A_S$

$A_B = 142.25 - 62.55 = 79.70\ BV$, (or 519.64 mL)

Since the total exchange capacity (Q_T) of the bed is given as in Equation 2.19:

$$Q_T = \frac{\int_0^{VT} (C_o - C)dV}{\rho_b h_T A_{c.s}}$$

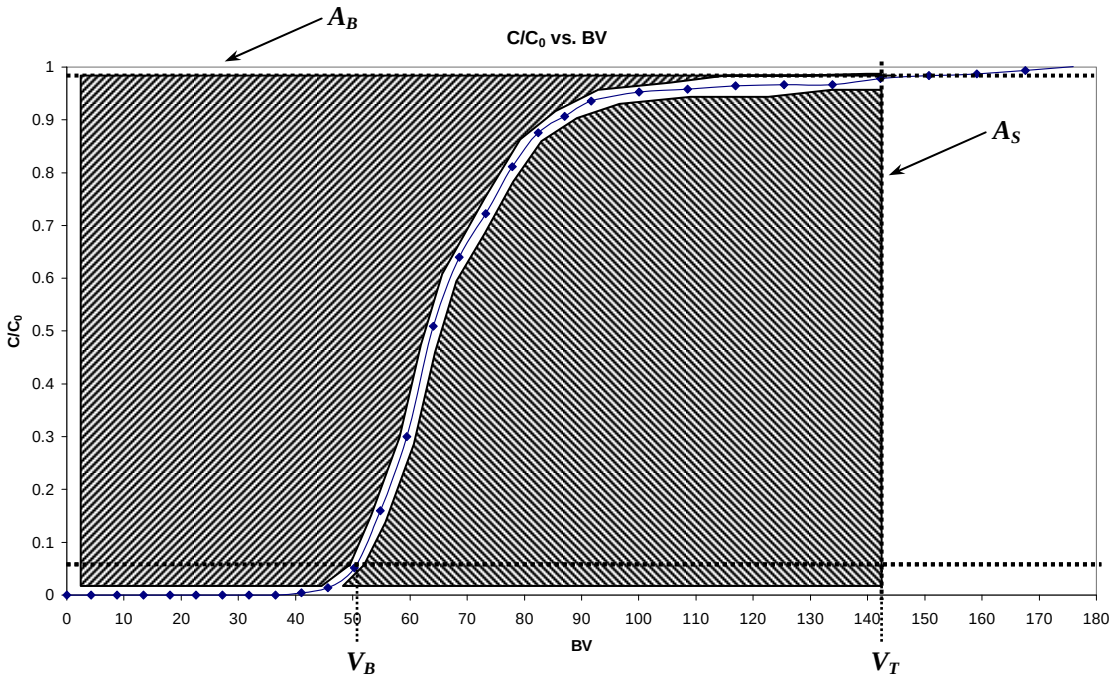

or

$$Q_T = \frac{C_o \int_0^{VT} (1 - \frac{C}{C_o}) dV}{\rho_b h_T A_{c.s}}$$

then

$$Q_T = \frac{(10 \frac{meq}{L})(79.70 \ \ BV(6.52 \times 10^{-3} \frac{L}{BV})}{5 g_{zeolite}} = 1.03 \frac{meq}{g_{zeolite}}$$

Also, the area above the breakthrough curve between breakthrough and exhaustion points (Q_z) will be:

Q_z = 79.70 - 48.59 = 31.11 *BV*

The Column Efficiency (η_c)

The column efficiency is calculated from equation 2.20:

$$\eta_C = \frac{Q_B}{Q_T}$$

$$\eta_C = \frac{0.633}{1.03} = 0.609$$

APPENDIX C

REPRODUCIBILITY OF THE EXPERIMENTS

The reproducibility of the experiments was checked for a specific a specific NH_4^+-Na^+ exchange experiment with initial influent concentration of 0.01 N, and flow rate of 8 mL/min. two experiments were conducted holding the same operating conditions, i.e. same flow rate, same influent concentration, same clinoptilolite particle size range, and both clinoptilolite samples were taken from the same NaCl-form clinoptilolite batch. The breakthrough curves for these two experiments are given in Figure C.1. The breakthrough capacity was found as 0.667 meq/g of zeolite in the first experiment, and the breakthrough capacity obtained from the reproducibility second experiment was 0.674 meq/g of zeolite. This showed that the percent error for reproducibility experiments was 1%.

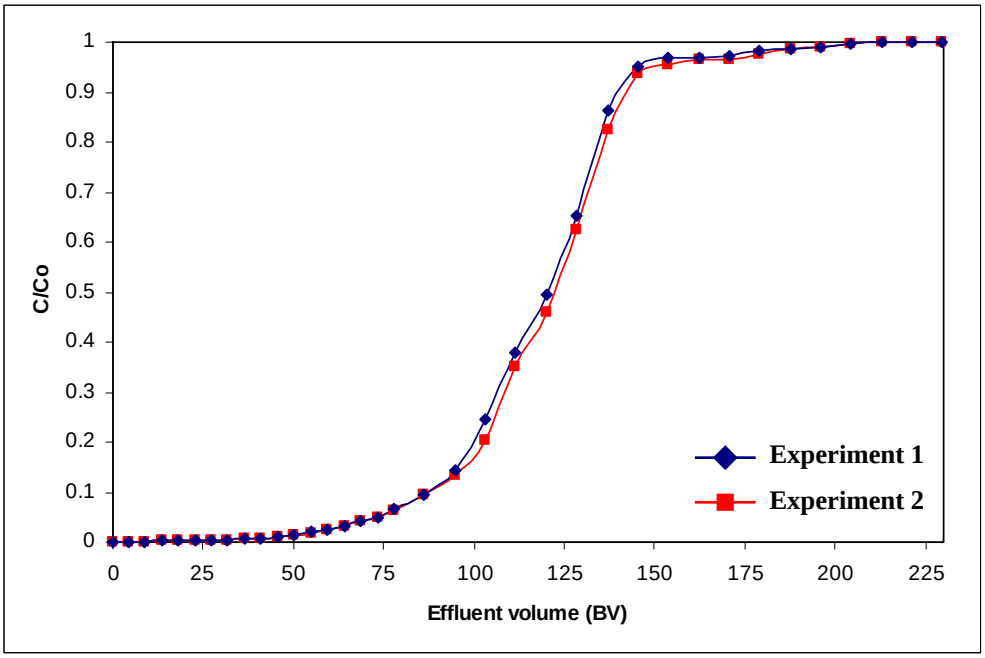

Figure C.1. The Breakthrough Curves of NH_4^+-Na^+ System - The Reproducibility Experiments

APPENDIX D

RAW DATA OF COLUMN EXPERIMENTS

Table D.1. Data for Binary Pb^{2+}-Na^{+} Exchange System, $\hat{O}$ = 8 *mL/min*, C_o = 0.01 *N*

Volume (*mL*)	Corrected Volume (*mL*)	Bed Volume (*BV*)	Concentration (*ppm*)	C/C_0
0	0	0.00	0.0	0
25	27.5	4.22	0.0	0
50	57.5	8.82	0.0	0
75	87.5	13.42	0.0	0
100	117.5	18.02	0.0	0
125	147.5	22.62	0.0	0
150	177.5	27.22	0.0	0
175	207.5	31.83	0.0	0
200	237.5	36.43	0.0	0
225	267.5	41.03	4.6	0
250	297.5	45.63	14.9	0.01
275	327.5	50.23	53.1	0.05
300	357.5	54.83	165.6	0.16
325	387.5	59.43	310.7	0.3
350	417.5	64.03	528.4	0.51
375	447.5	68.63	663.2	0.64
400	477.5	73.24	748.9	0.72
425	507.5	77.84	841.5	0.81
450	537.5	82.44	908.5	0.88
475	567.5	87.04	940.8	0.91
500	597.5	91.64	970.3	0.94
550	652.5	100.08	988.4	0.95
600	707.5	108.51	993.1	0.96
650	762.5	116.95	1000.5	0.96
700	817.5	125.38	1002.6	0.97
750	872.5	133.82	1003.8	0.97
800	927.5	142.25	1015.3	0.98
850	982.5	150.69	1024.0	0.99

Table D.1. (Continued)

900	1037.5	159.13	1029.1	0.99
950	1092.5	167.56	1036.0	1
1000	1147.5	176.00	1036.0	1

Table D.2. Data for Binary Pb^{2+}-Na^{+} Exchange System, $\hat{O}$ = 16 *mL/min*, C_o = 0.01 *N*

Volume (*mL*)	**Corrected Volume (*mL*)**	**Bed Volume (*BV*)**	**Concentration (*ppm*)**	**C/C_0**
0	0	0.00	0.0	0
25	27.5	4.22	0.0	0
50	57.5	8.82	0.0	0
75	87.5	13.42	2.9	0
100	117.5	18.02	22.8	0.02
125	147.5	22.62	48.7	0.05
150	177.5	27.22	106.7	0.1
175	207.5	31.83	205.7	0.2
200	237.5	36.43	400.8	0.39
225	267.5	41.03	645.8	0.62
250	297.5	45.63	752.4	0.73
275	327.5	50.23	841.3	0.81
300	357.5	54.83	900.6	0.87
325	387.5	59.43	937.7	0.91
350	417.5	64.03	958.5	0.93
375	447.5	68.63	975.8	0.94
400	477.5	73.24	998.6	0.96
425	507.5	77.84	1001.1	0.97
450	537.5	82.44	1012.1	0.98
475	567.5	87.04	1020.9	0.99
500	597.5	91.64	1026.5	0.99
550	652.5	100.08	1030.4	0.99
600	707.5	108.51	1035.7	1.00
650	762.5	116.95	1035.8	1.00
700	817.5	125.38	1036.0	1.00
750	872.5	133.82	1036.0	1.00
800	927.5	142.25	1036.0	1.00
850	982.5	150.69	1036.0	1.00
900	1037.5	159.13	1036.0	1.00
950	1092.5	167.56	1036.0	1.00
1000	1147.5	176.00	1036.0	1.00

Table D.3. Data for Binary Pb^{2+}-Na^{+} Exchange System, $\hat{O}$ = 32 *mL/min*, C_o = 0.01 *N*

Volume (*mL*)	**Corrected Volume (*mL*)**	**Bed Volume (*BV*)**	**Concentration (*ppm*)**	**C/C_0**
0	0	0.00	0.0	0
25	27.5	4.22	18.4	0.02
50	57.5	8.82	30.1	0.03
75	87.5	13.42	56.2	0.05
100	117.5	18.02	189.4	0.18
125	147.5	22.62	367.6	0.35
150	177.5	27.22	523.9	0.51
175	207.5	31.83	620.1	0.6
200	237.5	36.43	700.5	0.68
225	267.5	41.03	780.5	0.75
250	297.5	45.63	844.4	0.82
275	327.5	50.23	890.1	0.86
300	357.5	54.83	947.3	0.91
325	387.5	59.43	979.5	0.95
350	417.5	64.03	1012.4	0.98
375	447.5	68.63	1025.3	0.99
400	477.5	73.24	1035.4	1.00
425	507.5	77.84	1035.8	1.00
450	537.5	82.44	1035.9	1.00
475	567.5	87.04	1035.9	1.00
500	597.5	91.64	1035.9	1.00
550	652.5	100.08	1035.9	1.00
600	707.5	108.51	1036.0	1.00
650	762.5	116.95	1036.0	1.00
700	817.5	125.38	1036.0	1.00
750	872.5	133.82	1036.0	1.00
800	927.5	142.25	1036.0	1.00
850	982.5	150.69	1036.0	1.00
900	1037.5	159.13	1036.0	1.00
950	1092.5	167.56	1036.0	1.00
1000	1147.5	176.00	1036.0	1.00

Table D.4. Data for Binary Pb^{2+}-Na^{+} Exchange System, $\hat{O}$ = 8 *mL/min*, C_o = 0.005 *N*

Volume (*mL*)	**Corrected Volume (*mL*)**	**Bed Volume (*BV*)**	**Concentration (*ppm*)**	**C/C_0**
0	0	0.00	0.0	0.000
25	27.5	4.22	0.0	0.000
50	57.5	8.82	0.0	0.000
75	87.5	13.42	0.0	0.000
100	117.5	18.02	0.0	0.000
125	147.5	22.62	0.0	0.000
150	177.5	27.22	0.0	0.000
175	207.5	31.83	0.0	0.000
200	237.5	36.43	0.0	0.000
225	267.5	41.03	0.0	0.000
250	297.5	45.63	0.0	0.000
275	327.5	50.23	0.0	0.000
300	357.5	54.83	0.0	0.000
325	387.5	59.43	3.2	0.006
350	417.5	64.03	4.8	0.009
375	447.5	68.63	7.4	0.014
400	477.5	73.24	9.3	0.018
425	507.5	77.84	11.5	0.022
450	537.5	82.44	15.1	0.029
475	567.5	87.04	26.2	0.051
500	597.5	91.64	64.3	0.124
550	652.5	100.08	156.2	0.302
600	707.5	108.51	234.9	0.453
650	762.5	116.95	341.8	0.660
700	817.5	125.38	410.3	0.792
750	872.5	133.82	470.9	0.909
800	927.5	142.25	490.3	0.947
850	982.5	150.69	501.9	0.969
900	1037.5	159.13	504.6	0.974
950	1092.5	167.56	504.9	0.975
1000	1147.5	176.00	505.4	0.976
1050	1202.5	184.43	506.3	0.977
1100	1257.5	192.87	507.4	0.980
1150	1312.5	201.30	508.9	0.982
1200	1367.5	209.74	511.2	0.987
1250	1422.5	218.17	515.3	0.995
1300	1477.5	226.61	518.0	1.000
1350	1532.5	235.05	518.0	1.000

Table D.5. Data for Binary Pb^{2+}-Na^{+} Exchange System, $\hat{O}$ = 8 *mL/min*, C_o = 0.02 *N*

Volume (*mL*)	**Corrected Volume (*mL*)**	**Bed Volume (*BV*)**	**Concentration (*ppm*)**	**C/C_0**
0	0	0	0.0	0.00
25	27.5	4.218	20.4	0.01
50	57.5	8.819	93.8	0.05
75	87.5	13.42	241.0	0.12
100	117.5	18.02	460.4	0.22
125	147.5	22.62	841.2	0.41
150	177.5	27.22	1036.4	0.50
175	207.5	31.83	1330.2	0.64
200	237.5	36.43	1533.0	0.74
225	267.5	41.03	1663.0	0.80
250	297.5	45.63	1778.8	0.86
275	327.5	50.23	1846.2	0.89
300	357.5	54.83	1894.6	0.91
325	387.5	59.43	1967.0	0.95
350	417.5	64.03	2004.8	0.97
375	447.5	68.63	2024.6	0.98
400	477.5	73.24	2056.6	0.99
425	507.5	77.84	2072.0	1.00
450	537.5	82.44	2072.0	1.00
475	567.5	87.04	2072.0	1.00
500	597.5	91.64	2072.0	1.00
550	652.5	100.1	2072.0	1.00
600	707.5	108.5	2072.0	1.00
650	762.5	116.9	2072.0	1.00
700	817.5	125.4	2072.0	1.00
750	872.5	133.8	2072.0	1.00
800	927.5	142.3	2072.0	1.00
850	982.5	150.7	2072.0	1.00
900	1037.5	159.1	2072.0	1.00
950	1092.5	167.6	2072.0	1.00
1000	1147.5	176	2072.0	1.00

Table D.6. Data for Binary NH_4^+-Na^+ Exchange System, $\hat{O}$ = 8 *mL/min*, C_o = 0.01 *N*

Volume (*mL*)	**Corrected Volume (*mL*)**	**Bed Volume (*BV*)**	***mV***	**Concentration (*ppm*)**	**C/C_0**
0	0	0.00	0	0.00	0.00
25	27.5	4.22	22.6	0.15	0.00
50	57.5	8.82	34.3	0.26	0.00
75	87.5	13.42	40.2	0.35	0.00
100	117.5	18.02	44.4	0.42	0.00
125	147.5	22.62	48.4	0.51	0.00
150	177.5	27.22	53.3	0.64	0.00
175	207.5	31.83	61.5	0.94	0.01
200	237.5	36.43	67.2	1.23	0.01
225	267.5	41.03	71.2	1.48	0.01
250	297.5	45.63	76.6	1.91	0.01
275	327.5	50.23	83.7	2.67	0.01
300	357.5	54.83	89.8	3.55	0.02
325	387.5	59.43	95.7	4.69	0.03
350	417.5	64.03	100.2	5.80	0.03
375	447.5	68.63	106.3	7.72	0.04
400	477.5	73.24	109.9	9.14	0.05
450	507.5	77.84	115.4	11.84	0.06
500	562.5	86.27	123.3	17.17	0.09
550	617.5	94.71	132.1	25.96	0.14
600	672.5	103.14	143.3	43.95	0.24
650	727.5	111.58	152.6	68.04	0.38
700	782.5	120.02	158.4	89.36	0.49
750	837.5	128.45	164.2	117.37	0.65
800	892.5	136.89	170.2	155.61	0.86
850	947.5	145.32	172.2	170.95	0.95
900	1002.5	153.76	172.6	174.19	0.97
950	1057.5	162.19	172.6	174.19	0.97
1000	1112.5	170.63	172.7	175.01	0.97
1050	1167.5	179.06	172.9	176.67	0.98
1100	1222.5	187.50	173	177.50	0.99
1150	1277.5	195.94	173.1	178.34	0.99
1200	1332.5	204.37	173.2	179.18	1.00
1250	1387.5	212.81	173.3	180.02	1.00
1300	1442.5	221.24	173.3	180.02	1.00
1350	1497.5	229.68	173.3	180.02	1.00

Table D.7. Data for Binary NH_4^+-Na^+ Exchange System, $\hat{O}$ = 12 *mL/min*,C_o = 0.01 *N*

Volume (*mL*)	Corrected Volume (*mL*)	Bed Volume (*BV*)	Raw Clinoptilolite			Na Clinoptilolite		
			mV	Conc. (*ppm*)	C/C_0	*mV*	Conc. (*ppm*)	C/C_0
0	0	0.00	0	0.00	0.00	0	0.00	0.00
25	27.5	4.22	107.1	9.81	0.05	50.6	0.56	0.00
50	57.5	8.82	127	26.91	0.15	56.3	0.75	0.00
75	87.5	13.42	136.3	43.11	0.24	59.2	0.86	0.00
100	117.5	18.02	143.1	60.86	0.34	61.4	0.97	0.01
125	147.5	22.62	146.3	71.58	0.40	63.4	1.07	0.01
150	177.5	27.22	149.2	82.92	0.46	65.3	1.18	0.01
175	207.5	31.83	151.8	94.60	0.52	67.5	1.32	0.01
200	237.5	36.43	152.7	99.02	0.55	80.2	2.51	0.01
225	267.5	41.03	154	105.77	0.59	90.6	4.25	0.02
250	297.5	45.63	155.8	115.87	0.64	101.3	7.31	0.04
275	327.5	50.23	156.4	119.45	0.66	106.9	9.71	0.05
300	357.5	54.83	157.9	128.89	0.71	113.8	13.78	0.08
325	387.5	59.43	158.7	134.23	0.74	123.1	22.08	0.12
350	417.5	64.03	159.2	137.67	0.76	129.2	30.08	0.17
375	447.5	68.63	160.3	145.57	0.81	134.3	38.96	0.22
400	477.5	73.24	162.1	159.48	0.88	138.3	47.72	0.26
450	507.5	77.84	163.1	167.77	0.93	143.1	60.86	0.34
500	562.5	86.27	164	175.61	0.97	148.3	79.22	0.44
550	617.5	94.71	164.5	180.11	1.00	154.1	106.31	0.59
600	672.5	103.14	164.5	180.11	1.00	158.5	132.87	0.74
650	727.5	111.58	164.5	180.11	1.00	161.1	151.60	0.84
700	782.5	120.02	164.5	180.11	1.00	162.7	164.41	0.91
750	837.5	128.45	164.5	180.11	1.00	163.7	172.96	0.96
800	892.5	136.89	164.5	180.11	1.00	164.2	177.40	0.98
850	947.5	145.32	164.5	180.11	1.00	164.5	180.11	1.00
900	1002.5	153.76	164.5	180.11	1.00	164.5	180.11	1.00
950	1057.5	162.19	164.5	180.11	1.00	164.5	180.11	1.00
1000	1112.5	170.63	164.5	180.11	1.00	164.5	180.11	1.00
1050	1167.5	179.06	164.5	180.11	1.00	164.5	180.11	1.00
1100	1222.5	187.50	164.5	180.11	1.00	164.5	180.11	1.00
1150	1277.5	195.94	164.5	180.11	1.00	164.5	180.11	1.00
1200	1332.5	204.37	164.5	180.11	1.00	164.5	180.11	1.00
1250	1387.5	212.81	164.5	180.11	1.00	164.5	180.11	1.00
1300	1442.5	221.24	164.5	180.11	1.00	164.5	180.11	1.00
1350	1497.5	229.68	164.5	180.11	1.00	164.5	180.11	1.00

Table D.8. Data for Binary NH_4^+-Na^+ Exchange System, $\hat{O}$ = 16 *mL/min*, C_o = 0.01*N*

Volume (*mL*)	**Corrected Volume (*mL*)**	**Bed Volume (*BV*)**	***mV***	**Concentration (*ppm*)**	**C/C_0**
0	0	0.00	0	0.00	0.00
25	27.5	4.22	47.6	0.62	0.00
50	57.5	8.82	55.3	0.89	0.00
75	87.5	13.42	57.2	0.98	0.01
100	117.5	18.02	57.4	0.99	0.01
125	147.5	22.62	57.7	1.00	0.01
150	177.5	27.22	60.3	1.13	0.01
175	207.5	31.83	65.5	1.44	0.01
200	237.5	36.43	78.2	2.62	0.01
225	267.5	41.03	96.6	6.22	0.03
250	297.5	45.63	105.6	9.50	0.05
275	327.5	50.23	113.7	13.90	0.08
300	357.5	54.83	124.8	23.42	0.13
325	387.5	59.43	130.7	30.90	0.17
350	417.5	64.03	135.2	38.18	0.21
375	447.5	68.63	140.3	48.52	0.27
400	477.5	73.24	145.9	63.13	0.35
450	507.5	77.84	149.4	74.42	0.41
500	562.5	86.27	157.3	107.88	0.60
550	617.5	94.71	163.1	141.69	0.79
600	672.5	103.14	165.2	168.60	0.87
650	727.5	111.58	166.3	176.72	0.91
700	782.5	120.02	167.1	177.55	0.95
750	837.5	128.45	167.5	179.22	0.97
800	892.5	136.89	167.6	179.22	0.97
850	947.5	145.32	167.8	179.22	0.98
900	1002.5	153.76	167.9	179.22	0.99
950	1057.5	162.19	168.2	179.22	1.00
1000	1112.5	170.63	168.2	180.07	1.00
1050	1167.5	179.06	168.2	180.07	1.00
1100	1222.5	187.50	168.2	180.07	1.00
1150	1277.5	195.94	168.2	180.07	1.00
1200	1332.5	204.37	168.1	180.07	1.00
1250	1387.5	212.81	168.2	180.07	1.00
1300	1442.5	221.24	168.2	180.07	1.00
1350	1497.5	229.68	168.2	180.07	1.00

Table D.9. Data for Binary NH_4^+-Na^+ Exchange System, $\hat{O}$ = 32 *mL/min*, C_o = 0.01*N*

Volume (*mL*)	**Corrected Volume (*mL*)**	**Bed Volume (*BV*)**	***mV***	**Concentration (*ppm*)**	**C/C_0**
0	0	0.00	0	0.00	0.00
25	27.5	4.22	56.2	0.80	0.00
50	57.5	8.82	63.3	1.15	0.01
75	87.5	13.42	66.9	1.38	0.01
100	117.5	18.02	82.5	3.03	0.02
125	147.5	22.62	103.9	8.92	0.05
150	177.5	27.22	118.7	18.83	0.10
175	207.5	31.83	132.1	37.05	0.20
200	237.5	36.43	143.7	66.56	0.37
225	267.5	41.03	149.4	88.77	0.49
250	297.5	45.63	155.1	118.38	0.65
275	327.5	50.23	160.3	153.94	0.85
300	357.5	54.83	161.4	162.73	0.90
325	387.5	59.43	162.3	170.30	0.94
350	417.5	64.03	162.5	172.03	0.95
375	447.5	68.63	162.7	173.77	0.96
400	477.5	73.24	162.8	174.65	0.97
450	507.5	77.84	162.9	175.54	0.97
500	562.5	86.27	163.1	177.32	0.98
550	617.5	94.71	163.3	179.12	0.99
600	672.5	103.14	163.4	180.03	1.00
650	727.5	111.58	163.4	180.03	1.00
700	782.5	120.02	163.4	180.03	1.00
750	837.5	128.45	163.4	180.03	1.00
800	892.5	136.89	163.4	180.03	1.00
850	947.5	145.32	163.4	180.03	1.00
900	1002.5	153.76	163.4	180.03	1.00
950	1057.5	162.19	163.4	180.03	1.00
1000	1112.5	170.63	163.4	180.03	1.00
1050	1167.5	179.06	163.4	180.03	1.00
1100	1222.5	187.50	163.4	180.03	1.00
1150	1277.5	195.94	163.4	180.03	1.00
1200	1332.5	204.37	163.4	180.03	1.00
1250	1387.5	212.81	163.4	180.03	1.00
1300	1442.5	221.24	163.4	180.03	1.00
1350	1497.5	229.68	163.4	180.03	1.00

Table D.10. Data for Binary NH_4^+-Na^+ Exchange System, $\hat{O}$= 8 *mL/min*, C_o = 0.005*N*

Volume (*mL*)	**Corrected Volume (*mL*)**	**Bed Volume (*BV*)**	***mV***	**Concentration (*ppm*)**	**C/C_0**
0	0	0.00	0	0.00	0.00
25	27.5	4.22	1	0.05	0.00
50	57.5	8.82	1	0.05	0.00
75	87.5	13.42	1	0.05	0.00
100	117.5	18.02	1	0.05	0.00
125	147.5	22.62	1	0.05	0.00
150	177.5	27.22	1	0.05	0.00
175	207.5	31.83	1	0.05	0.00
200	237.5	36.43	1	0.05	0.00
225	267.5	41.03	1	0.05	0.00
250	297.5	45.63	1	0.05	0.00
275	327.5	50.23	1	0.05	0.00
300	357.5	54.83	1	0.05	0.00
325	387.5	59.43	1	0.05	0.00
350	417.5	64.03	1	0.05	0.00
375	447.5	68.63	1.1	0.05	0.00
400	477.5	73.24	4.1	0.06	0.00
450	507.5	77.84	10.1	0.08	0.00
500	562.5	86.27	63.5	0.80	0.01
550	617.5	94.71	73.1	1.21	0.01
600	672.5	103.14	81.1	1.71	0.01
650	727.5	111.58	87.3	2.23	0.02
700	782.5	120.02	110.1	5.96	0.05
750	837.5	128.45	133.3	16.17	0.15
800	892.5	136.89	143.3	24.87	0.24
850	947.5	145.32	150.1	33.32	0.33
900	1002.5	153.76	156.7	44.26	0.46
950	1057.5	162.19	160.9	53.03	0.56
1000	1112.5	170.63	165.1	63.53	0.68
1050	1167.5	179.06	169.4	76.45	0.83
1100	1222.5	187.50	171.6	84.04	0.92
1150	1277.5	195.94	172.1	85.87	0.95
1200	1332.5	204.37	172.3	86.61	0.95
1250	1387.5	212.81	172.4	86.98	0.96
1300	1442.5	221.24	172.5	87.36	0.96
1350	1497.5	229.68	172.6	87.73	0.97
1400	1552.5	238.11	172.6	87.73	0.97
1450	1607.5	246.55	172.7	88.11	0.97
1500	1662.5	254.98	172.7	88.11	0.97
1550	1717.5	263.42	172.9	88.87	0.98

Table D.10. (Continued)

1600	1772.5	271.86	173.1	89.64	0.99
1650	1827.5	280.29	173.2	90.03	1.00
1700	1882.5	288.73	173.2	90.03	1.00
1750	1937.5	297.16	173.2	90.03	1.00
1800	1992.5	305.60	173.2	90.03	1.00

Table D.11. Data for Binary NH_4^+-Na^+ Exchange System, $\hat{O} = 8$ *mL/min*, $C_o = 0.02N$

Volume (*mL*)	**Corrected Volume (*mL*)**	**Bed Volume (*BV*)**	***mV***	**Concentration (*ppm*)**	**C/C_0**
0	0	0.00	0	0.00	0.00
25	27.5	4.22	40.1	0.44	0.00
50	57.5	8.82	62.6	1.28	0.00
75	87.5	13.42	88.2	4.28	0.01
100	117.5	18.02	117.2	16.86	0.05
125	147.5	22.62	137.3	43.57	0.12
150	177.5	27.22	146.3	66.66	0.18
175	207.5	31.83	160.1	127.93	0.36
200	237.5	36.43	167.3	179.77	0.50
225	267.5	41.03	171.2	216.14	0.60
250	297.5	45.63	174	246.70	0.69
275	327.5	50.23	175.9	269.87	0.75
300	357.5	54.83	176.8	281.59	0.78
325	387.5	59.43	178.1	299.43	0.83
350	417.5	64.03	178.9	310.96	0.86
375	447.5	68.63	179.8	324.47	0.90
400	477.5	73.24	180.9	341.78	0.95
450	507.5	77.84	181.6	353.27	0.98
500	562.5	86.27	181.8	356.62	0.99
550	617.5	94.71	182	360.01	1.00
600	672.5	103.14	182	360.01	1.00
650	727.5	111.58	182	360.01	1.00
700	782.5	120.02	182	360.01	1.00
750	837.5	128.45	182	360.01	1.00
800	892.5	136.89	182	360.01	1.00
850	947.5	145.32	182	360.01	1.00
900	1002.5	153.76	182	360.01	1.00
950	1057.5	162.19	182	360.01	1.00
1000	1112.5	170.63	182	360.01	1.00
1050	1167.5	179.06	182	360.01	1.00
1100	1222.5	187.50	182	360.01	1.00
1150	1277.5	195.94	182	360.01	1.00
1200	1332.5	204.37	182	360.01	1.00

Table D.11. (Continued)

1250	1387.5	212.81	182	360.01	1.00
1300	1442.5	221.24	182	360.01	1.00
1350	1497.5	229.68	182	360.01	1.00

Table D.12. Data for Ternary Pb^{2+}-NH_4^+-Na^+ Exchange System, $\hat{O}$ = 8 *mL/min*, C_{oT}= 0.01 *N*, $C_o[Pb^{2+}]$ = 0.005*N*, $C_o\,[NH_4^+]$ = 0.005 *N*

Volume (*mL*)	Corrected Volume (*mL*)	Bed Volume (*BV*)	Lead		NH4	
			C (*ppm*)	C/C_0	C (*ppm*)	C/C_0
0	0	0.00	0.00	0.000	0	0.000
25	27.5	4.22	1.12	0.002	0.11	0.001
50	57.5	8.82	2.07	0.004	0.72	0.008
75	87.5	13.42	2.65	0.005	1.82	0.020
100	117.5	18.02	3.07	0.006	2.92	0.032
125	147.5	22.62	11.23	0.022	4.61	0.051
150	177.5	27.22	24.32	0.047	11.78	0.131
175	207.5	31.83	42.61	0.082	23.39	0.260
200	237.5	36.43	64.23	0.124	36.61	0.407
225	267.5	41.03	96.29	0.186	46.89	0.521
250	297.5	45.63	146.90	0.284	53.41	0.593
275	327.5	50.23	187.23	0.361	59.57	0.662
300	357.5	54.83	224.94	0.434	65.27	0.725
325	387.5	59.43	273.43	0.528	71.22	0.791
350	417.5	64.03	321.26	0.620	78.51	0.872
375	447.5	68.63	352.91	0.681	81.24	0.903
400	477.5	73.24	399.49	0.771	83.81	0.931
425	507.5	77.84	456.81	0.882	85.11	0.946
450	537.5	82.44	487.78	0.942	86.02	0.956
475	567.5	87.04	509.14	0.983	87.16	0.968
500	597.5	91.64	518.00	1.000	87.41	0.971
550	652.5	100.08	518.00	1.000	87.86	0.976
600	707.5	108.51	518.00	1.000	88.21	0.980
650	762.5	116.9	518.00	1.000	90	1.000
700	817.5	125.38	518.00	1.000	90	1.000
750	872.5	133.82	518.00	1.000	90	1.000
800	927.5	142.25	518.00	1.000	90	1.000
850	982.5	150.69	518.00	1.000	90	1.000
900	1037.5	159.13	518.00	1.000	90	1.000
950	1092.5	167.56	518.00	1.000	90	1.000
1000	1147.5	176.00	518.00	1.000	90	1.000
1050	1202.5	184.43	518.00	1.000	90	1.000
1100	1257.5	192.87	518.00	1.000	90	1.000

Table D.13. Data for Ternary Pb^{2+}-NH_4^+-Na^+ Exchange System, $\hat{O}$ = 16 *mL/min*, C_{oT}= 0.01 *N*, $C_o[Pb^{2+}]$ = 0.005*N*, $C_o\,[NH_4^+]$ = 0.005 *N*

Volume (*mL*)	**Corrected Volume (*mL*)**	**Bed Volume (*BV*)**	**Pb^{2+}**		**NH_4^+**	
			C (*ppm*)	**C/C_0**	**C (*ppm*)**	**C/C_0**
0	0	0.00	0.00	0.000	0	0.000
25	27.5	4.22	0.09	0.000	0.21	0.002
50	57.5	8.82	0.52	0.001	0.27	0.003
75	87.5	13.42	0.65	0.001	0.31	0.003
100	117.5	18.02	0.76	0.001	1.31	0.015
125	147.5	22.62	9.50	0.018	4.41	0.049
150	177.5	27.22	19.46	0.038	12.29	0.137
175	207.5	31.83	27.33	0.053	18.81	0.209
200	237.5	36.43	35.65	0.069	28.98	0.322
225	267.5	41.03	53.85	0.104	38.78	0.431
250	297.5	45.63	76.36	0.147	46.42	0.516
275	327.5	50.23	101.23	0.195	57.24	0.636
300	357.5	54.83	134.68	0.260	67.42	0.749
325	387.5	59.43	175.30	0.338	73.49	0.817
350	417.5	64.03	203.05	0.392	77.14	0.857
375	447.5	68.63	234.50	0.453	79.07	0.879
400	477.5	73.24	261.59	0.505	82.57	0.917
425	507.5	77.84	289.44	0.559	83.49	0.928
450	537.5	82.44	323.33	0.624	85.48	0.950
475	567.5	87.04	345.65	0.667	87.63	0.974
500	597.5	91.64	374.19	0.722	88.08	0.979
550	652.5	100.08	428.22	0.827	89.06	0.990
600	707.5	108.51	473.22	0.914	90	1.000
650	762.5	116.95	494.23	0.954	90	1.000
700	817.5	125.38	506.93	0.979	90	1.000
750	872.5	133.82	512.79	0.990	90	1.000
800	927.5	142.25	518.00	1.000	90	1.000
850	982.5	150.69	518.00	1.000	90	1.000
900	1037.5	159.13	518.00	1.000	90	1.000
950	1092.5	167.56	518.00	1.000	90	1.000
1000	1147.5	176.00	518.00	1.000	90	1.000
1050	1202.5	184.43	518.00	1.000	90	1.000
1100	1257.5	192.87	518.00	1.000	90	1.000

Table D.14. Data for Ternary Pb^{2+}-NH_4^+-Na^+ Exchange System, $\hat{O}$ = 32 *mL/min*, C_{oT}= 0.01 *N*, $C_o[Pb^{2+}]$ = 0.005*N*, $C_o\,[NH_4^+]$ = 0.005 *N*

Volume (*mL*)	Corrected Volume (*mL*)	Bed Volume (*BV*)	Pb^{2+}		NH_4^+	
			C (*ppm*)	C/C_0	C (*ppm*)	C/C_0
0	0	0.00	0.00	0.000	0	0.000
25	27.5	4.22	1.12	0.002	0.11	0.001
50	57.5	8.82	2.07	0.004	0.72	0.008
75	87.5	13.42	2.65	0.005	1.82	0.020
100	117.5	18.02	3.07	0.006	2.92	0.032
125	147.5	22.62	11.23	0.022	4.61	0.051
150	177.5	27.22	24.32	0.047	11.78	0.131
175	207.5	31.83	42.61	0.082	23.39	0.260
200	237.5	36.43	64.23	0.124	36.61	0.407
225	267.5	41.03	96.29	0.186	46.89	0.521
250	297.5	45.63	146.90	0.284	53.41	0.593
275	327.5	50.23	187.23	0.361	59.57	0.662
300	357.5	54.83	224.94	0.434	65.27	0.725
325	387.5	59.43	273.43	0.528	71.22	0.791
350	417.5	64.03	321.26	0.620	78.51	0.872
375	447.5	68.63	352.91	0.681	81.24	0.903
400	477.5	73.24	399.49	0.771	83.81	0.931
425	507.5	77.84	456.81	0.882	85.11	0.946
450	537.5	82.44	487.78	0.942	86.02	0.956
475	567.5	87.04	509.14	0.983	87.16	0.968
500	597.5	91.64	518.00	1.000	87.41	0.971
550	652.5	100.08	518.00	1.000	87.86	0.976
600	707.5	108.51	518.00	1.000	88.21	0.980
650	762.5	116.9	518.00	1.000	90	1.000
700	817.5	125.38	518.00	1.000	90	1.000
750	872.5	133.82	518.00	1.000	90	1.000
800	927.5	142.25	518.00	1.000	90	1.000
850	982.5	150.69	518.00	1.000	90	1.000
900	1037.5	159.13	518.00	1.000	90	1.000
950	1092.5	167.56	518.00	1.000	90	1.000
1000	1147.5	176.00	518.00	1.000	90	1.000
1050	1202.5	184.43	518.00	1.000	90	1.000
1100	1257.5	192.87	518.00	1.000	90	1.000

Table D.15. Data for Ternary Pb^{2+}-NH_4^+-Na^+ Exchange System, $\hat{O}$ = 8 *mL/min*, $C_o[Pb^{2+}]$ = 0.0025*N*, $C_o\,[NH_4^+]$ = 0.0075 *N*

Volume (*mL*)	**Corrected Volume (*mL*)**	**Bed Volume (*BV*)**	**Pb^{2+}**		**NH_4^+**	
			C (*ppm*)	**C/C_0**	**C (*ppm*)**	**C/C_0**
0	0	0.00	0.00	0.00	0.00	0.00
25	27.5	4.22	0.00	0.00	0.67	0.00
50	57.5	8.82	0.00	0.00	1.00	0.01
75	87.5	13.42	0.00	0.00	1.22	0.01
100	117.5	18.02	0.00	0.00	1.35	0.01
125	147.5	22.62	0.00	0.00	1.43	0.01
150	177.5	27.22	1.43	0.01	1.49	0.01
175	207.5	31.83	1.46	0.01	1.54	0.01
200	237.5	36.43	1.46	0.01	1.78	0.01
225	267.5	41.03	1.46	0.01	2.07	0.02
250	297.5	45.63	1.46	0.01	6.16	0.05
275	327.5	50.23	1.46	0.01	10.45	0.08
300	357.5	54.83	1.46	0.01	17.32	0.13
325	387.5	59.43	1.57	0.01	29.13	0.22
350	417.5	64.03	1.57	0.01	56.84	0.42
375	447.5	68.63	1.57	0.01	82.71	0.61
400	477.5	73.24	1.60	0.01	108.80	0.81
425	507.5	77.84	1.60	0.01	121.53	0.90
450	537.5	82.44	1.60	0.01	130.00	0.96
475	567.5	87.04	1.60	0.01	132.52	0.98
500	597.5	91.64	1.61	0.01	135.10	1.00
550	652.5	100.08	1.90	0.01	135.10	1.00
600	707.5	108.51	4.20	0.02	135.10	1.00
650	762.5	116.9	12.00	0.05	135.10	1.00
700	817.5	125.38	20.44	0.08	135.10	1.00
750	872.5	133.82	45.88	0.18	135.10	1.00
800	927.5	142.25	84.28	0.33	135.10	1.00
850	982.5	150.69	132.10	0.51	135.10	1.00
900	1037.5	159.13	168.10	0.65	135.10	1.00
950	1092.5	167.56	188.10	0.73	135.10	1.00
1000	1147.5	176.00	208.30	0.80	135.10	1.00
1050	1202.5	184.43	221.56	0.86	135.10	1.00
1100	1257.5	192.87	233.78	0.90	135.10	1.00
1150	1312.5	201.30	239.79	0.93	135.10	1.00
1200	1367.5	209.74	243.65	0.94	135.10	1.00
1250	1422.5	218.17	249.11	0.96	135.10	1.00
1300	1477.5	226.61	250.78	0.97	135.10	1.00
1350	1532.5	235.05	251.90	0.97	135.10	1.00
1400	1587.5	243.48	254.98	0.98	135.10	1.00

Table D.16. Data for Ternary Pb^{2+}-NH_4^+-Na^+ Exchange System, $\hat{O}$ = 8 *mL/min*, $C_o[Pb^{2+}]$ = 0.0075*N*, $C_o\,[NH_4^+]$ = 0.0025 *N*

Volume (*mL*)	Corrected Volume (*mL*)	Bed Volume (*BV*)	Pb^{2+}		NH_4^+	
			C (*ppm*)	C/C_0	C (*ppm*)	C/C_0
0	0	0.00	0.00	0.000	0.00	0.00
25	27.5	4.22	0.19	0.000	0.42	0.01
50	57.5	8.82	0.46	0.001	0.67	0.01
75	87.5	13.42	0.98	0.001	0.99	0.02
100	117.5	18.02	11.21	0.014	1.16	0.03
125	147.5	22.62	15.34	0.020	1.67	0.04
150	177.5	27.22	19.37	0.025	2.25	0.05
175	207.5	31.83	27.43	0.035	2.58	0.06
200	237.5	36.43	31.31	0.040	3.21	0.07
225	267.5	41.03	39.00	0.050	4.25	0.09
250	297.5	45.63	45.44	0.058	7.77	0.17
275	327.5	50.23	65.44	0.084	12.77	0.28
300	357.5	54.83	79.30	0.102	18.82	0.42
325	387.5	59.43	123.55	0.159	24.24	0.54
350	417.5	64.03	161.61	0.208	31.89	0.71
375	447.5	68.63	207.88	0.268	36.66	0.81
400	477.5	73.24	256.93	0.331	39.62	0.88
425	507.5	77.84	304.43	0.392	41.29	0.92
450	537.5	82.44	347.89	0.448	43.04	0.96
475	567.5	87.04	399.72	0.514	43.94	0.98
500	597.5	91.64	463.21	0.596	44.62	0.99
550	652.5	100.08	531.12	0.684	44.85	1.00
600	707.5	108.51	605.11	0.779	44.85	1.00
650	762.5	116.9	655.56	0.844	44.85	1.00
700	817.5	125.38	689.70	0.888	44.85	1.00
750	872.5	133.82	721.45	0.929	44.85	1.00
800	927.5	142.25	748.38	0.963	44.85	1.00
850	982.5	150.69	759.66	0.978	44.85	1.00
900	1037.5	159.13	768.46	0.989	44.85	1.00
950	1092.5	167.56	776.10	0.999	44.85	1.00
1000	1147.5	176.00	776.30	0.999	44.85	1.00
1050	1202.5	184.43	776.40	0.999	44.85	1.00
1100	1257.5	192.87	776.4	0.999	44.85	1.00
1150	1312.5	201.30	776.5	0.999	44.85	1.00
1200	1367.5	209.74	777.1	1.000	44.85	1.00
1250	1422.5	218.17	777.1	1.000	44.85	1.00
1300	1477.5	226.61	777.1	1.000	44.85	1.00